Norwegian University of Life Sciences

Master's Thesis 2021 60 ECTS
Faculty of Environmental Sciences and Natural Resource Management (MINA)

Testing a new methodology for measuring aggregate stability

Thomas Julseth Brown
Plant sciences
Faculty of Biosciences

Preface & Acknowledgements

MSc thesis completed as a part of a MSc degree in plant sciences (spec: Plant Biotechnology) at the Norwegian University of Life Sciences (NMBU). This MSc thesis focuses on soil physical properties and is linked to the Faculty of Environmental Sciences and Natural Resource Management (MINA). The MSc thesis covers 60 ECTS and both laboratory and theoretical work was performed between January and December 2021 (spring and autumn semesters).

I would like to say a particular thanks to my two supervisors Mathieu Lamandé and Susanne Eich-Greatorex for support, detailed advice, and constructive criticism throughout the year of 2021. Also, a thanks to Trond Børresen for patiently answering all my foolish questions. In addition, I would like to convey my thanks to Irene E. Eriksen and Øyvind Vartdal for helping me with laboratory analysis, and the latter for good conversation on how bad Manchester United have been playing recently.

A special thanks to my father Robert Brown for reading through my thesis several times to uncover my grammatical mistakes, of which there were many; it must have been a tiresome affair. I also pass on my gratitude to my mum, sister and family and friends for continuous support. Especially my girlfriend Live deserves recognition for lifting my spirits and showing patience when my mind was subconsciously thinking about my thesis.

This thesis marks the end of my time as a student in Ås; 5 years of my life that I will never forget.

Norwegian University of Life Sciences

Oslo, 10.12.21

Thomas Julseth Brown

Abstract

Soil aggregate stability is an important measure of a soils' physical and structural condition. Good aggregate stability is paramount in order to sustain crop productivity, limit soil erosion and promote healthy and sustainable soil. Improving aggregate stability promotes an idealistic soil state known as optimal tilth. In such conditions, the soil is perfectly loose and porous to allow for the assemblage of stable aggregates, which further enhances free infiltration and movement of water and air, resulting in easy cultivation and planting, unobstructed germination, seedling emergence, and growth of roots. In other words, good aggregate stability is crucial for sustainable agriculture. Most conventional aggregate stability measurement methods currently used are difficult to operate, slow, expensive, and require a laboratory. The conventional method used in this thesis is the rainfall simulator, which is the standard aggregate stability measurement method used at the Norwegian University of Life Sciences (NMBU). An application called SLAKES may be on the verge of offering an alternative to the older existing aggregate stability measurement methods. SLAKES is an application invented in Australia by the University of Sydney. In contrast to the conventional methods, SLAKES offers an easy, quick, and inexpensive method of measuring aggregate stability. In addition, no laboratory is needed, and SLAKES is available to anyone who owns a smartphone. After 10 mins, SLAKES is able to produce an aggregate stability measurement that is displayed on the smartphone screen using only water, a petri dish, 3 soil aggregates (2-15 mm), and a smartphone with the SLAKES application installed. A text-file including additional data is automatically downloaded to the smartphone's memory after the 10 min slaking interval. Four experimental sites are used to measure aggregate stability with SLAKES and the rainfall simulator: one organic fertilizer experiment and three tillage experiments. The aim is to determine if SLAKES can detect differences between treatments, and if these differences correspond to the results from the rainfall simulator. All four experimental fields have different soil textures: Silt loam, silty clay loam, clay, and sandy loam. In two out of three fields, mean values from SLAKES show higher significant separation between treatments than the rainfall simulator. In one field, significance cannot be established as there is only one repetition. Analysis suggests that the rainfall simulator can better detect correlations between aggregate stability and organic matter than SLAKES. Although SLAKES has flaws, this thesis gives evidence to suggest that the application is a valid alternative to conventional aggregate stability measurement methods such as the rainfall simulator.

Table of contents

1 – Introduction

There is wide scientific consensus that soil quality is improved through sustainable farming practises, compared to conventional ones (Birkhofer et al., 2008, Marinari et al., 2006, Krauss et al., 2020). As the world shifts towards a more sustainable future, more detailed insights into specific benefits of organic fertilizers and reduced tillage on different soil parameters will be required. To begin with, it is necessary to define soil quality. It may be described as the capacity of a given soil to function "normally" (Karlen et al., 1997). "Normal" soil function depends on the ecosystem, either it is natural, or managed. Also, the function of a soil is judged on its ability to sustain plant and animal productivity, to maintain or enhance water and air quality, and to support human health and habitation (Karlen et al. 1997). Another definition of soil quality is that it is the measure of soil condition (physically, chemically, biologically) depending on type of land-use, climate patterns, cropping sequences and farming systems (Rajani, 2019). Soil quality can be evaluated according to many different indicators. Table 1.1 shows an example. In conventionally managed systems, soil quality is often in decline due to traditional tillage practices (e.g., ploughing), and excessive use of mineral fertilizer and pesticides. Adoption of reduced tillage practices and increased use of organic fertilizers may have many positive effects on several soil quality parameters, like the ones listed in Table 1.1. Of these variables, aggregation is fundamentally important, simply because aggregates are the building blocks of soil. An aggregate/ped/clod is a small clump or mass consisting of primary soil particles (clay, silt, and sand), bound together by clay and organic matter (Oades, 1984, Six et al., 2004).

Table 1.1 - Parameters affecting soil quality (Karlen et al., 1997).

Table 1. Selected indicators of soil quality and some processes they impact.

Measurement	Process affected
Organic matter	Nutrient cycling, pesticide and water retention, soil structure
Infiltration	Runoff and leaching potential, plant water use efficiency, erosion potential
Aggregation	Soil structure, erosion resistance, crop emergence, infiltration
pH	Nutrient availability, pesticide absorption and mobility
Microbial biomass	Biological activity, nutrient cycling, capacity to degrade pesticides
Forms of N	Availability to crops, leaching potential, mineralization and immobilization rates
Bulk density	Plant root penetration, water- and air-filled pore space, biological activity
Topsoil depth	Rooting volume for crop production, water and nutrient availability
Conductivity or salinity	Water infiltration, crop growth, soil structure
Available nutrients	Capacity to support crop growth, environmental hazard

This thesis focuses on the stability of soil aggregates, and particularly on aggregate stability measurement methods. Conventional methods used to measure aggregate stability are old, difficult to operate, expensive and require a laboratory. A new method for measuring aggregate stability involving an application called SLAKES is suggested to be less time consuming and cheaper than conventional methods, but it has yet to be tested on Norwegian soils. SLAKES is compared to the traditional method used at the Norwegian University of Life Sciences, the rainfall simulator.

1.1 – Aggregate stability

Soil aggregate stability is a measurement of the strength of the chemical bonds that hold an aggregate together when exposed to external destructive forces (e.g., rainfall and/or water submergence). Aggregate stability is a major soil physical property that influences, and is influenced by other physical, chemical, and biological factors (Tisdall & Oades, 1982). For instance, aggregate stability influences the ability of the soil to retain organic carbon, its ability to uphold soil porosity, water infiltration, water retention, aeration, and hydraulic conductivity, and to avoid compactability, thus increasing the capacity of the soil to withstand erosion due to rainfall and overland flow (Masciandaro et al., 2018). To understand aggregate stability, one must be aware of three vital factors affecting aggregation, namely clay content, roots, and organic matter.

1.2 – Aggregation

1.2.1 – Clay

Clay content is essential for the formation of aggregates, because of the tendency of clay to flocculate (Hillel et al., 1998). In addition, cohesiveness between clay particles is the paramount binding force within microaggregates. Depending on the amount of calcium carbonate and aluminium oxides present in clay molecules (determined by the mineralogy of the soil), these molecules convey substantial stability to otherwise weak aggregates (Hillel et al., 1998). Tropical soils often contain little organic matter, and the impressive stability these soils portray is due to aluminium oxides. Although flocculation is a necessary ingredient for aggregation, it is not enough. Presence of roots and organic matter is equally crucial, as is it promotes

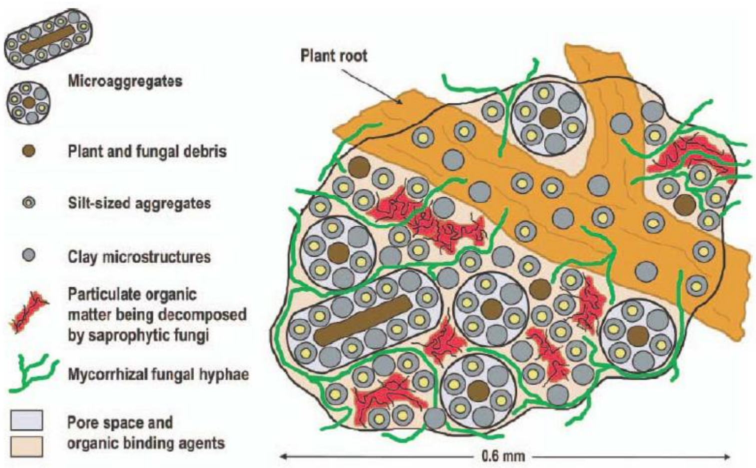

Figure 1.1 – "Conceptual diagram depicting the hierarchical organisation of micro-aggregates within a macro- aggregate" (Jastrow & Miller, 1998).

formation of stable aggregates. Figure 1.1 shows essential components of a typically stable soil aggregate.

1.2.2 – Organic matter, roots and microbes

Various soil organisms present in organic matter (especially fungi and bacteria), as well plant roots, apply force and secrete compounds that act as glue to cement/bind aggregates together (Jastrow & Miller, 1998). Cementation is especially important for the stability of aggregates. Roots provide both physical and chemical cementation. Vast expanses of roots below the soil surface entangle and permeate aggregates, applying enormous pressures that both compact some aggregates, and separate others. Another physical cementation property of roots is water uptake, which "causes differential dehydration, shrinkage, and the opening of numerous small cracks" (Hillel et al., 1998). Chemically, roots cement aggregates together by secreting root exudates, mucilage, and sloughed off cells and tissues. Also, these secretions promote nutrient uptake, and protect roots and aggregates from drying out; they also improve soil-root contact, inhibit the uptake of unwanted substances (e.g., aluminium), and increase microbial activity in the rhizosphere, all of which benefit further aggregation (Hillel et al., 1998). Dead roots and root hairs are especially beneficial, as they nurture soil microorganisms by acting as carbon and nitrogen sources. In other words, dead roots left in the soil, and plant residues left on the surface, increase soil organic matter, thus encouraging microbial activity and the production of humic cements. In turn, this stabilizes aggregates and provides plant available nutrients (Fig. 1.2).

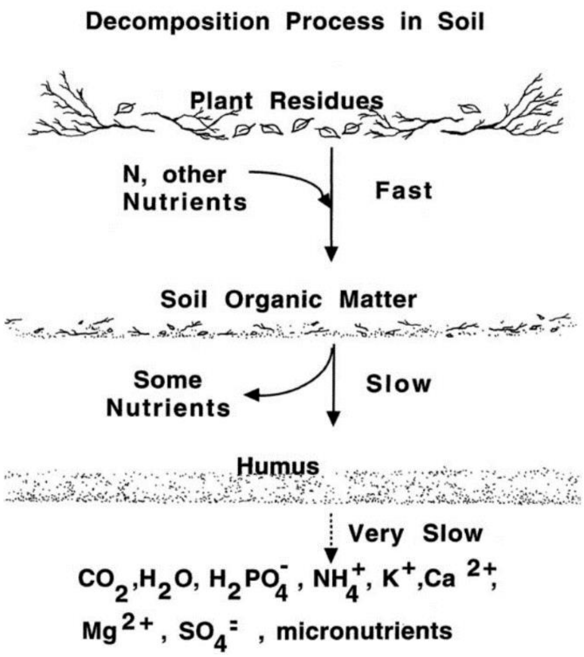

Figure 1.2 – "Decomposition in soil. plant or animal remains in soils decompose breaking down into organic matter with eventual formation of humus and release of many plant nutrients" (Keefer, 2000).

Although dead roots provide organic matter to the soil; in annual cropping systems this is not always enough because some organic matter is removed from the soil during harvest. Moreover, there is often little to no plant residues left on the soil surface to nurture the microorganisms in the soil. As Hillel et al. (1998) explains, annual cropping systems hasten the decomposition of humus and the destruction of soil aggregates. If there is a continuous lack of addition of organic matter in these systems, and the soil surface is left barren and exposed, aggregates are left unprotected towards desiccation and heavy rainfall. Roots and microbes both act as cements, but microbes have some additional functions influencing aggregation and aggregate stability. This leads us in more depth to the importance of soil organic matter. Fungi, bacteria, protozoa, and many other species, make up the trillions of microorganisms present in soil, and organic matter feeds these organisms. Especially rhizospheric bacteria (e.g., nitrogen-fixing bacteria) and fungi (e.g., mycorrhiza) that function in direct relation with roots are very beneficial. In addition to cementation by secreted mucilaginous products, microorganisms also bind aggregates by complex mechanisms like adsorption, and physical entanglement and envelopment (Hillel et al., 1998). Among the main microbial products exuded and capable of cementing aggregates together are polysaccharides, hemicelluloses or uronides, and many other natural polymers (Coleman & Crossley, 1996). These organic products are of the utmost importance for inter- and intra-aggregate bonding and thus the stability of an aggregate. These polymers attach to clay surfaces through hydrogen bonding, van der Waals forces, cation bridges and anion adsorption mechanisms; and especially polysaccharides have large, linear, and supple structures that are required to form multiple bonds with numerous particles at the same time (Hillel et al., 1998). Hillel et al. (1998) adds that in some instances, individual clay particles barely become perforated by organic compounds, instead a shielding capsule-like cover is formed around soil peds. In other instances, organic substances may enter soil aggregates, where they precipitate into almost irreversible insoluble cements, while remaining biologically degradable (Hillel et al., 1998). The two latter instances are often examples of organo-clay complexes in which the organic substances are innately hydrophobic or become so as they dehydrate. This reduces the complexes' affinity for water and is specifically critical in relation to promoting aggregate stability by reducing wettability and swelling of aggregates (Hillel et al., 1998).

1.2.3 – Importance of stable aggregates

In relation to aggregate stability, one can now begin to see the importance of clay content, extensive root networks, and amount and quality of organic matter. It is essential to emphasize the significance of these factors in assuring strong inter- and intra-aggregate bonding, as well as their function linked to reduced wettability and swelling of aggregates. These three aggregate qualities are necessary components of a stable aggregate. Without good aggregate stability, irregular and heavy rainfall increases the risk of aggregate slaking (disintegration due to water submergence) and erosion. Aggregate slaking may lead to soil crusting, and in such a circumstance, smaller particles resulting from fragmented surface aggregates form a layer of dispersed mud upon wetting, usually several millimetres thick (Hillel et al., 1998). Macropores are often filled with this mud, reducing water and gas infiltration. Frequently this is called a surface seal, and “upon drying, the dispersed layer shrinks to become a dense, hard crust, which impedes seedling emergence by its hardness and tears seedling roots as it cracks” (Hillel et al., 1998).

Water fragments aggregates in two distinct ways, erosion by heavy rainfall, and slaking by water submergence. Slaking of aggregates often follows erosion when subjected to a deluge of rain. However, the physical processes of disintegration are entirely different for aggregates eroded by rainfall compared to aggregates slaked during water immersion. It is important to be aware of this difference, as the rainfall simulator largely mimics erosion by heavy rainfall, while SLAKES imitates slaking by sudden water submergence – this will be explained further in the sections dedicated to the two different aggregate stability measurement methods. In a world increasingly affected by climate change, with periods of drought followed by torrential rain impacting cropping systems across the globe; the importance of understanding aggregation and aggregate stability, as well as the destructive forces influencing these parameters, becomes evident. In Norway and other subarctic regions, climate change is occurring more rapidly than on world average. According to the Paris agreement (2015), the world wants to limit the average global temperature to 1.5 ^{o}C, but in most subsequent years, Norway is already exceeding that temperature limit. In 2020, the mean temperature for Norway was 2.4 ^{o}C above average (State of the Environment Norway, 2021). The Norwegian Meteorological Institute predicts warmer, wilder, and wetter weather. Prolonged drought periods during summer are expected, particularly in southern and eastern parts of Norway. When precipitation first arrives, it will come in larger quantities and within a shorter period of time than before, likely causing flooded farmland (Norwegian Meteorological Institute, 2021).

1.3 – SLAKES

SLAKES is a mobile application software invented by Fajardo & McBratney (2019) at The University of Sydney. It is based on a scientific paper by the same authors (Fajardo et al. 2016). The app can be downloaded to both Android and Apple devices from Google Play and App Store. The physics behind SLAKES is sudden water submergence of desiccated aggregates. Dry aggregates are particularly vulnerable to sudden water submergence. The reason for this is that prior to submergence, all pores within an aggregate contain air, but no water. When aggregates suddenly become submerged in water, the entire periphery of the

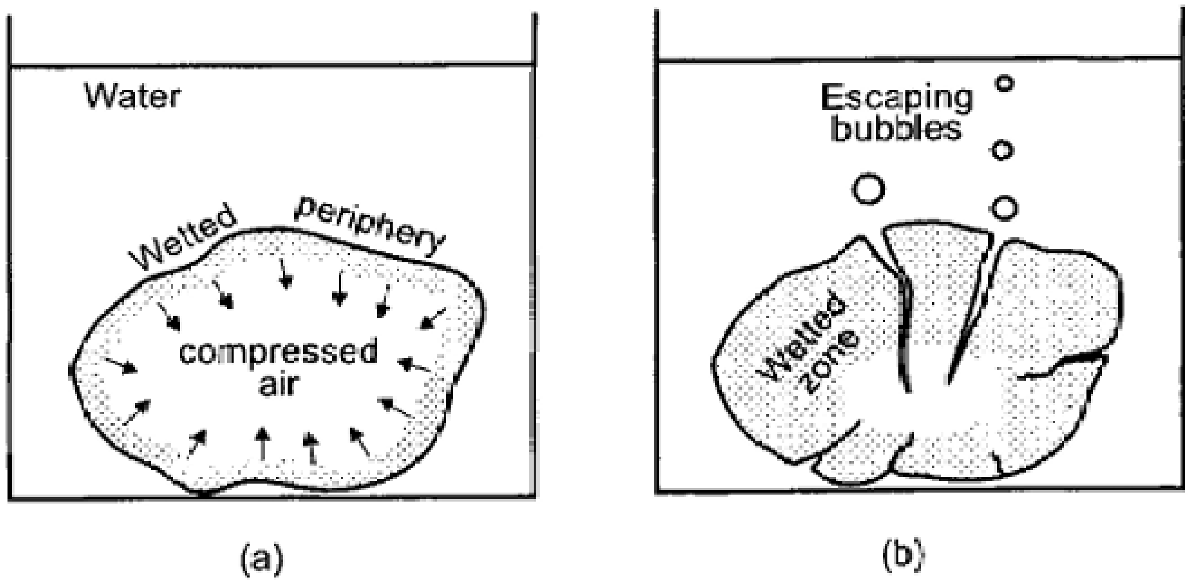

Figure 1.3 – «Air slaking of an initially dry aggregate suddenly submerged in water. (a) Early stage: The periphery of the aggregate is wetted, and water moves into the aggregate compressing the air inside. (b) Bursting stage: As the wetted zone is weakened by swelling and the pressure of entrapped air increases in proportion to its compression, eventually the aggregate is shattered and air bubbles out. This point may be quite abrupt and result in the collapse of the shattered aggregate." (Hillel et al., 1998).

aggregate is surrounded by water and there is nowhere for air to escape. As the water gradually, but quickly, moves into the aggregate, the air inside becomes increasingly compressed. Simultaneously, water induces swelling of the soil ped, weakening the cohesive strength between soil particles. As Hillel et al. (1998) describes, eventually the growing pressure exerted upon the entrapped air inside the clod becomes too large and the soil aggregate may explode. A series of small explosions is however more typical and is often observed as a bubble of air escaping from the aggregate, followed by the disintegration of the aggregate (Fig. 1.3). This process is known as air slaking, hence the name of the application. Depending on the aggregate stability of the soil ped, the degree of slaking varies. SLAKES appears to be a good alternative to more traditional aggregate stability measurement methods, such as the rainfall simulator. Being an application, SLAKES has its advantages. It requires less equipment therefore reducing expenses. Also, the measuring of aggregate stability is much quicker and needs less technical know-how with simple instructions.

1.4 – Rainfall simulator

One of the traditional methods commonly used, and the one used in this experiment is the Rainfall Simulator, developed at the Norwegian University of Life Sciences (NMBU). Developed by Marti in 1984, it is a relatively old method which requires expensive equipment, it is also time consuming, and it needs to be performed in a laboratory. The physical mode of action applied upon soil aggregates by the rainfall simulator is the destroying impact of heavy rainfall. Although slaking also occurs because of the wetting of rainfall, the main reason as to why the aggregates disintegrate using this method, is due to the battering force of raindrops. Since dry aggregates are very susceptible to slaking, aggregates need to be pre-wetted so that only mechanical breakdown affects disaggregation.

The rainfall simulator is the method used at NMBU, and is far from the most common way of measuring aggregate stability. A few other methods for measuring aggregate stability include wet sieving (Tiulin, 1928; Yoder, 1936; De Leenheer & De Boodt, 1958), the wet aggregate stability test (Ogden, 1997), the drop method (McCalla, 1944), and the permeability method (Reeve, 1965).

1.5 – Objectives

Mainly, the thesis assesses SLAKES and its advantages and disadvantages compared to the rainfall simulator. Furthermore, the thesis evaluates if SLAKES is sensitive enough to detect differences between various organic fertilizers, even in a short-term experiment. In such a brief experiment the treatment dissimilarities are expected to be small, so the question is if SLAKES can be as sensitive as the rainfall simulator. Included are also three long-term tillage experiments where the differences between treatments are expected to be substantial. Here the aim is to find out if SLAKES shows similar aggregate stability measurements compared to the rainfall simulator.

1.6 – Hypothesis

Based on the experiments conducted by Flynn et al. (2019), there is optimism linked to the ability of SLAKES to accurately measure aggregate stability. Flynn et al. (2019) found SLAKES to be more sensitive to tillage treatment than the Cornell wet aggregate stability test. It is hypothesized that the application may be a simpler and better way of measuring aggregate stability than traditional methods.

The following hypotheses were tested in this thesis:

1. SLAKES shows sensitivity similar to the rainfall simulator method in detecting differences in aggregate stability between organic fertilizer treatments.
2. SLAKES shows sensitivity similar to the rainfall simulator method in detecting differences in aggregate stability between different tillage treatments.

2 – Materials and methods

2.1 – Experimental sites

All experimental sites are located in the Oslofjord region of eastern Norway (Fig. 2.1). One of the field experiments focuses on the effect of organic fertilizers on different soil properties (E166), whereas the three other field experiments focus on how tillage practise affects various soil properties (A85, A45, & Kjuus).

According to Köppen climate classification, areas around the Oslo fjord have a hemiboreal climate (*Dfb*). A *Dfb* climate means average temperatures below -3 ^{o}C in the coldest month, and at least four months where temperatures rise above +10 ^{o}C, as well as a year-round moist and cool climate (Mamen, 2020). Average annual rainfall ranges between 750 – 1000 mm.

Particle size distribution analysis has categorized the soil type for each of the four different experimental sites (Fig. 2.2). Field E166 is a silt loam, field A85 is a silty clay loam, field A45 is a clay, and field Kjuus is a sandy loam.

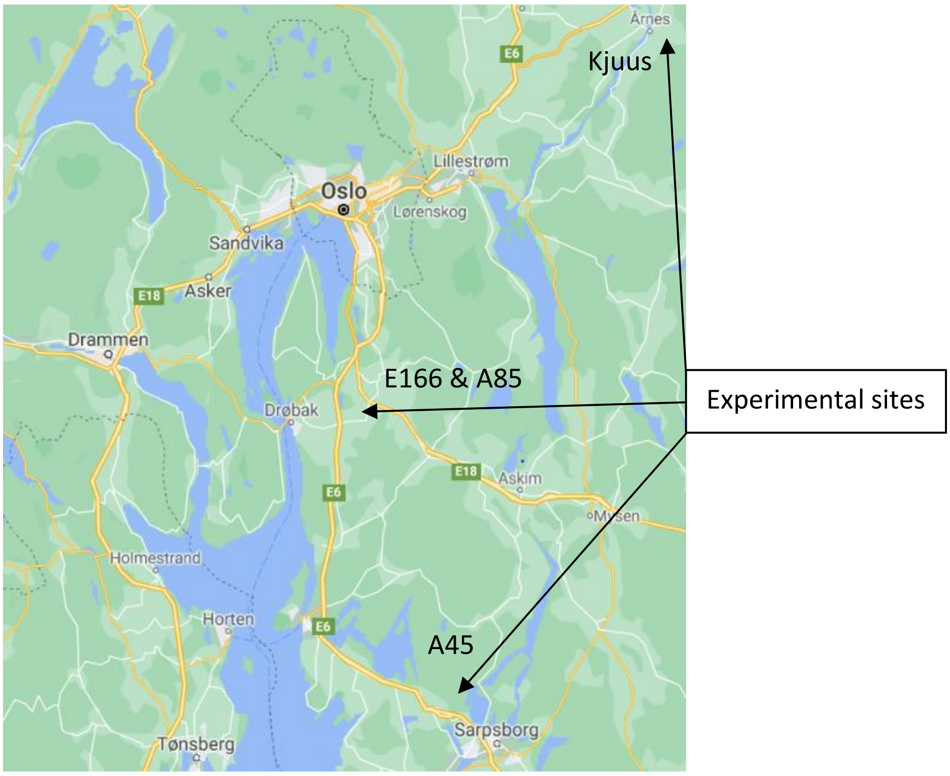

Figure 2.1 – Map of the Oslofjord region. Arrows point to experimental sites. 1 field in Årnes (TR), 2 fields in Ås (M), and 1 field in Sarpsborg (BR) (Google, n.d.).

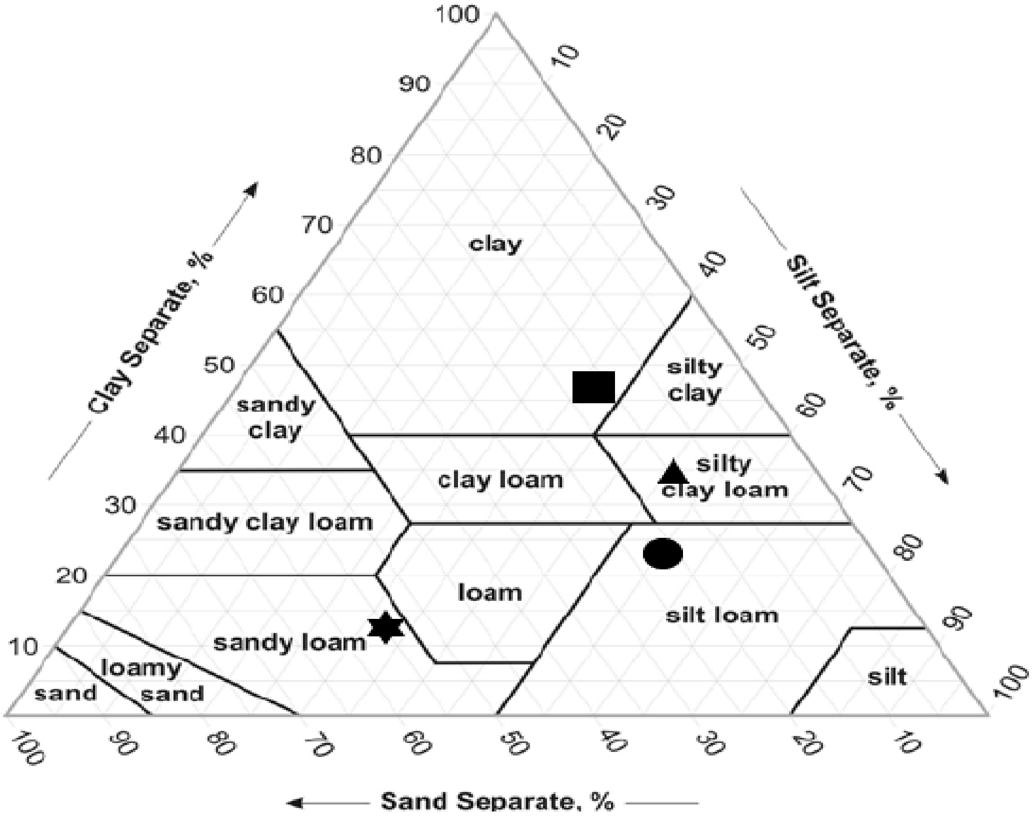

Figure 2.2 – Soil texture triangle (USDA soil texture triangle). Field E166 (oval shape): 23 % clay, 55 % silt, 2 % sand = silt loam. Field A85 (triangle shape): 34 % clay, 51 % silt, 15 % sand = silty clay loam. Field A45 (square shape): 45 % clay, 38 % silt, 17 % sand = clay. Field Kjuus (star shape): 13 % clay, 34 % silt, 53 % sand = sandy loam.

2.1.1 – Organic waste fertilizer experiment (E166 – Digestate)

- Field: E166
- Location: Ås, Norway
- Coordinates (DMS): 59º 39’ 50.87” N, 10º 46’ 16.35” E

1	2	3	4	5	6	7	8	9	10	11	12	13
6	**13**	**4**	**8**	**10**	**5**	**12**	**11**	**3**	**2**	**9**	**7**	**1**
							108					
14	15	16	17	18	19	20	21	22	23	24	25	26
7	**10**	**9**	**13**	**3**	**6**	**1**	**12**	**4**	**8**	**5**	**2**	**11**
27	28	29	30	31	32	33	34	35	36	37	38	39
4	**3**	**12**	**7**	**1**	**2**	**11**	**6**	**9**	**10**	**13**	**8**	**5**

Figure 2.3 – Overview of experimental field E166

Table 2.1 - Overview of fertilizer treatments applied on field E166.

	Treatment
1	Control
2	Mineral fertilizer
3	Animal manure
4	Digestate – food waste
5	Digestate – sludge + food waste

An experiment with organic fertilizers was started in 2014 on field E166, consisting of three blocks/rows (Fig. 2.3 – plots 1-39). E166 is so far a relatively short-term experiment. The entire field covers an area of 1248 m^2, where each block covers 273 m^2, and individual plots cover 21 m^2. Of the 13 treatments listed in Table 2.1, only the 5 treatments highlighted are used for analysis. There are 3 repetitions, and all 5 treatments are randomly spaced within the 3 repetition blocks, adding up to a total of 15 plots (3 x 5). The 5 treatments used in this study are a control with no fertilizer added (T1), mineral fertilizer (T3), animal manure (T5), biogas digestate based on food waste (T7), and biogas digestate based on sewage sludge and food waste (T9) (Tab. 2.1). All fertilizers are given at a rate of 10 kg of plant available N/daa. The biogas digestate fertilizers are organic residual products derived from biogas production, whereas the animal manure fertilizer is slurry derived from livestock at Ås farm. Usual amounts of animal manure applied is 7 – 8 tons per daa with a dry matter content of approximately 6 % (g/100g). For digestate based on food waste, the usual amount applied is 6 tons per daa, whereas it is 7 tons per daa for digestate food waste and sewage sludge – both digestate fertilizers have an approximate dry matter content of 3 % (g/100g). Every year, spring ploughing and clod crushing are performed prior to adding fertilizer treatments, which are subsequently harrowed into the soil, before cereal crops are sown (barley 2020, wheat 2019). Harrowing after fertilization was performed on the 23rd of April 2020.

2.1.2 – Reduced tillage experiments

2.1.2.1 – Ås – tillage spring and autumn (A85)

- Field: A85
- Location: Ås, Norway
- Coordinates (DMS): 59º 39’ 50.87” N, 10º 46’ 16.35” E

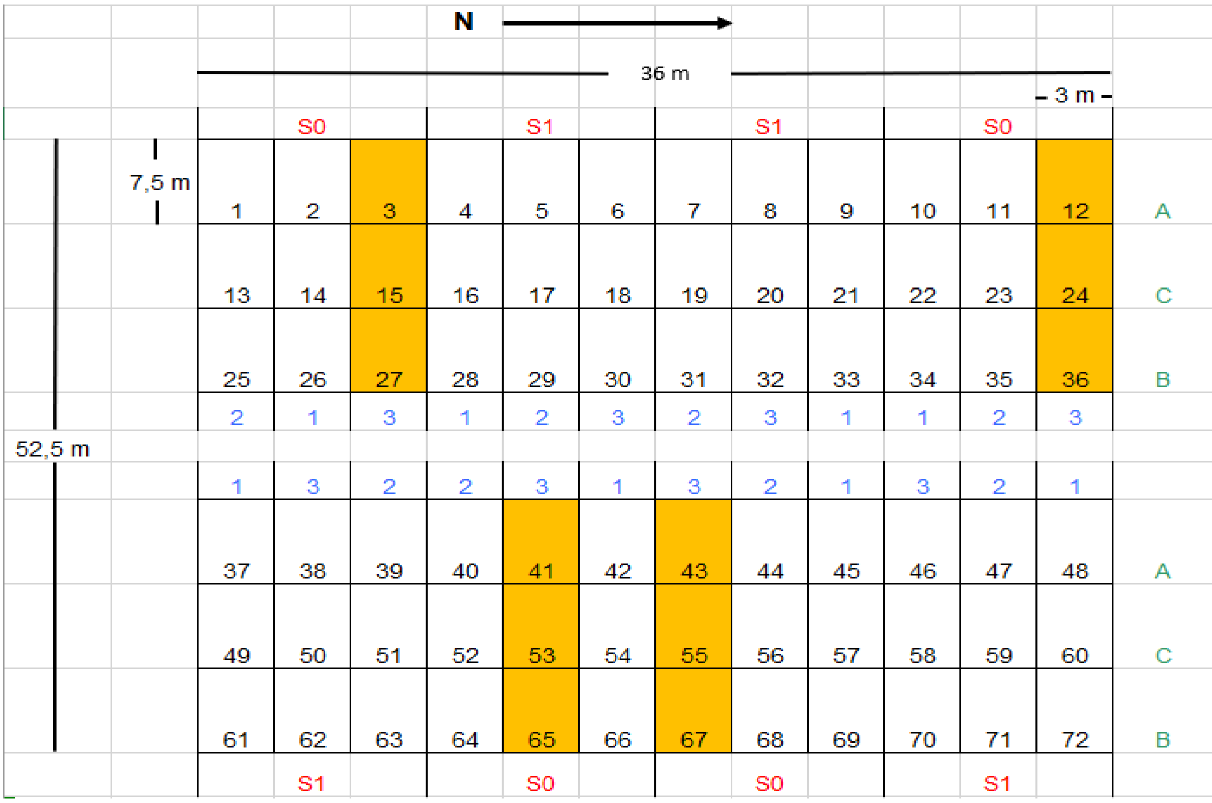

Figure 2.4 - Overview of experimental field A85. Highlighted grids are plots used for analysis (Børresen, 2019).

Table 2.2 – Overview of tillage treatments applied on field A85. S0 means no stubble harrowing, whereas 3 means no soil compaction. Main treatments are A, B, and C.

	Main tillage treatment
S0 + 3 + main tillage treatment (A)	Autumn ploughing, 20-22 cm depth (A)
S0 + 3 + main tillage treatment (B)	Spring ploughing, 12-14 cm depth (B)
S0 + 3 + main tillage treatment (C)	No ploughing, spring harrowing, 4-6 cm depth

Experimental field A85 was established in 1989 by NMBU and is a long-term experiment (Fig. 2.4). The entire field covers an area of 1890 m^2, with individual plots covering 22,5 m^2. Plots used are: 3, 15, 27 → 12, 24, 36 → 41, 53, 65 → 43, 55, 67 – these are highlighted in Figure 2.4. There are 3 main treatments (A, B, C), with 4 repetitions, thus 12 plots. Treatments used for analysis on field A85 are always S0 + 3 (no stubble harrowing + no soil compaction) + the main treatments, which are either A, B, or C (autumn ploughing, spring ploughing, and spring harrowing, respectively) (Tab. 2.2). Every spring, 50-53 kg/daa of compound NPK fertilizer (22-3-10) is added to the soil. Fertilization is immediately followed by sowing of spring cereal crops, which are usually a rotation between barley, oats, and wheat.

2.1.2.2 – Øsaker – tillage spring and autumn (A45)

- Field: A45
- Location: Øsaker, Sarpsborg, Norway
- Coordinates: 59^{o} 19’ 12.58” N, 11^{o} 2’ 32.64” E

Table 2.3 – Overview of tillage treatments applied on field A85.

	Tillage treatment
B	Autumn & spring harrowing, 4-6 cm depth
D	Autumn ploughing 20 cm depth

Experimental field A45 was established in 1976 by the Norwegian Agricultural Extension Services south-east (NLR SørØst). Experiments only involved autumn ploughing until 1995, which is when spring harrowing and other treatments were introduced (Tab. 2.3). There are 2 main treatments (B, D), with 4 repetitions, thus 8 plots. Treatment B represents autumn & spring harrowing, while treatment D represents autumn ploughing (Tab. 2.3). Every spring, 55 kg/daa of compound NPK fertilizer (22-3-20) is added to the soil. Fertilization is immediately followed by sowing of spring cereal crops, which are usually a rotation between barley, oats, and wheat.

2.1.2.3 – Kjuus – tillage spring (Kjuus)

- Field: "Kjuus"
- Location: Årnes, Nes, Norway
- Coordinates: 60º 7' 29.89" N, 11º 29' 31.78" E

Figure 2.5 – Overview of experimental field "Kjuus". One entire row (280 m) = 1 plot. Left row treatment is spring ploughing, middle left row treatment is direct sowing, middle right row treatment is spring harrowing, and right row treatment is autumn harrowing (not used in this experiment). Photo by Kjuus (2020).

Table 2.4 – Overview of tillage treatments applied on field "Kjuus".

	Tillage treatment
1	Spring ploughing, 20 cm depth
2	Direct sowing, no tillage
3	Spring harrowing, 4 – 6 cm depth

"Kjuus" is a large-scale experimental field established in 1999 by farmer and agricultural advisor Lars Kjuus (Fig. 2.5). In a large-scale experiment like this, every plot covers a large area, in this case 280 m x 12 m = 3 360 m^2. In 2017 the width of all plots apart from the "direct sowing" plot was increased to 15 m, meaning the area covered by these plots is now 280 m x 15 m = 4200 m^2. "Kjuus" is also considered a long-term experiment. There are 3 main treatments, without repetitions. Treatment 1 is spring ploughing, treatment 2 represents direct sowing, and treatment 3 represents spring harrowing (Tab. 2.4). Every spring, 3-4 kg/daa of compound NP fertilizer (12-23) is added to the soil as an initial fertilization followed by 10 kg/daa of compound NPK fertilizer (24-3,5-6). Normal N-levels are 14-15 kg N/daa for spring cereals, and 20 kg N/daa for winter cereals. Fertilization is immediately followed by sowing of spring cereal crops, which are usually a rotation between barley, oats, and wheat.

2.2 – Sampling

Due to prolonged rainfall in the autumn of 2020, corona virus restrictions, and inaccessibility, personal soil sampling was not possible. Therefore, older samples were provided for E166, A85, and Kjuus, as well as more recently taken samples from A45. Soil samples from E166 were taken 24.04.2020 at a depth of 0 – 10 cm. Soil samples from A85 were extracted 20.09.2019 at a depth of 0 – 10 cm, but also at a depth of 10 – 20 cm. The latter depth is only used for loss on ignition and pH in a few plots from A85, due to lack of sampling material at depth 0 – 10 cm. Soil samples from "Kjuus" were extracted 01.09.2020 at a depth of 0 – 8 cm. Soil samples from A45 were extracted 30.04.2021 at a depth of 0 – 10 cm.

2.2.1 – Sampling procedure and soil pre-treatment

Since soil samples are not taken personally, the sampling procedure is provided by Lamandé (2020):

Soil samples are taken at a random location within the plots in every field. Using a shovel, soil is extracted from the desired depth. Without disturbing the soil too much, fractions are removed from the shovel and put into a 2-litre cardboard carton. The carton is then marked with the plot number and sampling depth. The soil samples are left to air dry at room temperature for at least one week before various analyses may begin.

2.3 – Dry matter & soil organic matter content (loss on ignition)

As explained in the introduction, soil organic matter is closely related to soil aggregate stability. Therefore, soil organic matter measurements are included to see the correlation between soil organic matter and soil aggregate stability. Loss on ignition is a common procedure used to determine soil organic matter.

Figure 2.6 – (a) Weighing of individual crucibles with soil before (b) placing them in a drying cabinet overnight at 105 °C. (c) Crucibles containing the dried soil are placed in the calcination furnace for 3 hours at 550 °C. (d) Soil after calcination. Photos: Thomas J. Brown (2021).

Porcelain crucibles (approx. 20 ml) are weighed and labelled with an individual number. Then the crucibles are weighed once more, this time containing 3 – 5 grams of soil from their designated plots (Fig. 2.6 a). The next step is to place the crucibles in a drying cabinet at a temperature of 105 °C (+/- 5 °C) overnight (Fig. 2.6 b). The crucibles are cooled before weighing and the dry matter content is calculated. To determine loss on ignition, the crucibles with dry soil are placed in a calcination furnace where the soil is left to calcinate at a temperature of 550 °C for 3 hours (Fig. 2.6 c). Once the calcination furnace has cooled down sufficiently, the crucibles are removed (Fig. 2.6 d), weighed once more, and loss on ignition is calculated.

Calculations needed to find organic matter content (g/100g):

$$Loss\ on\ ignition\ \left(\frac{g}{100g}\right) = \left(\frac{m_2 - m_3\ (g)}{m_2 - m_1\ (100g)}\right)$$

Where: m_1 = weight of crucible

m_2 = weight of crucible and soil sample after drying

m_3 = weight of crucible and soil sample after calcination

Loss on ignition by itself does not give an accurate image of organic matter content (g/100g) in mineral soils. This is because clay contains chemically bound water that does not evaporate before temperatures reach 150 °C or higher. A correction is needed and is dependent on clay content (%) in the given soil:

- E166: Silt loam, 10 – 24 % clay – correction: 2 g/100 g
- A85: Silty clay loam, 25 – 39 % clay – correction: 2.5 g /100 g
- A45: Clay, 40 – 59 % clay – correction: 3.5 g/100 g
- Kjuus: Sandy loam, 10 – 24 % clay – correction: 2 g/100 g

$$OM\ (g/100g) = Loss\ on\ ignition\ (g/100g) - Correction\ (g/100g)$$

The procedure used can also be found in *JORD 200 Field and Laboratory Methods* (Krogstad & Børresen, 2015).

2.4 – Acidity

The soil pH is measured in H_2O with a soil solution ratio of 1:2:5. 10 ml of soil from each plot is transferred into plastic containers using a 10 ml measuring spoon (Fig. 2.7 a). 25 ml of deionized water is added to each beaker, the lid of the beakers closed, and all beakers are then shaken by hand until the soil is properly mixed with the water (Fig. 2.7 b). The beakers are left until the next day. Before beginning pH measurements, the following day, the samples are shaken once more, and left to precipitate for 15 mins. The pH meter is calibrated with two buffer solutions, one buffer with a pH of 4.00 and one with pH 7.00 (6.88). After 15 mins, the electrode is placed in a beaker, suspending it so that the glass membrane and the salt bridge remain just above the precipitated soil (Fig. 2.7 c). When the pH instrument shows a stable pH-value, the reading is logged in an excel sheet.

The procedure used can also be found in *JORD 200 Field and Laboratory Methods* (Krogstad & Børresen, 2015).

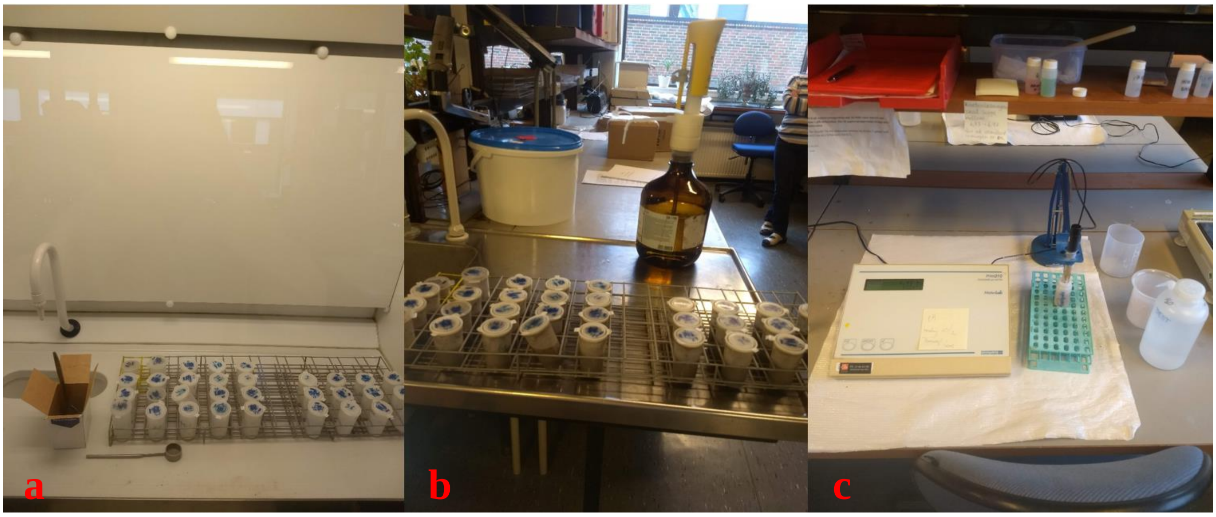

Figure 2.7 – (a) 10 ml of soil transferred to a specific beaker. (b) Beakers filled with 25 ml of deionized water. (c) Electrode suspended in a beaker and a pH reading is given on the pH-instrument. Photos: Thomas J. Brown (2021).

2.5 – Fraction 0.6 – 6 mm (from aggregate size distribution)

When the soil is finished air drying, it needs to be weighed and sieved prior to aggregate stability measurements. Through mechanical sieving, various fractions are found and known as aggregate size distribution. Mechanical sieving provides us with information about the quality of a seedbed. Many coarse lumps or too much fine material is not ideal, and approximately 50 % of the aggregates should range between 0.5 – 5 mm (Børresen & Lamandé, 2019). Since the sieves only provide fractions 6-2 mm and 2-0.6 mm, adjustment is made so that approximately 50 % of aggregates should range between 0.6 – 6 mm. The aggregate size distribution from all sieving fractions can be found in appendix 1.

Firstly, weighing of soil samples takes place. A scale with an accuracy down to one decimal point is used. Next, an empty bowl is placed on the scale and the tare button is pressed so that the displayed weight is zero. Then the air-dried soil within the 2-litre carton is emptied into the bowl, stones are removed, and the weight is logged (Fig. 2.8).

Secondly, sieving of the weighed soil is performed. The bowl containing the soil sample is tipped into a motorized sieve (Fig. 2.9). There are 5 compartments within the sieve, each with a different mesh-diameter, thus letting through different sized aggregates. The sieve works by applying a rapid back and forth motion, shaking the soil so that the different sized aggregates sieve through the variously sized mesh. Before commencing the sieving process, a ventilator fan is started to suck away excess dust. To initiate sieving, the start button is pressed (Fig. 2.10). Sieving lasts for 3 minutes. After sieving, the first sieve compartment contains aggregates > 20 mm, the second compartment contains aggregates between 20 – 6 mm, the third compartment contains aggregates between 6 – 2 mm, the fourth compartment contains aggregates between 2 – 0.6 mm, and finally the fifth compartment contains aggregates < 0.6 mm. All fractions are now weighed individually. The individual fractions are then calculated as the percentage of the total sample-weight.

Figure 2.8 – Weighing of soil sample. Photo: Thomas J. Brown (2021).

Figure 2.9 – Motorized sieve. Photo: Thomas J. Brown (2021).

Figure 2.10 – Start button motorized sieve. Photo: Thomas J. Brown (2021).

Calculations needed to find g/100 g of soil aggregates ranging between 0.6 – 6 mm:

$$Weight\ of\ fraction\ (g/100g) = \left(\frac{weight\ of fraction\ (g)}{total\ weight\ of\ sample\ (100g)}\right)$$

$$Weight\ of\ fraction\ 0.6 - 6\ mm\ \left(\frac{g}{100g}\right) = fraction\ 2 - 6\ mm + fraction\ 2 - 0.6\ mm$$

In order to find the mean weight of all fractions within the 0.6 – 6 mm interval for each treatment (T), all samples from one treatment need to be included.

2.6 – Rainfall simulator

Figure 2.11 – Weighing 20g of soil per parallel. Photo: Thomas J. Brown (2021).

Figure 2.12 – Weighing of filter paper. Photo: Thomas J. Brown (2021).

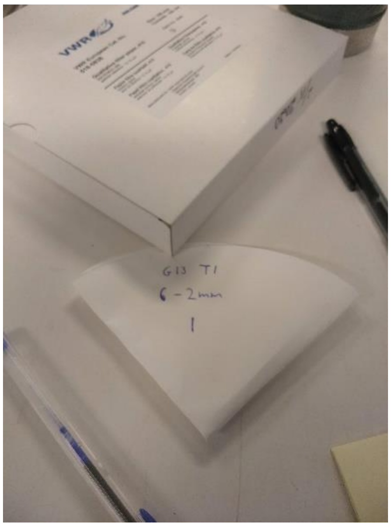

Figure 2.13 – Folded filter paper with plot number (G), treatment number (T), parallel number, and fraction. Photo: Thomas J. Brown (2021).

Aggregates ranging between 6 – 2 mm and 2 – 0.6 mm are the fractions chosen to determine aggregate stability using the rainfall simulator. For all field experiment plots, each aggregate stability measurement is performed twice so that there is a parallel. Thus, there are 4 measurements per plot in total (2 for fraction 6 – 2 mm & 2 for fraction 2 – 0.6 mm).

First, using a scale with an accuracy down to two decimal points, 20 g of soil is weighed per parallel (Fig. 2.11). In preparation for drying the aggregates at the end of the process, filter paper is weighed, folded into a funnel shape, and marked with plot number, treatment number, parallel number, and aggregate fraction size (Fig. 2.12 & 2.13). Then the 20 g of soil per parallel is tipped into respective pre-wetted sieves and left to soak for 5 mins before

Figure 2.14 – 4 marked and pre-wetted sieves. Photo: Thomas J. Brown (2021).

Figure 2.15 – The rainfall simulator with 4 sieves placed on the rotating platform. Photo: Thomas J. Brown (2021).

Figure 2.16 – Barometer set at 1.5 bar units. Photo: Thomas J. Brown (2021).

initiating the rainfall simulator (Fig. 2.14). Each sieve is marked 1, 2, 3, 4. Sieve 1 contains the 20 g of soil corresponding to parallel 1 fraction 6 – 2 mm, sieve 2 contains the 20 g of soil corresponding to parallel 2 fraction 6 – 2 mm, sieve 3 contains the 20 g of soil corresponding to parallel 1 fraction 2 – 0.6 mm, and sieve 4 contains the 20 g of soil corresponding to parallel 2 fraction 2 – 0.6 mm. The reason why the soil is pre-wetted by capillary forces is to avoid abrupt disintegration of soil aggregates due to air slaking. This way, disintegration of soil aggregates can almost only be attributed to the battering force of rain drops.

Immediately after the aggregates have been soaked for 5 mins, the sieves are placed in the rainfall simulator (Fig. 2.15). For the rainfall to be evenly distributed, the simulator needs to be rotating, therefore the rotation switch is turned on before the “rain”. The rainfall simulation is performed for 3mins with a water pressure of 1.5 bar units (Fig. 2.16).

After 3mins, the aggregates remaining in the sieves are washed into corresponding bowls marked 1, 2, 3, and 4, respectively (Fig. 2.17). Here they are left to sediment for 6mins.

Immediately after 6mins, the excess water in the bowls is drained. To avoid losing the precipitated soil, some water is left in the bowls along with the soil. The little water that is left + the soil contents in the bowls are then rinsed into funnels containing the funnel-folded filter paper and left to air-dry for 7 days (Fig. 2.18 & 2.19). When 7 days have passed, the desiccated filter paper with soil is weighed and the result is logged in an excel sheet (Fig. 2.20).

Figure 2.17 – Soil left to precipitate for 6mins in ceramic bowls. Photo: Thomas Brown (2021).

Figure 2.18 – Excess water and precipitated soil are rinsed into funnels with filter paper. Photo: Thomas Brown (2021).

Figure 2.19 – Soil left to air-dry in funnels for 7 days. Photo: Thomas Brown (2021).

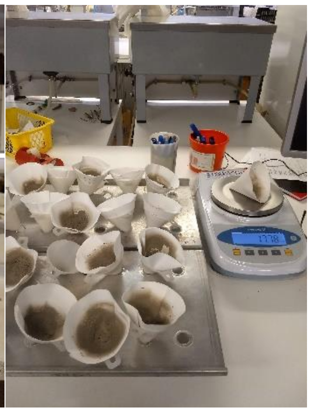

Figure 2.20 – Filter paper containing dry soil is weighed and results logged. Photo: Thomas Brown (2021).

For easier comparison with SLAKES, an aggregate stability index is used for the rainfall simulator, called Rainfall Stability Index (RSI). RSI represents the percentage of soil lost due erosion by the rainfall simulator, in other words the loss of aggregate stability. A soil loss of around 10 % (RSI = 10) is considered as excellent aggregate stability, 20 % (RSI = 20) loss as good, 30 % (RSI = 30) loss as moderate, more than 30 % (RSI > 40) and especially more than 40 % (RSI > 40) loss is considered as poor aggregate stability (Børresen, 2021[1]).

Calculation needed to find the percentage of aggregate stability that is lost during the rainfall simulator:

$$Rainfall\ Stability\ Index = 100 - \left(\left(\frac{Dry\ weight\ soil\ after\ rain\ (g)}{Dry\ weight\ soil\ before\ rain\ (g)}\right) * 100\right) \quad (1)$$

2.7 – SLAKES

In contrast to what is common for the rainfall simulator, aggregates need to have a size between 2 – 15 mm to determine aggregate stability using SLAKES. Therefore, the only fraction used from the aggregate size distribution is the one containing aggregates ranging between 6 – 2 mm in size. For each experimental plot, 3 aggregates are used. Thus, there are 3 parallels/measurements per plot.

First, the SLAKES application is used on a Motorola Moto G5 Plus smart phone with a 12 MP main camera. All procedures described here follow the step-by-step instructions provided by the application.

Figure 2.21 – 3 aggregates per petri dish for each plot. Photo: Thomas J. Brown (2021).

For each plot, 3 similarly sized aggregates are picked at random from the aggregates between 6 – 2 mm. These 3 aggregates are then placed in a petri dish without water, with a corresponding label representing which plot and treatment they belong to (Fig. 2.21).

[1] Trond Børresen, personal communication.

Next, an experimental setup is made from two laboratory stands with clamps (Fig. 2.22). The stands are placed with the right distance between each other to be able to suspend the smartphone. The clamps are attached at the correct height for the smartphone to lie level, and for the 100 mm petri dish underneath to exactly fit within the image obtained by the smartphone. To provide contrast between the soil aggregates and the background, a white piece of A4 paper is positioned beneath the petri dish. Lighting includes overhead fluorescent laboratory lighting, but for proper contrast to be achieved, extra lighting is also necessary. Two LED overhead lamps are installed directly above the smartphone. Without suitable lighting SLAKES tends to mistake soil peds for shadows or fails to distinguish between soil peds and the background.

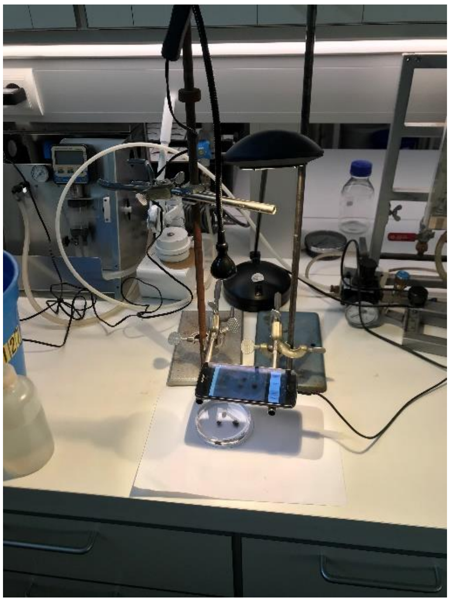

Figure 2.22 – Experimental setup displaying aggregates submerged in water in a petri dish. Photo: Thomas J. Brown (2021).

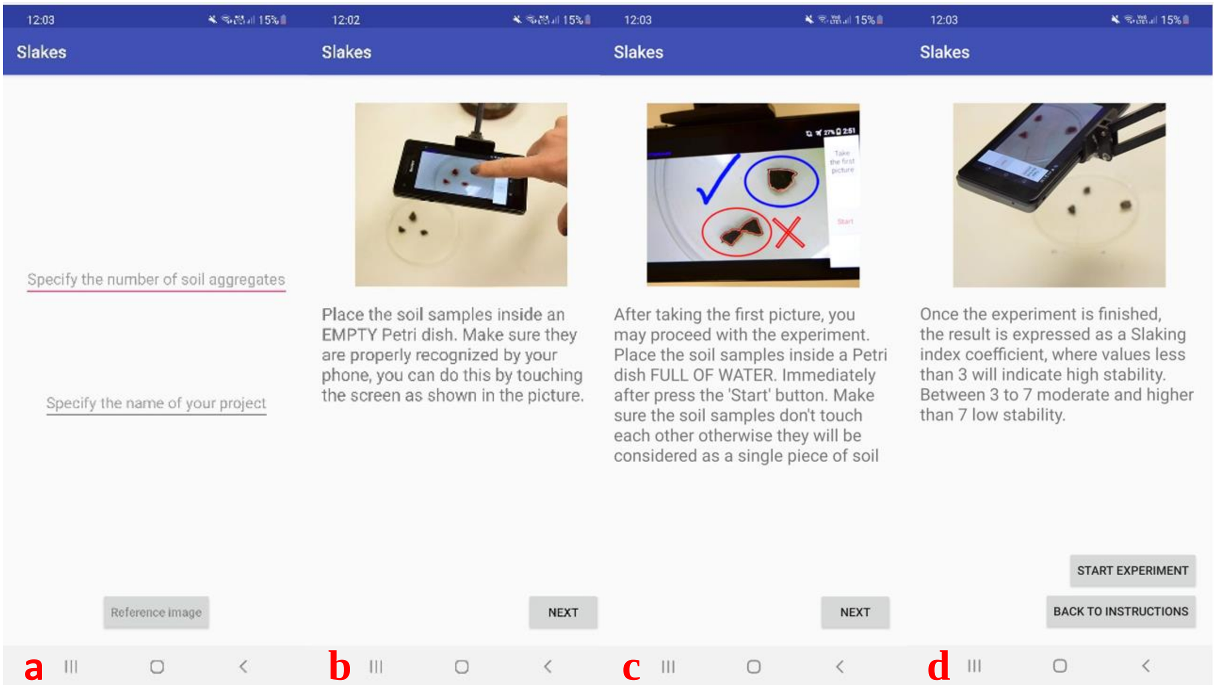

Figure 2.23 – Instructions provided by the smartphone app SLAKES. (A) Number of soil aggregates present in the petri dish is specified along with the name of the project. (B) A reference image is taken of the soil aggregates in an empty petri dish. (C) Soil aggregates are simultaneously submerged in a petri dish filled with water and start button is pressed. (D) Slaking Index coefficient a is shown on the smartphone screen after 10 mins of slaking (Fajardo & McBratney, 2019).

Following the instructions provided by the app, the number of soil aggregates in the petri dish is specified (Fig. 2.23 a), along with the name of the project, which in this case is the plot number and treatment number.

A petri dish containing 3 soil aggregates (and no water) is then placed on the white paper below the smartphone. By touching the smartphone screen red rings occur around the soil peds if there is adequate contrast. When sure that the aggregates are in focus, the button "reference image" is pressed and a reference image is taken (Fig. 2.23 b). This is to measure the initial size of the aggregates prior to water submergence.

Next, the dry petri dish containing the 3 aggregates is removed from the white sheet of paper. Another petri dish is filled to the brim with water and placed on the white sheet of paper. The 3 desiccated aggregates are then submerged as simultaneously as possible into the petri dish full of water, and immediately the start button in the app is pressed (Fig. 2.23 c). It is important to make sure that the aggregates are similarly arranged in the petri dish full of water as they were in the reference image. This is because the app is measuring the area change of the initial soil ped prior to water submergence, compared to after submergence – the surface area of the soil peds may be different depending on what side they lie on, due to their non-uniformity. After the start button is pressed, it takes 10 mins before measurements are complete.

When 10 mins have passed, the smartphone screen displays a number with one decimal point (Fig. 2.23 d). This number is known as coefficient *a* (Slaking Index (SI) coefficient), or the predicted aggregate stability. Coefficient *a* is the predicted maximum slaking value as an average of all 3 soil aggregates. A Slaking Index (SI)-value is an observed measurement of the aggregate stability in the soil aggregates. A coefficient *a* and SI-value of 1-3 is considered as good aggregate stability, 3-7 is considered as moderate aggregate stability, and > 7 is considered as poor aggregate stability.

An additional file is automatically downloaded to the smartphone's internal memory after the 10 min calculation. The file is an Excel sheet showing slaking values and area changes (disaggregation) for each soil ped over the 10 min (*t*) slaking interval. When measuring surface area change, SLAKES takes images in an exponential-like time interval; the first 4 images are taken in the first 4s, whereas the last 4 images are taken in the last 320s. Along with coefficient *a*, the excel file also reveals slaking coefficients *b* and *c* represented as the arithmetic mean of the 3 soil aggregates, as well as the standard deviation for coefficient *a*. Coefficient *b* illustrates the initial slaking of aggregates, while coefficient c is the continuous rate of slaking. An important SI-value to notice from the excel sheet is SI-600, which is the observed SI-value after 600s (10 mins), or the observed aggregate stability. The SI is modelled by the Gompertz equation (Gompertz, 1825):

$$SI = ae^{\{-be^{[-clog(t)]}\}} \quad \text{where } e \text{ is the Euler's number} \tag{2}$$

Originally, Benjamin Gompertz (1825) developed the Gompertz function in order to describe human mortality rate, but in more recent times the function has been used to describe growth in plants and animals and bacteria and cancer cells (Tjørve & Tjørve, 2017). More recently the Gompertz function has been used to describe the spread of SARS-CoV-2 (Ohnishi et al., 2020).

In the text file saved on the smartphone after the 10-minute slaking interval, coefficients *a*, *b*, and *c* are displayed as the arithmetic mean of the three soil peds (Flynn et al., 2019). Therefore, Excel data analysis and Excel solver are used to find the values of coefficients *a*, *b*, and *c* for each soil aggregate. Calculations needed to find SI-600 are also given.

To find coefficient *a*, *b*, and *c* for each soil ped, the Gompertz equation (Gompertz, 1825) is fitted to the observed slaking values, represented here as f(t):

$$SI_t = f(t) \tag{3}$$

Calculation of SI-600 is the area change at t = 600 compared to t = 0 (reference image) (SI-600 is also given at t = 600):

$$SI - 600 = \frac{A_{600} - A_0}{A_0} \tag{4}$$

Although the most important findings SLAKES provides are related to coefficient *a* (predicted aggregate stability) and SI-600 (observed aggregate stability), the SLAKES app should explain what coefficients *b* and *c* represent. For example: "What do high coefficient *b* and *c* values mean?" Fajardo et al. (2016) offer a short, but not easily understandable explanation: Coefficient *b* is the displacement along the x-axis, which can be interpreted as the initial time of fast slaking, and coefficient *c* can be interpreted as the rate of disaggregation (easier to comprehend). A more detailed explanation of coefficients *b* and *c* is offered and assisted by Figure 2.24. Coefficient *b* has a high value in Figure 2.24 (coefficient *b* = 446) because the initial slaking suddenly jumps from a low Slaking Index to a much higher Slaking Index rather than continuing a steady slaking course. From second 25 to second 26, the Slaking Index jumps from 0.15 – 0.66, which is due to a sudden area change. The likely explanation for such an area change is an internal explosion within the aggregate.

As explained in the introduction, an explosion like this is due to water forcing its way into the aggregate, building up pressure on the entrapped air, eventually rupturing and dispersing the aggregate. This sudden area change also results in a high coefficient *c* value, or slaking rate, because coefficient *c* is the arithmetic mean of the of the difference between each SI-value – e.g., second 1 to second 600 (((SI-2 – SI-1) + (SI-3 – SI-2) + ... + (SI-600 – SI-480))/54).

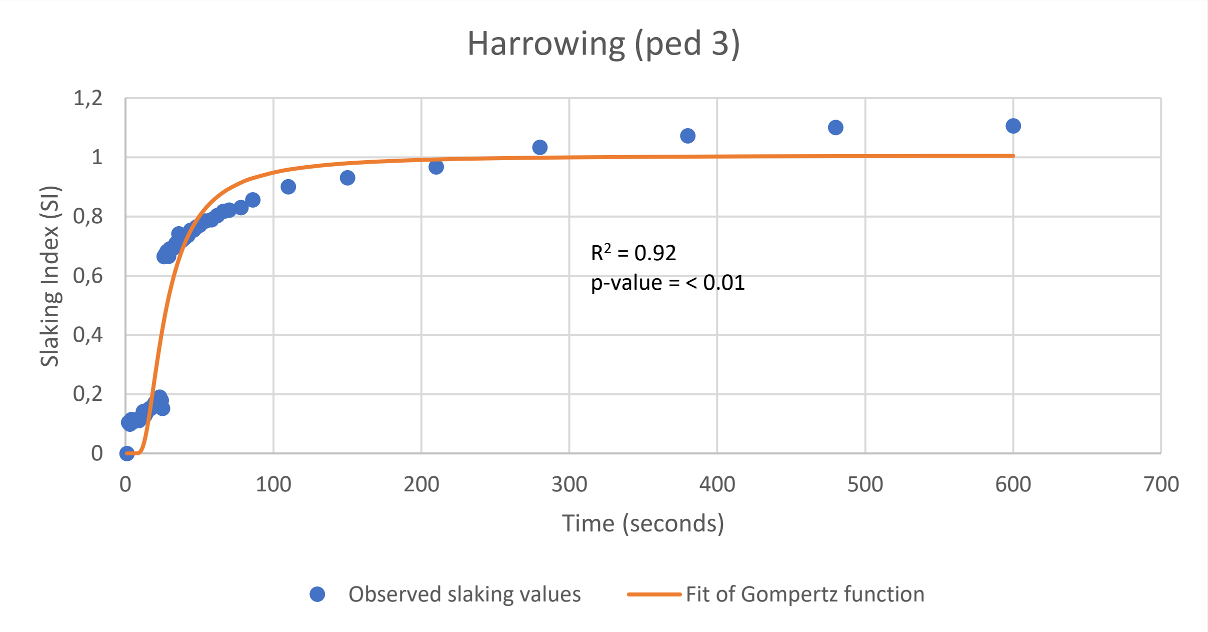

Figure 2.24 – An example-aggregate from the harrowing treatment in experimental field Kjuus. Observed jump in SI-value from second 25 (0.15) to second 26 (0.66).

2.8 – Statistical analysis

All statistical analysis including one-way ANOVA, paired t-test, regression analysis and correlation analysis are produced using Microsoft Excel version 2110. Statistical analysis is performed with a significance level of p = 0.05. Lower-case letters are used to represent the significance between treatments; different letters mean treatment results are significantly different from each other. Field Kjuus only provides one repetition per treatment and thus cannot yield a p-value.

3 – Results

The thesis focuses on comparing the results from the rainfall simulator and SLAKES. The results acquired from the organic matter- and pH analysis are used to see if there is a correlation between organic matter/pH and aggregate stability. The pH value range is very small within each field, so no real correlation is expected between aggregate stability and pH. Increasing the pH up to a certain point (approx. 7.5) has been found to increase aggregate stability (Getahun et al., 2021).

3.1 – Organic matter and acidity

Table 3.1 – Organic matter content and pH for different treatments on the four test sites. Different letters indicate statistically significant differences between treatments within an experimental.

Field	Treatment	OM (g/100g)	pH
E166	Control (T1)	4.38 a	6.54 ac
E166	Mineral Fertilizer (T3)	4.81 a	6.28 bc
E166	Livestock Manure (T5)	5.01 a	6.65 a
E166	Digestate – Food Waste (T7)	5.03 a	6.49 abc
E166	Digestate – Sludge + Food Waste (T9)	5.20 a	6.40 bc
A85	Autumn ploughing (A)	4.60 a	5.71 a
A85	Spring ploughing (B)	4.61 a	5.64 a
A85	Spring harrowing (C)	4.79 a	5.63 a
A45	Autumn & Spring harrowing (B)	4.28 a	6.45 a
A45	Autumn ploughing (D)	3.08 b	6.59 a
Kjuus	Spring ploughing (T1)	3.30 NA	6.30 NA
Kjuus	Direct sowing (T2)	4.30 NA	6.40 NA
Kjuus	Spring harrowing (T3)	4.00 NA	6.30 NA

Table 3.1 presents the average organic matter content (%) and pH between the different treatments on each experimental field.

For fields E166 and A85 there are no significant differences between treatments in organic matter content ($p > 0.05$). There is however a clear trend, for field E166 there is a higher average organic matter content for the organic fertilizer treatments than for treatment 1 (control) and treatment 3 (mineral fertilizer). For field A85, the trend is less clear, but there is a higher average organic matter content where there are reduced tillage treatments. Field A45 portrays a significantly higher organic matter content ($p < 0.05$) for autumn & spring harrowing (treatment B) than for autumn ploughing (treatment D). On average, direct sowing and spring harrowing (treatments T2 & T3) in field Kjuus have higher organic matter content than the spring ploughing treatment.

For field A85 and A45 there are no significant differences between treatments for pH ($p > 0.05$). In field E166 there are significant differences in pH-value: Treatment 3 (mineral fertilizer) has significantly lower pH than treatment 5 (animal manure), and treatment 5 (animal manure) has significantly lower pH than treatment 9 (digestate – sludge + food waste).

3.2 – Fraction 0.6 – 6 mm (from aggregate size distribution)

Table 3.2 – Average relative weight (g/100g) of fraction 0.6 – 6 mm in relation total weight of all fractions for different treatments on the four test sites. Different letters indicate statistically significant differences between treatments within an

Field	Treatment	Mean weight of fraction 0.6 – 6 mm (g/100g)
E166	Control (T1)	45.5 abc
E166	Mineral Fertilizer (T3)	47.5 a
E166	Livestock Manure (T5)	46.3 ab
E166	Digestate – Food Waste (T7)	43.3 c
E166	Digestate – Sludge + Food Waste (T9)	42.8 c
A85	Autumn ploughing (A)	62.6 a
A85	Spring ploughing (B)	48.6 b
A85	Spring harrowing (C)	58.1 a
A45	Autumn & Spring harrowing (B)	43.8 a
A45	Autumn ploughing (D)	46.7 b
Kjuus	Spring ploughing (T1)	26.3 NA
Kjuus	Direct sowing (T2)	26.5 NA
Kjuus	Spring harrowing (T3)	23.3 NA

For each treatment in all fields (E166, A85, A45, and Kjuus): The average weight of fraction 0.6 – 6 mm is given as the percentage of the average total weight of all fractions (Tab 3.2).

Field E166: Treatment 3 (mineral fertilizer) exhibits the highest mean percentage of soil in fraction 0.6 – 6 mm (47.5 %), while treatment 9 (digestate sludge + food waste) displays the lowest percentage (42.8 %). Treatment 3 (mineral fertilizer) and Treatment 5 (animal manure) are significantly different from treatment 7 (digestate food waste) and treatment 9 (digestate sludge + food waste), $p < 0.05$.

Field A85: Treatment A (autumn ploughing) exhibits the highest mean percentage of soil in fraction 0.6 – 6 mm (62.6 %), while treatment B (spring ploughing) displays the lowest percentage (48.6 %). Treatment A (autumn ploughing) and treatment C (spring harrowing) are not significantly different from each other ($p > 0.05$), however, they are both significantly different from treatment B (spring ploughing), $p < 0.05$.

Field A45: Treatment C (autumn ploughing) exhibits the highest mean percentage of soil in fraction 0.6 – 6 mm (46.73 %), while treatment A (spring harrowing) displays the lowest percentage (43.79 %). There is a significant difference between these two treatments ($p < 0.05$).

Field Kjuus: Treatment T1 (spring ploughing) exhibits the highest mean percentage of soil in fraction 0.6 – 6 mm (25.67 %), while treatment T3 (spring harrowing) displays the lowest percentage (19.38 %).

3.3 – Aggregate Stability

3.3.1 – Organic waste fertilizer experiment (E166 – Digestate)

3.3.1.1 – Rainfall simulator

One-way ANOVA revealed a non-significant p-value for fraction 6 – 2 mm ($p > 0.05$), and a significant p-value for fraction 2 – 0.6 mm ($p < 0.05$), the treatment differences for each fraction can be seen in Figures 3.1 & 3.2. High Rainfall Stability Index (RSI)-values correspond to increased loss of soil during rainfall simulation and thus lower aggregate stability and vice versa.

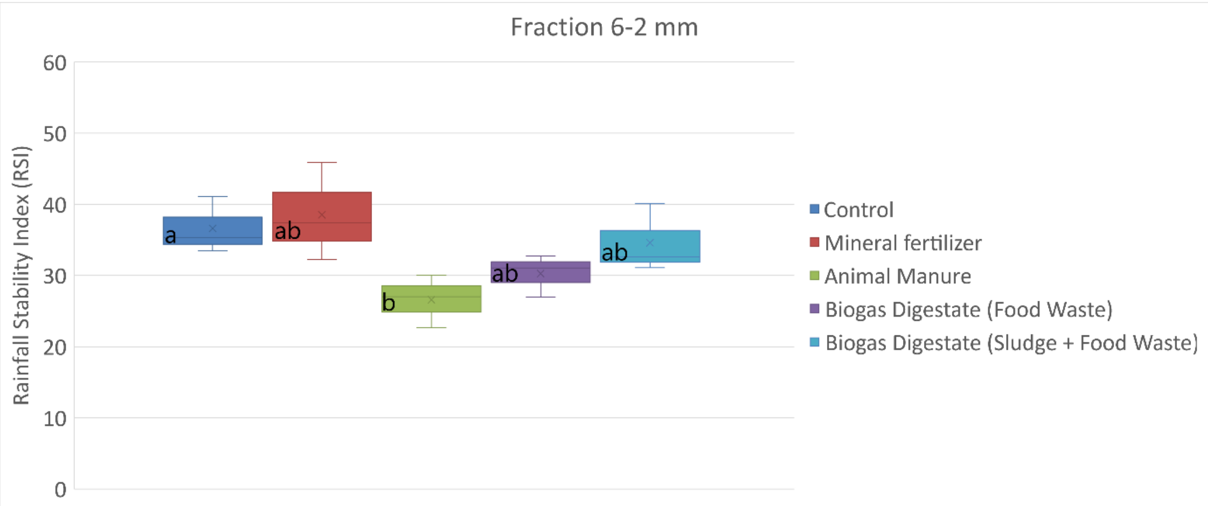

Figure 3.1 - Box plots including standard deviations and significance showing the Rainfall Stability Index (RSI) during rainfall simulation for each treatment for fraction 6 – 2 mm.

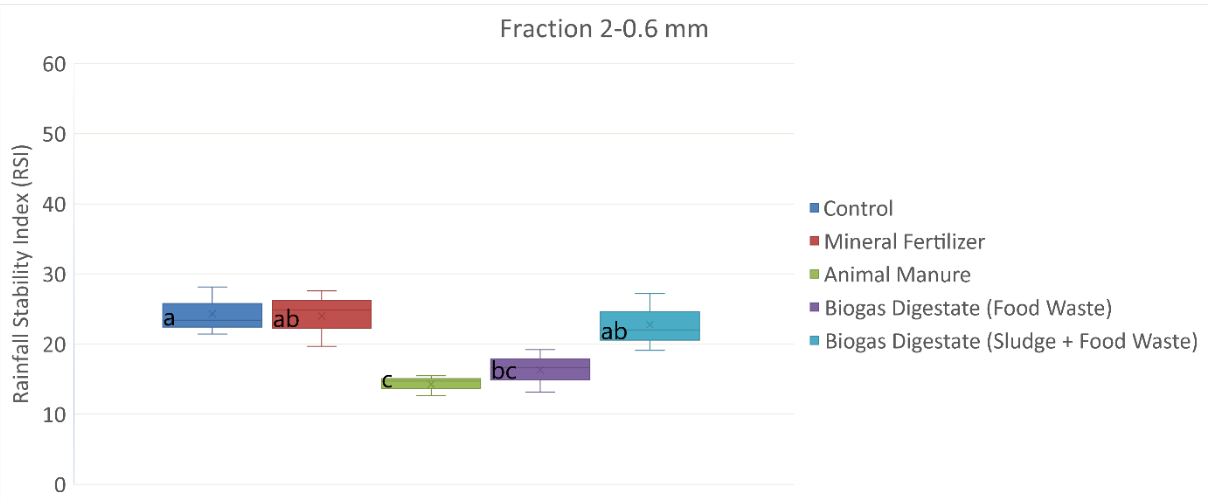

Figure 3.2 - Box plots including standard deviations and significance showing the Rainfall Stability Index (RSI) for each treatment for fraction 2 – 0.6 mm.

Box plots for fraction 6 – 2 mm and 2 – 0.6 mm are also made to show the differences in Rainfall Stability Index (RSI) between treatments (Fig. 3.1 & 3.2). For both fractions, treatment 1 (control) and treatment 3 (mineral fertilizer) have the lowest aggregate stability (losing most soil during rainfall simulation). The organic fertilizer treatments (5, 7, 9) maintain a higher aggregate stability (losing less soil during rainfall simulation). However, treatment 9 (digestate sludge and food waste) does not in any of the t-test comparisons have statistically better aggregate stability than treatments 1 and 3 (control & mineral fertilizer). For fraction 2 – 0.6 mm there are significant differences between treatment 1 (control) and treatments 5 and 7 (animal manure & digestate food waste). For the same fraction there is also

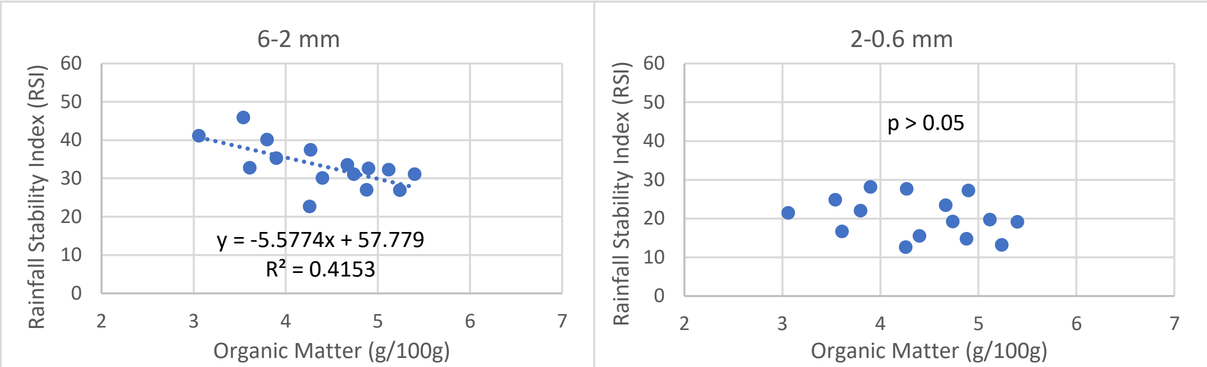

Figure 3.3 – Linear regression statistics showing the correlation between the Rainfall Stability Index (RSI) and organic matter content in the soil. The chart displays fractions 6 – 2 mm and 2 – 0.6 mm.

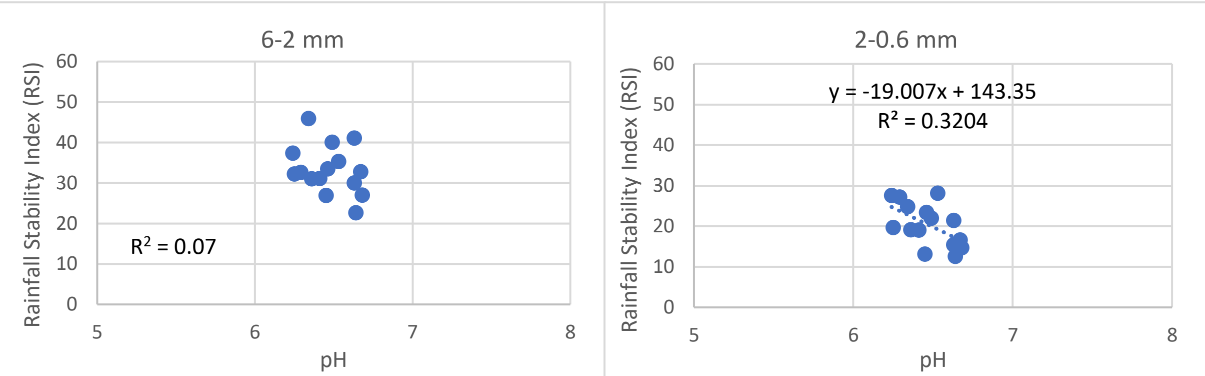

Figure 3.4 – Linear regression statistics showing the correlation between the Rainfall Stability Index (RSI) and pH in the soil. The chart displays fractions 6 – 2 mm and 2 – 0.6 mm.

significant difference between treatment 3 (mineral fertilizer) and treatment 5 (animal manure). In fraction 6 – 2 mm there is only statistical significance between treatment 1 (control) and treatment 5 (animal manure).

Linear regression statistics are created to reveal if there is a correlation between the RSI and organic matter content (g/100g) and pH (Fig. 3.3 & 3.4).

There is a moderate but significant negative correlation between the RSI and organic matter content in fraction 6 – 2 mm, with an R^2-value of 0.42 and a $p < 0.05$ (Fig. 3.3) However in fraction 2 – 0.6 mm there is a much weaker negative correlation, with an R^2-value of 0.07 and a $p > 0.05$ (not significant).

When it comes to the correlation between RSI and pH, there is a weak negative correlation in fraction 6 – 2 mm ($R^2 = 0.09$), but the correlation is not significant ($p > 0.05$). In fraction 2 – 0.6 mm however, the negative correlation is stronger ($R^2 = 0.32$) and significant ($p < 0.05$).

3.3.1.2 – SLAKES

One-way ANOVA revealed a $p > 0.05$ for coefficient *a* (not significant), and a $p > 0.05$ for SI-600 (not significant), the treatment differences for both coefficient *a* & SI-600 can be seen in Figures 3.5 & 3.6. High SI-values correspond to increased aggregate dispersion and thus lower aggregate stability and vice versa.

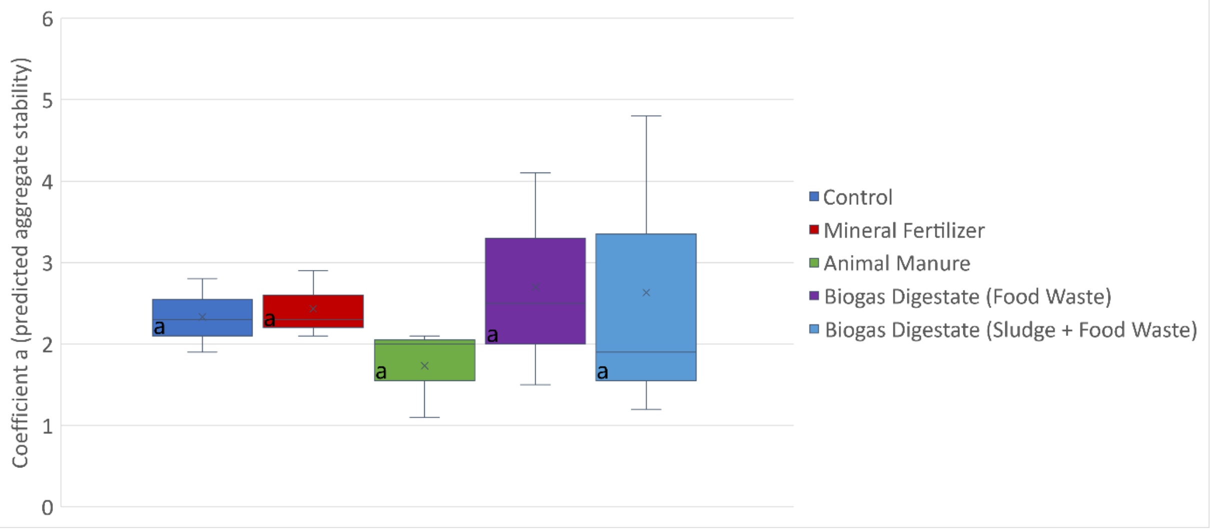

Figure 3.5 – Box plots including standard deviations and significance showing coefficient a-values for each treatment.

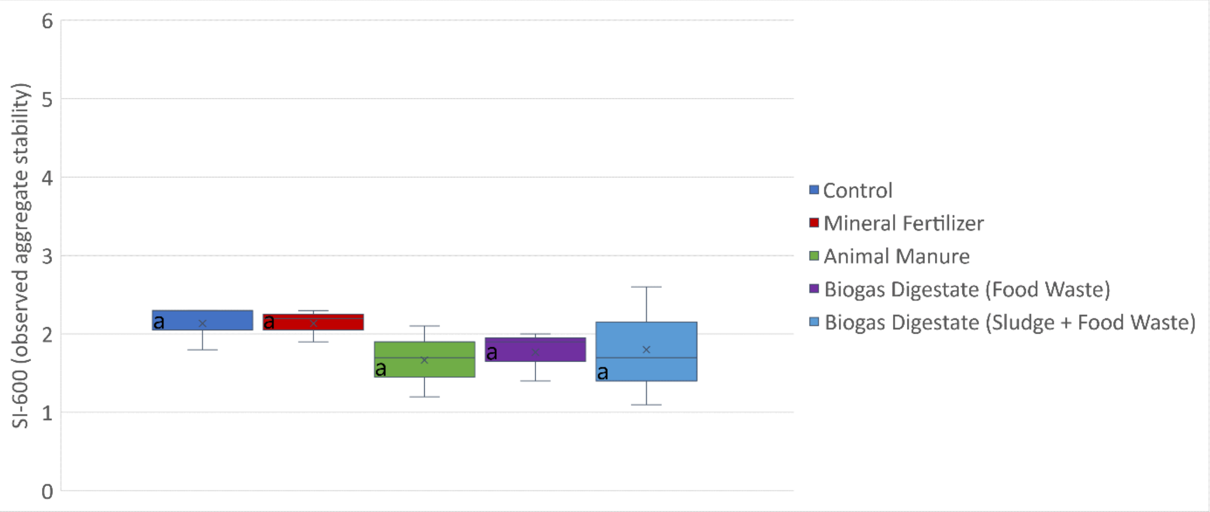

Figure 3.6 – Box plots including standard deviations and significance showing SI-600-values for each treatment.

Box plots for both coefficient *a* and SI-600 are also made to show the differences between treatments (Fig. 3.5 & 3.6). On average, SI-600 suggests that treatment 1 (control) and treatment 3 (mineral fertilizer) have the lowest aggregate stability (aggregates dispersing the most during slaking), while the organic fertilizers maintain a higher aggregate stability (aggregates dispersing the least during slaking) (Fig. 3.6). On the other hand, coefficient *a* averages suggest there are no real differences in aggregate stability between treatments (Fig. 3.5). T-tests comparing treatments confirm that there are no significant differences between treatments for both SI-600 and coefficient *a* ($p > 0.05$).

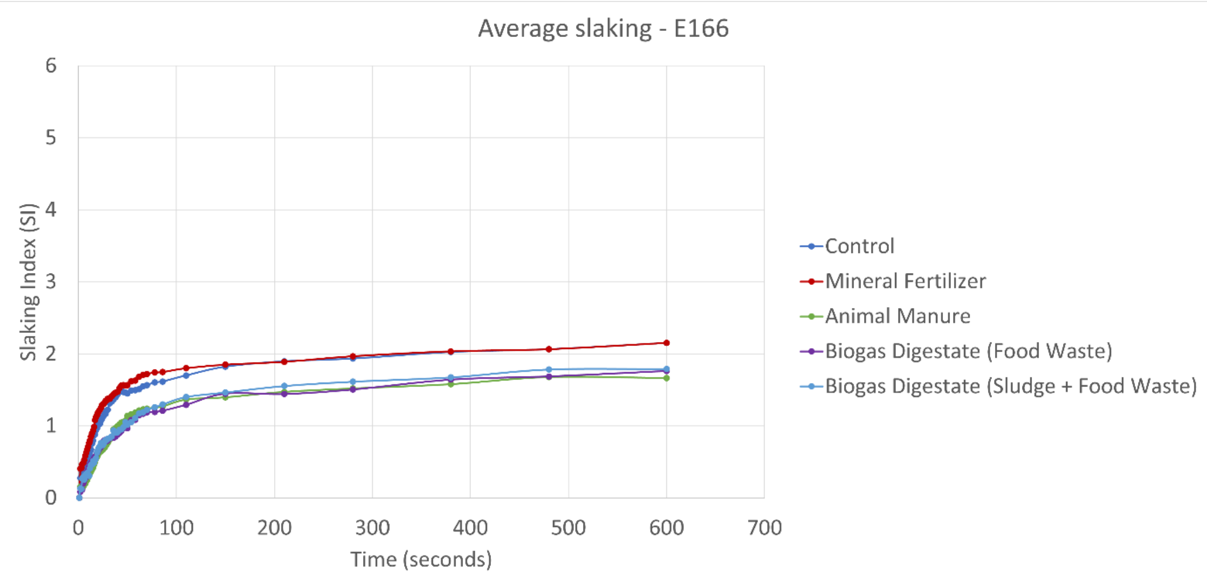

Figure 3.7 – Average slaking values for each treatment. Each data point is the mean slaking value of 9 soil aggregates at a particular time (t).

Although coefficient *a* and SI-600 are not able to display significant differences between treatments, the average SI-values over the 600 second time interval in Figure 3.7 display an interesting trend. The mean SI-values from 54 image observations per treatment reveal that treatment 1 (control) and treatment 3 (mineral fertilizer) on average have higher SI-values and thus lower aggregate stability than the organic fertilizer treatments.

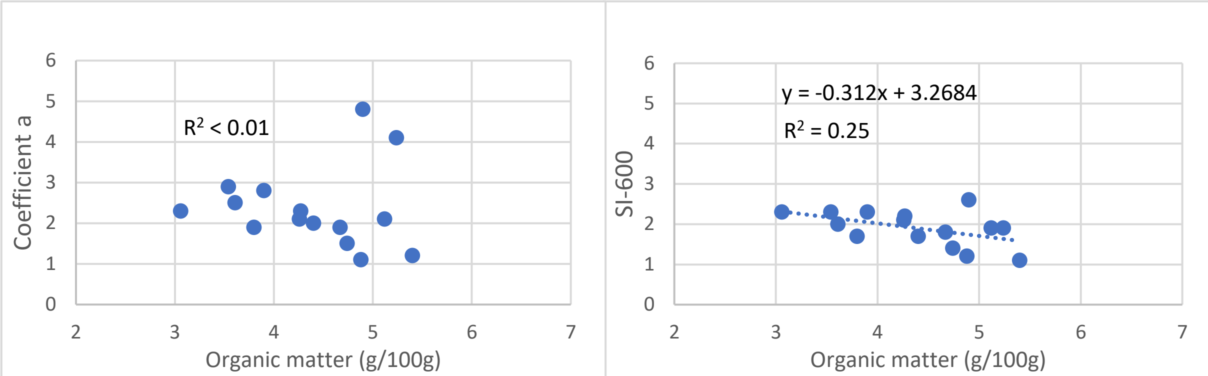

Figure 3.8 - Linear regression statistics showing the correlation between coefficient a & SI-600 and organic matter content in the soil.

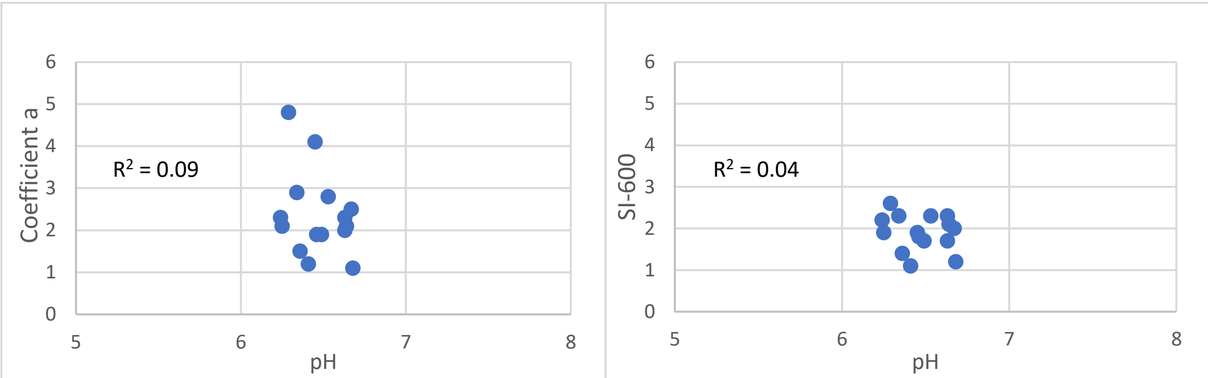

Figure 3.9 - Linear regression statistics showing the correlation between coefficient a & SI-600 and pH in the soil.

Linear regression statistics are created to reveal if there is a correlation between coefficient *a* & SI-600 and organic matter content (g/100g) & pH (Fig. 3.8 & 3.9).

There is a weak but significant correlation between SI-600 and organic matter content, with an R^2-value of 0.25 and a $p = 0.05$ (Fig. 3.8) However, for coefficient *a* there is no correlation, with an R^2-value of < 0.01 and a $p > 0.05$ (not significant).

When it comes to the correlation between coefficient *a* and pH, there is a weak correlation ($R^2 = 0.09$), but the correlation is not significant ($p > 0.05$). For SI-600 the correlation is even weaker ($R^2 = 0.04$) and not significant ($p > 0.05$).

3.3.1.3 – Comparison of rainfall simulator & SLAKES

To directly compare the rainfall simulator to SLAKES; values achieved from the rainfall simulator (6-2 mm) are plotted against the natural log-values achieved from SLAKES (SI-600). This leads to a linear regression plot showing the relationship between the two methods for measuring aggregate stability (Fig. 3.10). There is a weak positive correlation ($R^2 = 0.15$) in Figure 3.10, but it is not significant ($p > 0.05$).

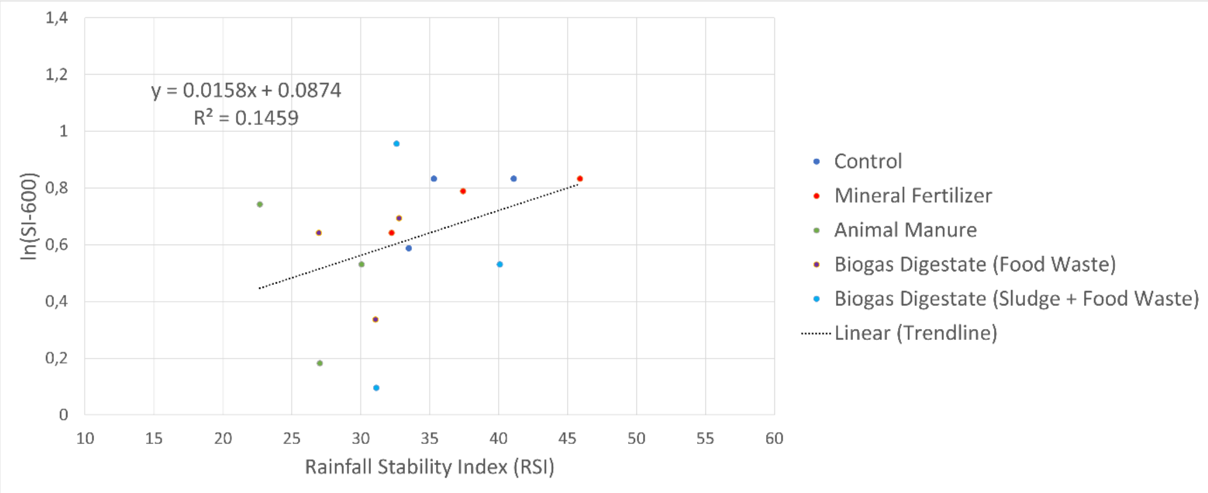

Figure 3.10 – Linear regression statistic showing the correlation between the natural log of SLAKES' Slaking Index at 600s (SI-600) and the Rainfall Stability Index (RSI) from fraction 6-2 mm.

3.3.2 – Ås – tillage spring and autumn (A85)

3.3.2.1 – Rainfall simulator

One-way ANOVA revealed a $p < 0.05$ for fraction 6 – 2 mm (significant), and a $p < 0.05$ for fraction 2 – 0.6 mm (significant), the treatment differences for each fraction can be seen in Figures 3.11 & 3.12. High Rainfall Stability Index (RSI)- values correspond to increased loss of soil during rainfall simulation and thus lower aggregate stability and vice versa.

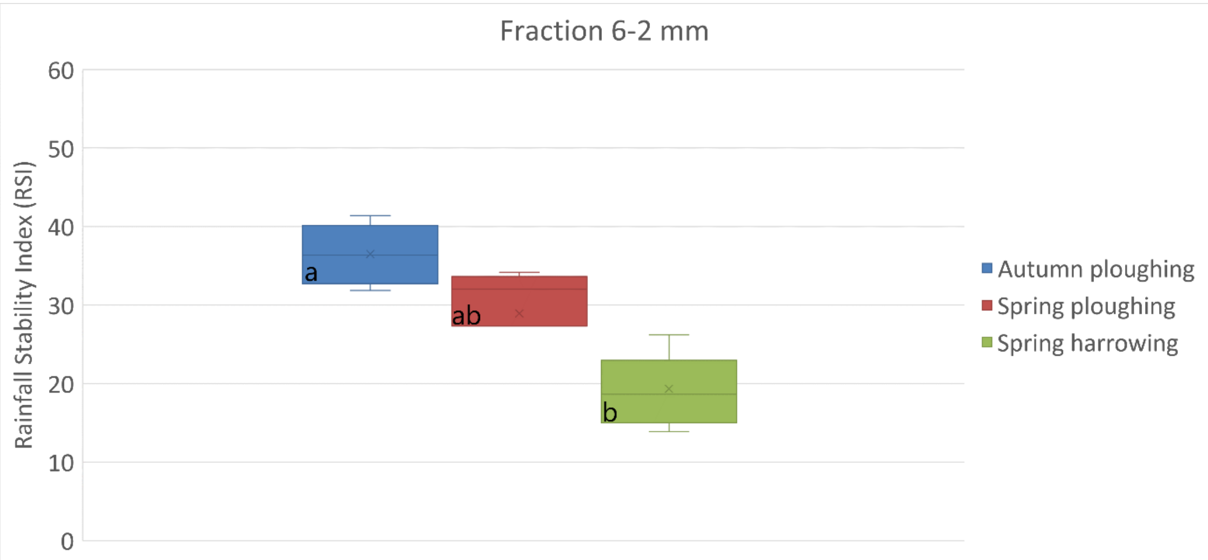

Figure 3.11 - Box plots including standard deviations and significance showing the Rainfall Stability Index (RSI) for each treatment for fraction 6 – 2 mm.

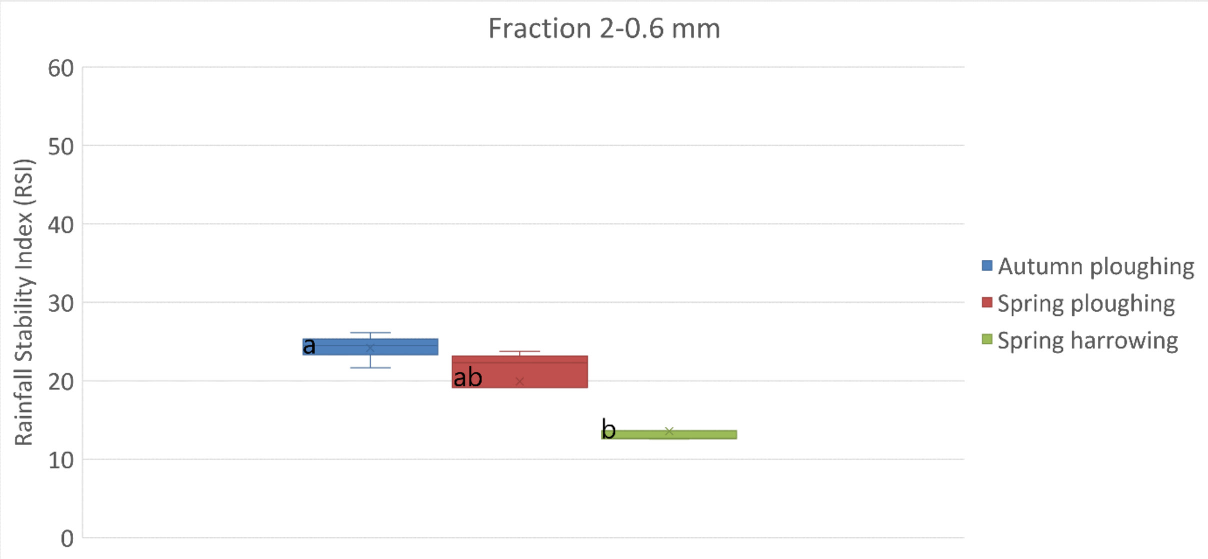

Figure 3.12 - Box plots including standard deviations and significance showing the Rainfall Stability Index (RSI) for each treatment for fraction 2 – 0.6 mm.

Box plots for each fraction are also made to show the differences in Rainfall Stability Index (RSI) between treatments (Fig. 3.11 & 3.12). From the boxplots one can see a clear trend. In both fractions, treatment A (autumn ploughing) has the lowest average aggregate stability (losing most soil during rainfall simulation), closely followed by treatment B (spring ploughing), while treatment C (spring harrowing) has the highest aggregate stability (losing least soil during rainfall simulation). T-tests comparing treatments confirm that treatment A (autumn ploughing) and treatment B (spring ploughing) have the lowest aggregate stability, but they are not significantly different from each other in either of the soil fractions. Treatment A (autumn ploughing) has significantly lower aggregate stability than treatment C (spring harrowing) in both fractions; however, no significant p-value is found between treatment B (spring ploughing) and treatment C (spring harrowing) in either of the fractions.

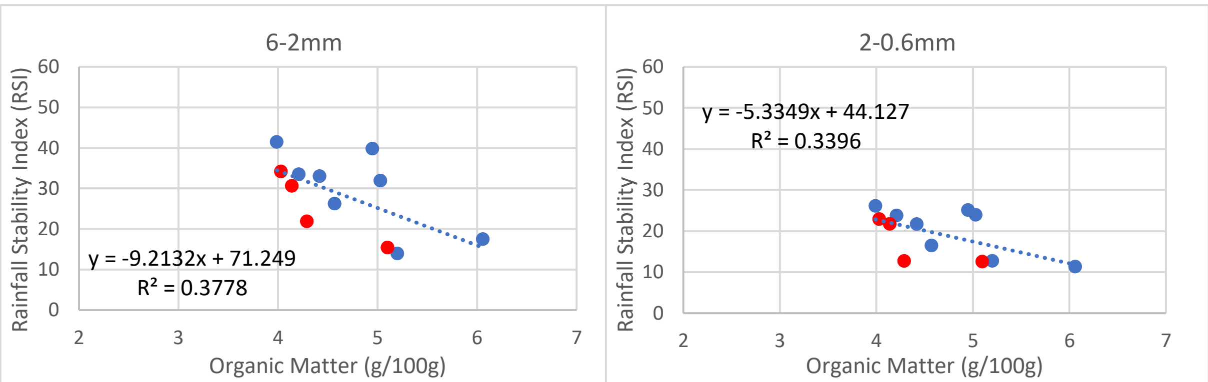

Figure 3.13 – Linear regression statistics showing the correlation between the Rainfall Stability Index (RSI) and organic matter content in the soil. The chart displays fractions 6 – 2 mm and 2 – 0.6 mm. ***Red data*** *points symbolize that soil used for organic matter measurements for these plots are taken at depth 10 – 20 cm rather than 0 – 10 cm.*

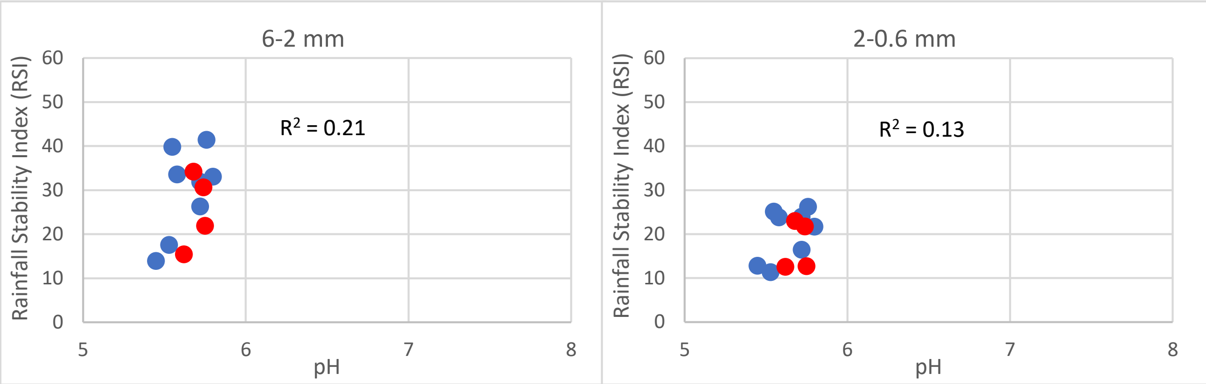

Figure 3.14 – Linear regression statistics showing the correlation between the Rainfall Stability Index (RSI) and pH in the soil. The chart displays fractions 6 – 2 mm and 2 – 0.6 mm. ***Red data*** *points symbolize that soil used for pH measurements for these plots are taken at depth 10 – 20 cm rather than 0 – 10 cm.*

Linear regression statistics are created to reveal if there is a correlation between the RSI and organic matter content (g/100g) and pH (Fig. 3.13 & 3.14).

There is a moderate but significant negative correlation between the RSI and organic matter content in fraction 6 – 2 mm, with an R^2-value of 0.38 and a $p < 0.05$ (Fig. 3.13) In fraction 2 – 0.6 mm there is a slightly weaker negative correlation, with an R^2-value of 0.34 and a $p = 0.05$ (significant).

When it comes to the correlation between the RSI and pH, there is a weak positive correlation in fraction 6 – 2 mm ($R^2 = 0.21$), but the correlation is not significant ($p > 0.05$). In fraction 2 – 0.6 mm the correlation is weaker ($R^2 = 0.13$) and not significant ($p > 0.05$).

3.3.2.2 – SLAKES

One-way ANOVA revealed a $p < 0.05$ for coefficient *a* (significant), and a $p < 0.05$ for SI-600 (significant), the treatment differences for both coefficient *a* & SI.600 can be seen in Figures 3.15 & 3.16. High SI-values correspond to increased aggregate dispersion and thus lower aggregate stability and vice versa.

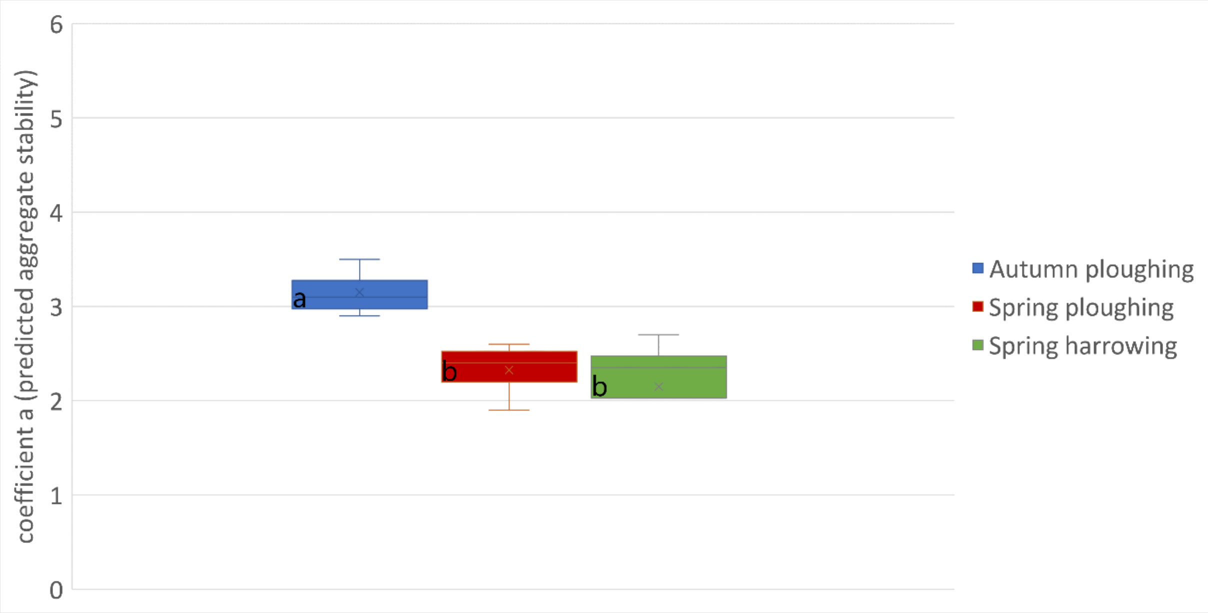

Figure 3.15 – Box plots including standard deviations and significance showing coefficient a-values for each treatment.

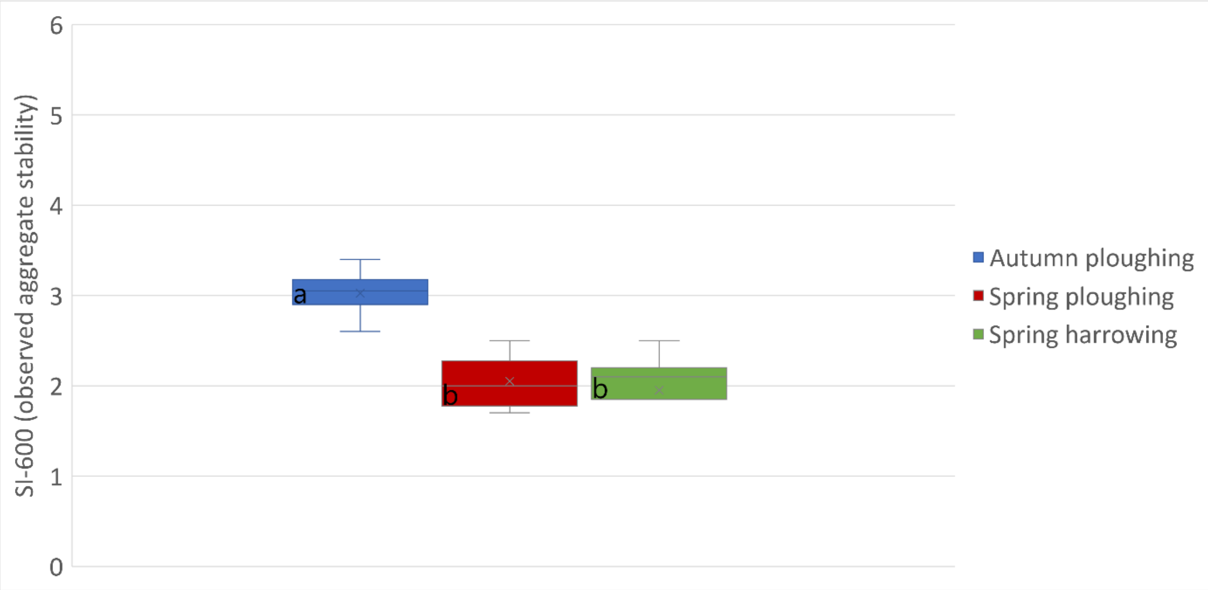

Figure 3.16 – Box plots including standard deviations and significance showing SI-600 values for each treatment.

Box plots for both coefficient *a* and SI-600 are also made to show the differences between treatments (Fig. 3.15 & 3.16). From the boxplots one can see a clear trend. For both coefficient *a* and SI-600, treatment A (autumn ploughing) has on average the lowest aggregate stability (aggregates dispersing the most during slaking), while both treatment B (spring ploughing) and treatment C (spring harrowing) have the highest aggregate stability (aggregates dispersing the least during slaking). T-tests comparing treatments confirm that treatment A (autumn ploughing) has the lowest aggregate stability, and that this treatment is significantly different from both treatment B (spring ploughing) and treatment C (spring harrowing) for both coefficient *a* and SI-600. There is no significant difference found between treatment B (spring ploughing) and treatment C (spring harrowing) for both coefficient *a* and SI-600.

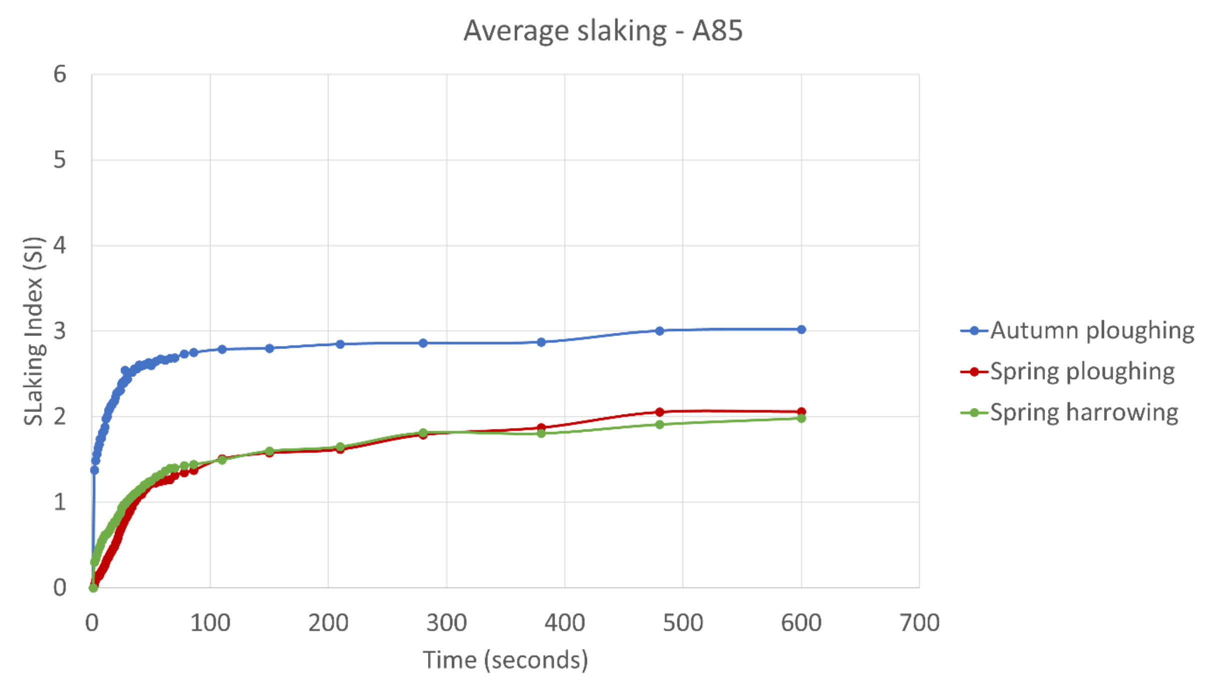

Figure 3.17 – Average slaking values for each treatment. Each data point is the mean slaking value of 12 soil aggregates at a particular time (t).

Figure 3.17 shows the average SI-values over the 600 second slaking interval. The trend is that treatment A (autumn ploughing) has the highest mean SI-values from 54 image observations, whereas treatment B (spring ploughing) and treatment C (spring harrowing) have the lowest SI-values and cannot be separated, which corresponds to the results obtained from the t-tests comparing treatments in coefficient *a* and SI-600.

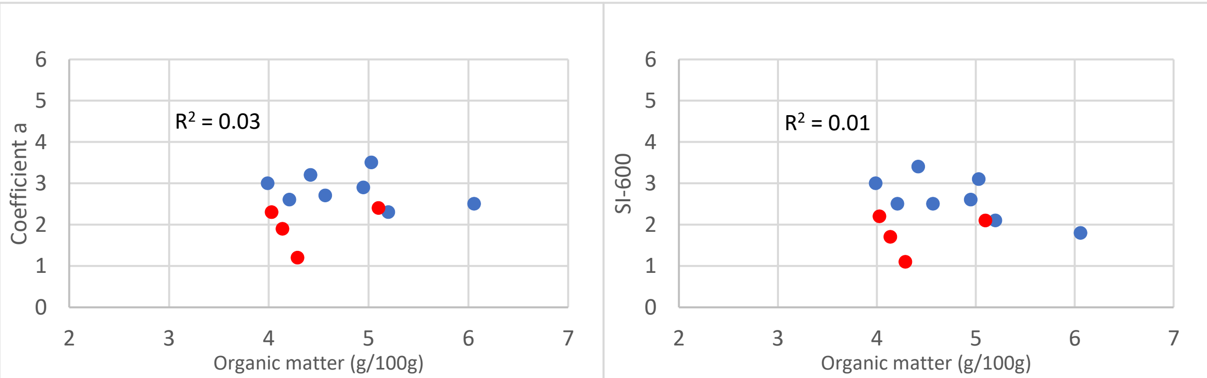

*Figure 3.18 – Linear regression statistics showing the correlation between Coefficient a & SI-600 and organic matter content in the soil. **Red data** points symbolize that soil used for pH measurements for these plots are taken at depth 10 – 20 cm rather than 0 – 10 cm.*

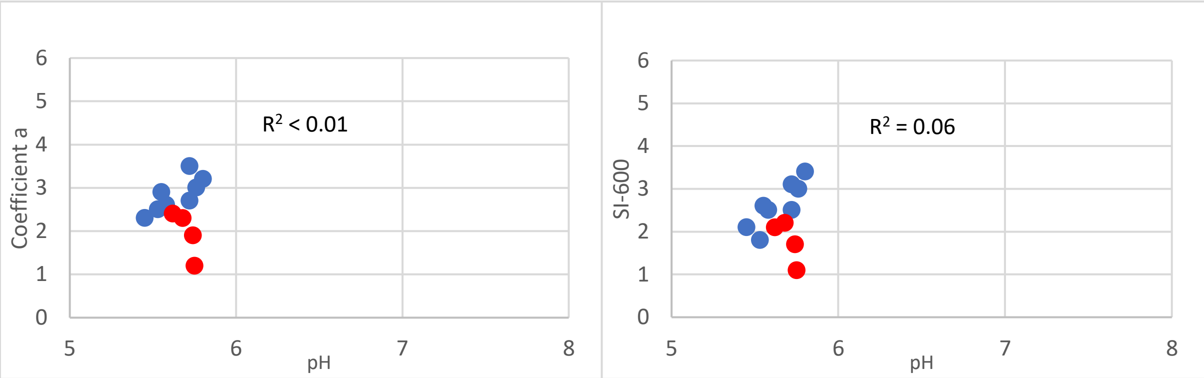

Figure 3.19 – Linear regression statistics showing the correlation between coefficient a & SI-600 and pH in the soil. ***Red data*** *points symbolize that soil used for organic matter measurements for these plots are taken at depth 10 – 20 cm rather than 0 – 10 cm.*

Linear regression statistics are created to reveal if there is a correlation between coefficient *a* & SI-600 and organic matter (g/100g) & pH (Fig. 3.18 & 3.19).

There are weak and non-significant correlations between coefficient *a* & SI-600 and organic matter content, with an R^2-value of 0.03 and a $p > 0.05$ for coefficient *a*, and an R^2-value of 0.01 and a $p > 0.05$ for SI-600.

There is no significant correlation between coefficient *a* and SI-600 and pH. For coefficient *a* there is no correlation ($R^2 < 0.01$), with a $p > 0.05$. For SI-600 there is a weak correlation ($R^2 = 0.06$), which is not significant ($p > 0.05$).

3.3.2.3 – Comparison of rainfall simulator & SLAKES

To directly compare the rainfall simulator to SLAKES, values achieved from the rainfall simulator (6-2 mm) are plotted against the natural log-values achieved from SLAKES (SI-600). This leads to a linear regression plot showing the relationship between the two methods for measuring aggregate stability (Fig. 3.20). There is a moderate positive correlation (R^2 = 0.29) in Figure 3.20, but it is not significant ($p > 0.05$).

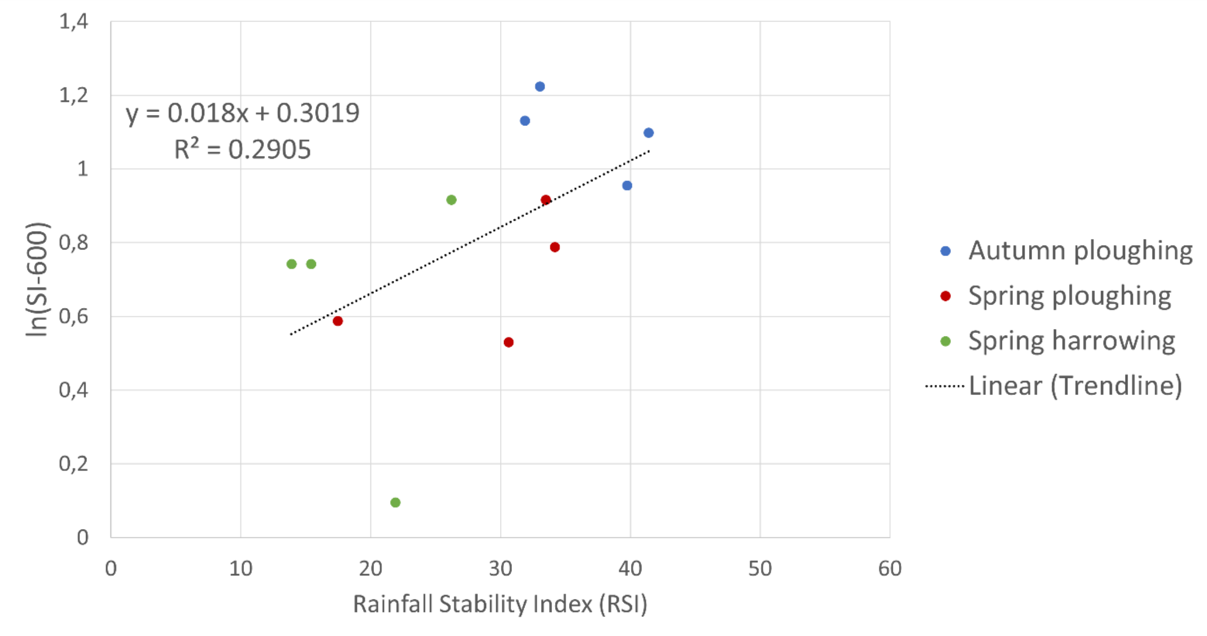

Figure 3.20 – Linear regression statistic showing the correlation between the natural log of SLAKES' Slaking Index at 600s and the Rainfall Stability Index (RSI) from fraction 6-2 mm.

3.3.3 – Øsaker – tillage spring and autumn (A45)

3.3.3.1 – Rainfall simulator

One-way ANOVA revealed a $p > 0.05$ for fraction 6 – 2 mm (not significant), and a $p < 0.05$ for fraction 2 – 0.6 mm (significant), the treatment differences for each fraction can be seen in Figures 3.21 & 3.22. High Rainfall Stability Index (RSI) values correspond to increased loss of soil during rainfall simulation and thus lower aggregate stability and vice versa.

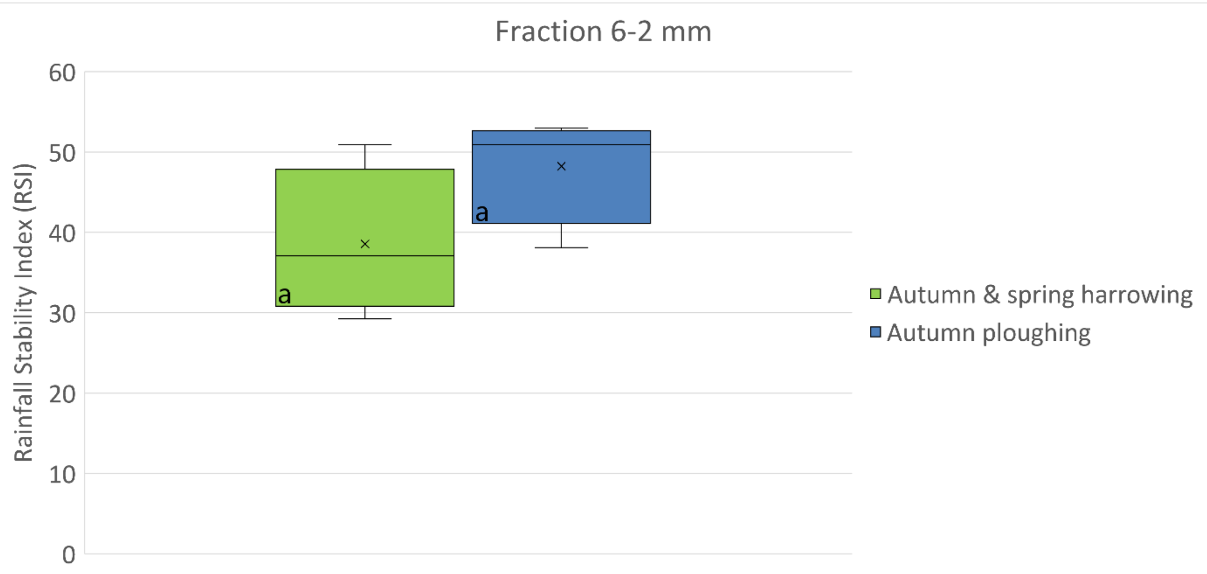

Figure 3.21 - Box plots including standard deviations and significance showing the Rainfall Stability Index (RSI) for each treatment for fraction 6 – 2 mm.

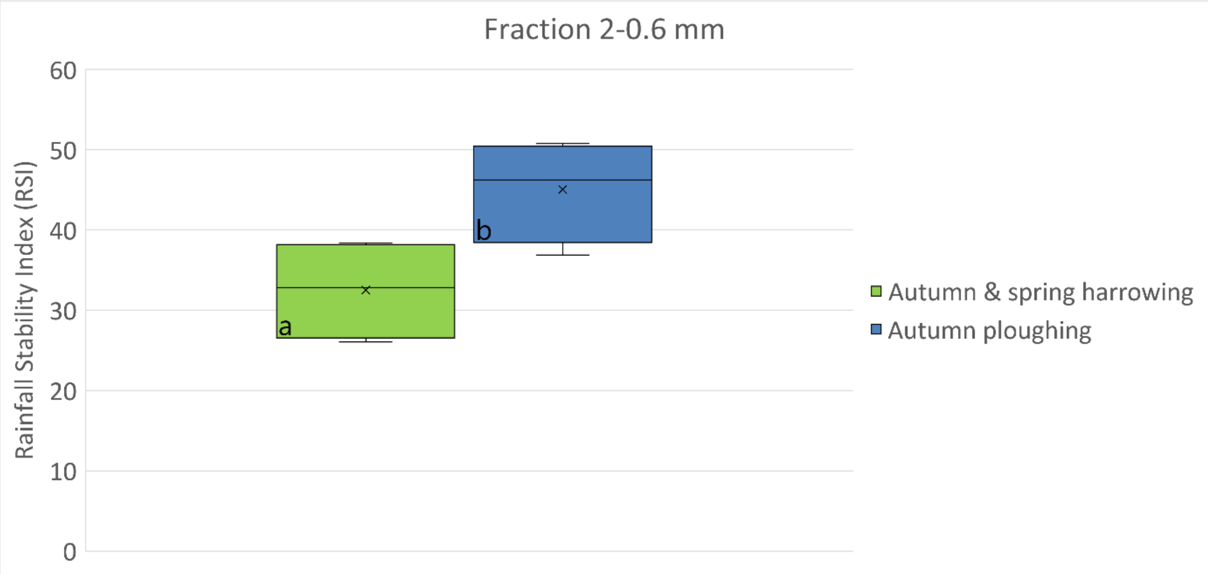

Figure 3.22 - Box plots including standard deviations and significance showing the Rainfall Stability Index (RSI) for each treatment for fraction 2 – 0.6 mm.

Box plots for each fraction are also created to show the differences in Rainfall Stability Index (RSI) between treatments (Fig. 3.21 & 3.22). From the boxplots one can see a clear trend. On average for both fractions, treatment D (autumn ploughing) has the lowest aggregate stability (losing most soil during rainfall simulation), while treatment B (autumn & spring harrowing), has the highest aggregate stability (losing least soil during rainfall simulation).

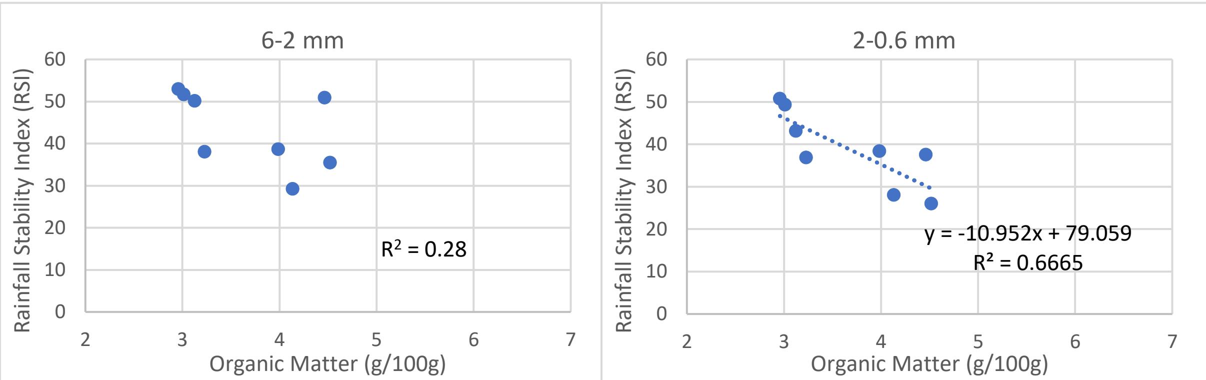

Figure 3.23 – Linear regression statistics showing the correlation between the Rainfall Stability Index (RSI) and organic matter content in the soil. The chart displays fractions 6 – 2 mm and 2 – 0.6 mm.

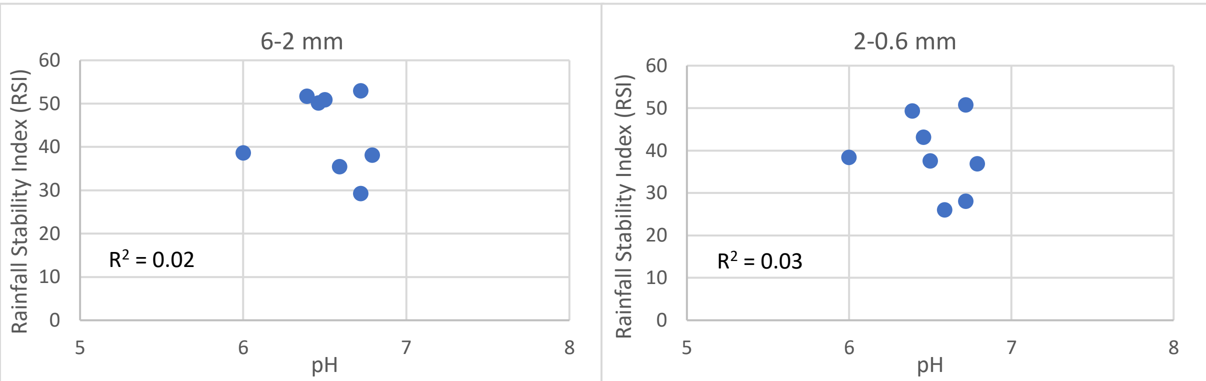

Figure 3.24 – Linear regression statistics showing the correlation between the Rainfall Stability Index (RSI) and pH in the soil. The chart displays fractions 6 – 2 mm and 2 – 0.6 mm.

Linear regression statistics are created to reveal if there is a correlation between the RSI and organic matter (g/100g) & pH (Fig. 3.23 & 3.24).

There is a moderate but non-significant negative correlation between RSI and organic matter content in fraction 6 – 2 mm, with an R^2-value of 0.28 and a $p > 0.05$. In fraction 2 – 0.6 mm there is a much stronger negative correlation, with an R^2-value of 0.67 and a $p < 0.05$ (significant).

When it comes to the correlation between the RSI and pH, there is no correlation in fraction 6 – 2 mm ($R^2 = 0.02$), and thus not significant ($p > 0.05$). There is no correlation in fraction 2 – 0.6 mm either ($R^2 = 0.03$) and nor is it significant ($p > 0.05$).

3.3.3.2 – SLAKES

One-way ANOVA revealed a $p < 0.05$ for coefficient *a* (significant), and a $p < 0.05$ for SI-600 (significant), the treatment differences for both coefficient *a* & SI-600 can be seen in Figures 3.25 & 3.26. High SI-values correspond to increased aggregate dispersion and thus worse aggregate stability and vice versa.

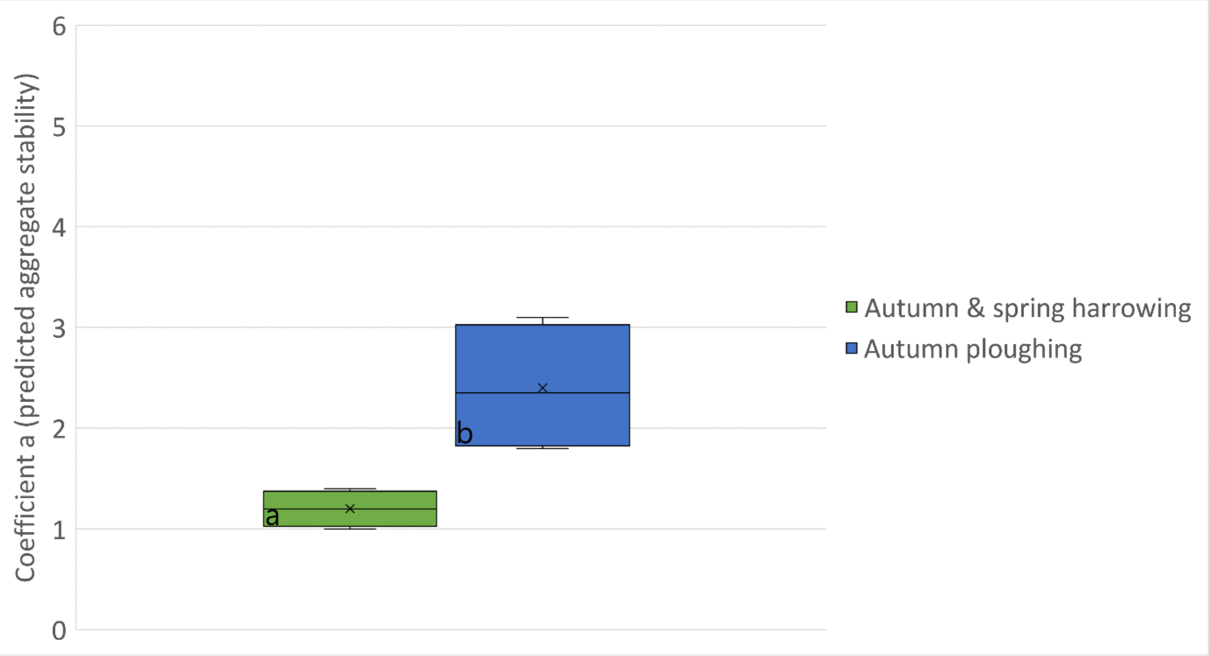

Figure 3.25 – Box plots including standard deviations and significance showing coefficient a-values for each treatment in coefficient a.

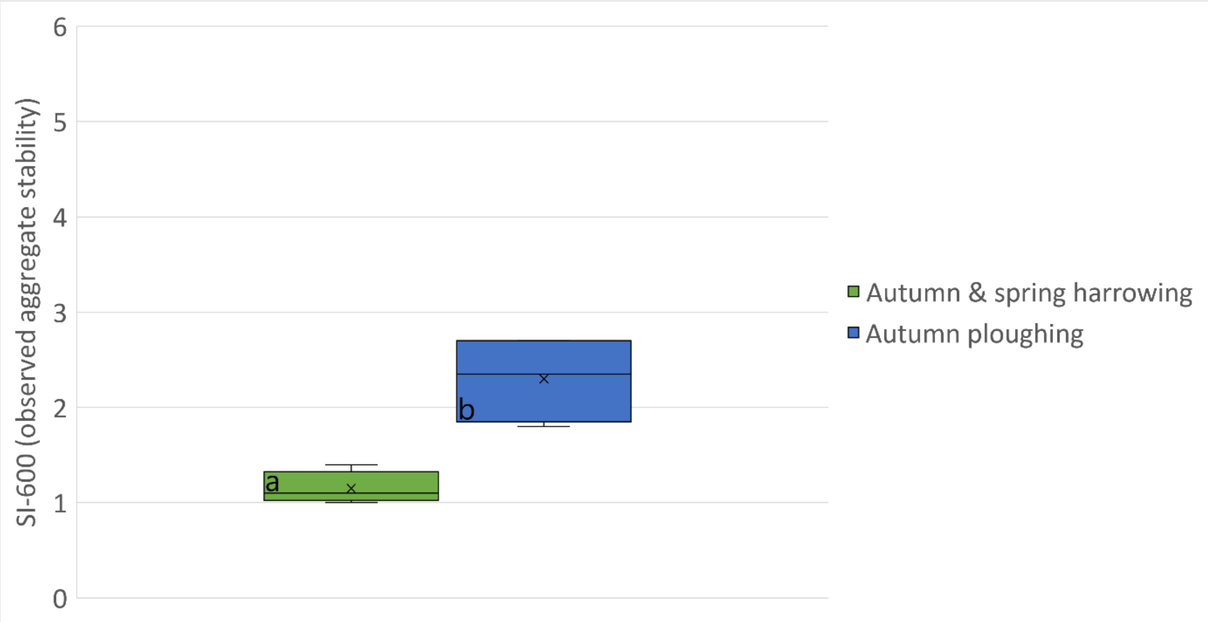

Figure 3.26 – Box plots including standard deviations and significance showing SI-600-values for each treatment in SI-600.

Box plots for both coefficient *a* and SI-600 are also created to show the differences between treatments (Fig. 3.25 & 3.26). For both coefficient *a* and SI-600, treatment D (autumn ploughing) has the lowest aggregate stability on average (aggregates dispersing the most during slaking), while treatment B (autumn & spring harrowing) has the highest aggregate stability on average (aggregates dispersing the least during slaking).

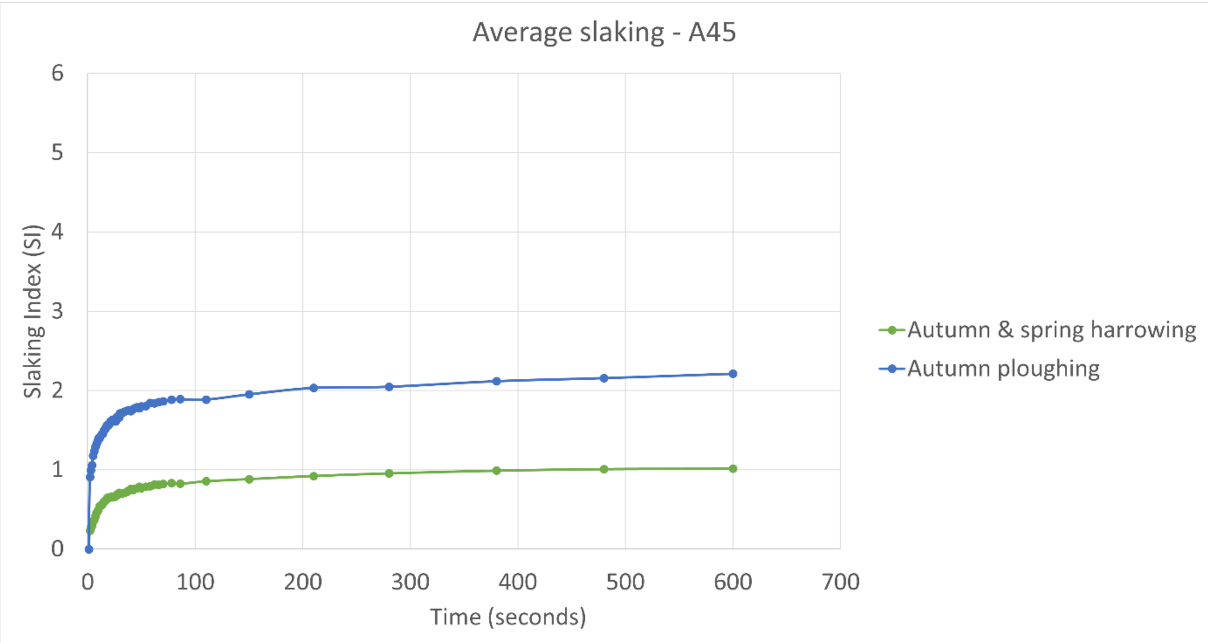

Figure 3.27 – Average slaking values for each treatment. Each data point is the mean slaking value of 12 soil aggregates at a particular time (t).

Figure 3.27 shows the average SI-values over the 600 second slaking interval. The graph displays that treatment D (autumn ploughing) has the highest mean SI-values from 54 image observations, whereas treatment B (autumn & spring harrowing) has the lowest SI-values.

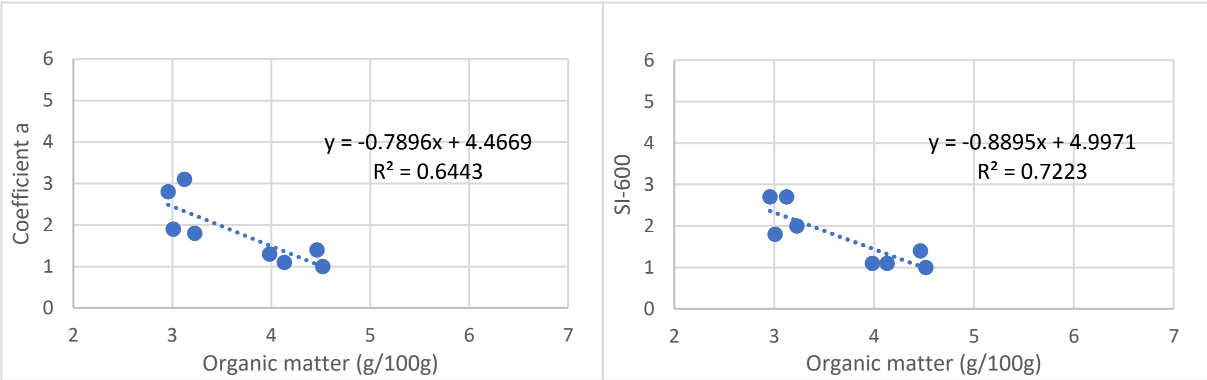

Figure 3.28 – Linear regression statistics showing the correlation between coefficient a & SI-600 and organic matter content in the soil.

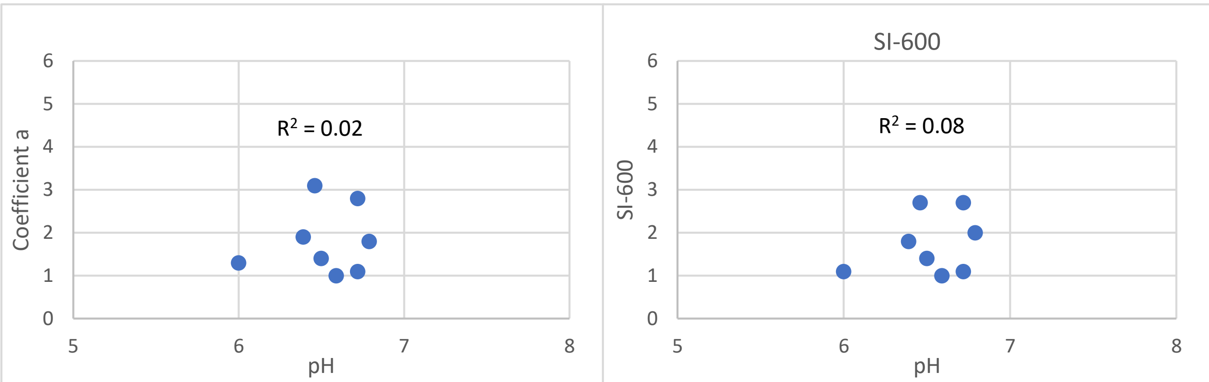

Figure 3.29 - Linear regression statistics showing the correlation between coefficient a & SI-600 and pH in the soil.

Linear regression statistics are compiled to reveal if there is a correlation between coefficient *a* & SI-600 and organic matter (g/100g) and pH (Fig. 3.28 & 3.29).

There are strong and significant correlations between coefficient *a* & SI-600 and organic matter content, with an R^2-value of 0.64 and a $p < 0.05$ for coefficient *a*, and an R^2-value of 0.72 and a $p < 0.05$ for SI-600.

There is no significant correlation between coefficient *a* and pH ($R^2 = 0.02$), with a $p > 0.05$. For SI-600 there is a weak correlation ($R^2 = 0.08$), which is not significant ($p > 0.05$).

3.3.3.3 – Comparison of rainfall simulator & SLAKES

To directly compare the rainfall simulator to SLAKES, values achieved from the rainfall simulator (6-2 mm) are plotted against the natural log of the values achieved from SLAKES (SI-600). This leads to a linear regression plot showing the relationship between the two methods for measuring aggregate stability (Fig. 3.30). There is a moderate positive correlation ($R^2 = 0.51$) in Figure 3.30, and it is significant ($p < 0.05$).

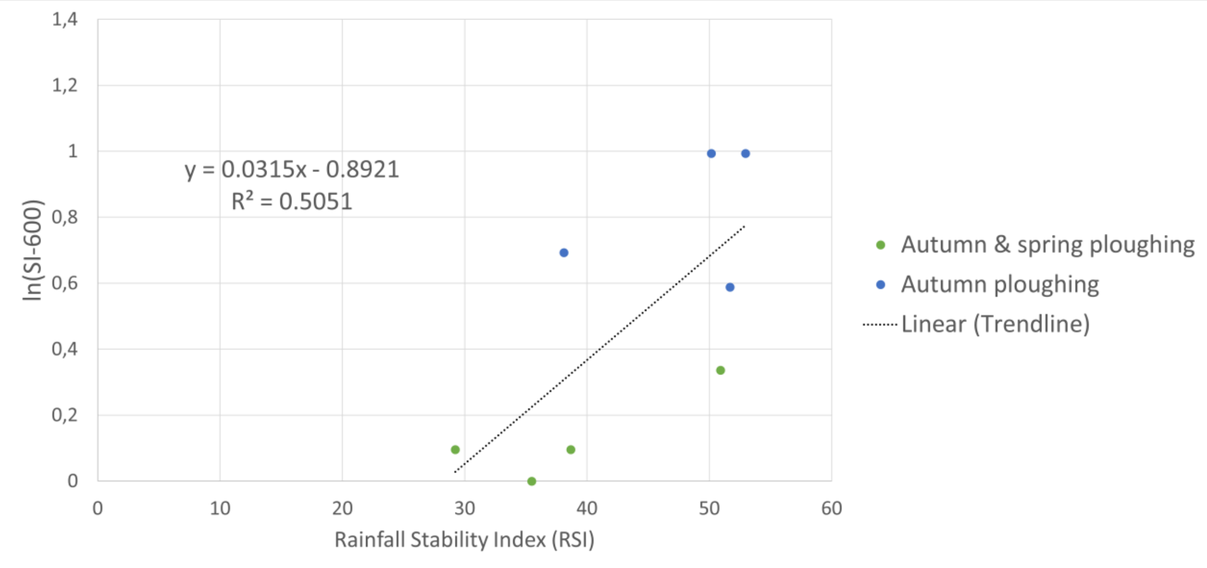

Figure 3.30 – Linear regression statistic showing the correlation between the natural log of SLAKES' Slaking Index at 600s and the Rainfall Stability Index (RSI) from fraction 6-2 mm.

3.3.4 – Kjuus – tillage spring

3.3.4.1 – Rainfall simulator

Box plots for each fraction are created to show the differences in Rainfall Stability Index (RSI) between treatments (Fig. 3.31 & 3.32). From the boxplots one can see a clear trend. For both fractions, Treatment 1 (spring ploughing) has the lowest aggregate stability on average (losing most soil during rainfall simulation), while treatment 2 (direct sowing) and treatment 3 (spring harrowing) have the highest aggregate stability (losing least soil during rainfall simulation). There is no way to confirm the significance of the results obtained in Figures 3.31 & 3.32 as there are no repetitions for either of the treatments.

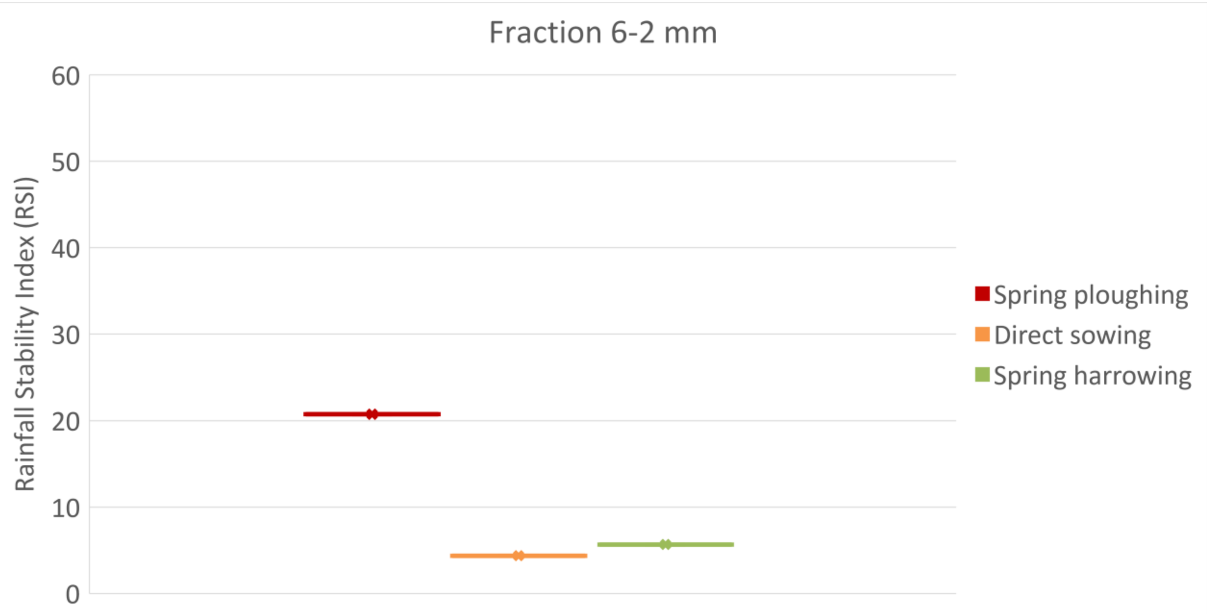

Figure 3.31 – Box plots showing the average Rainfall Stability Index (RSI) for each treatment for fraction 6 – 2 mm.

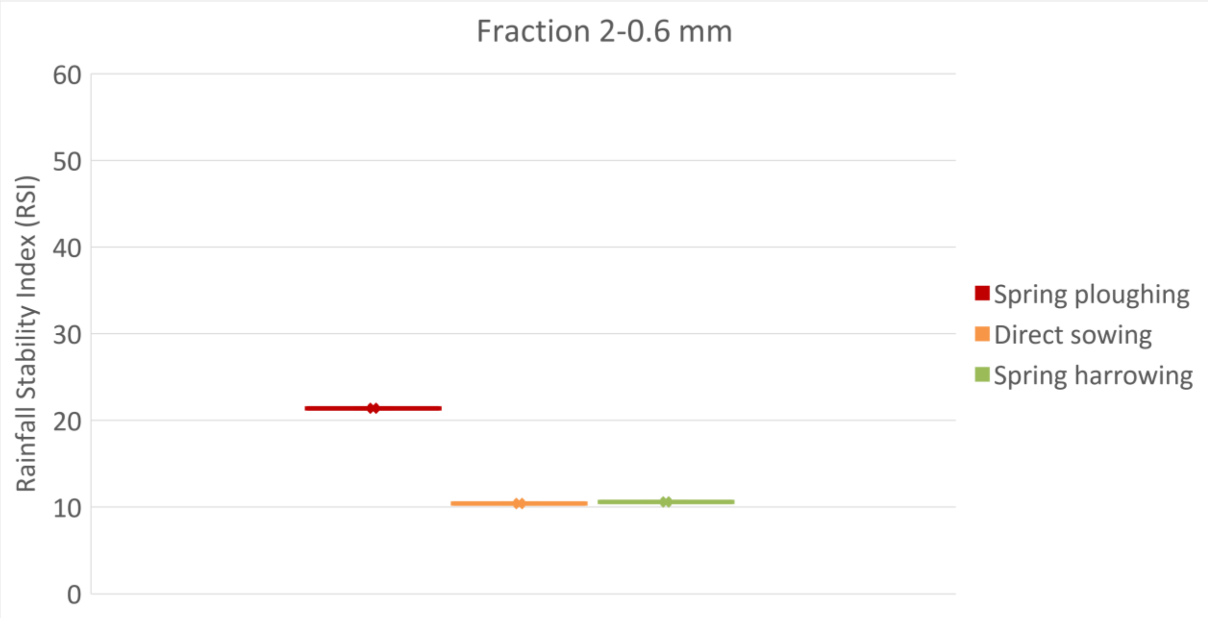

Figure 3.32 – Box plots showing the average Rainfall Stability Index (RSI) for each treatment for fraction 2 – 0.6 mm.

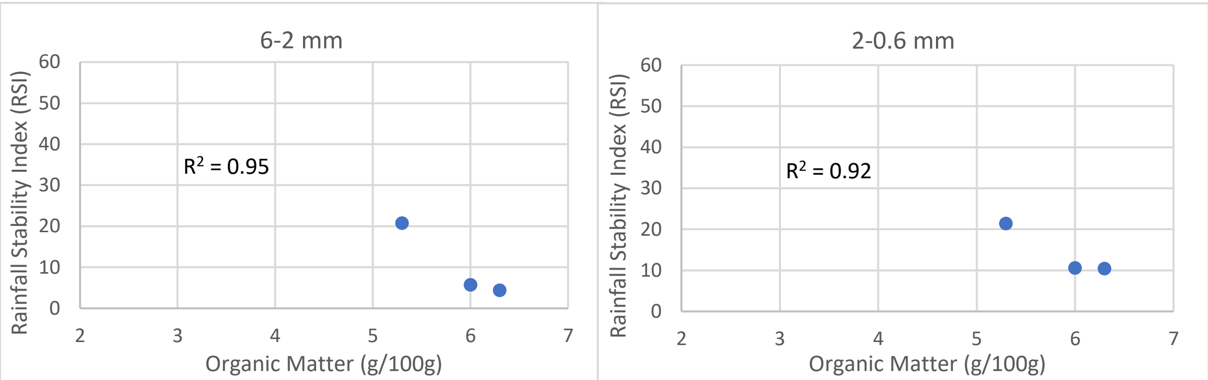

Figure 3.33 – Linear regression statistics showing the correlation between the Rainfall Stability Index (RSI) and organic matter content in the soil. The chart displays fractions 6 – 2 mm and 2 – 0.6 mm.

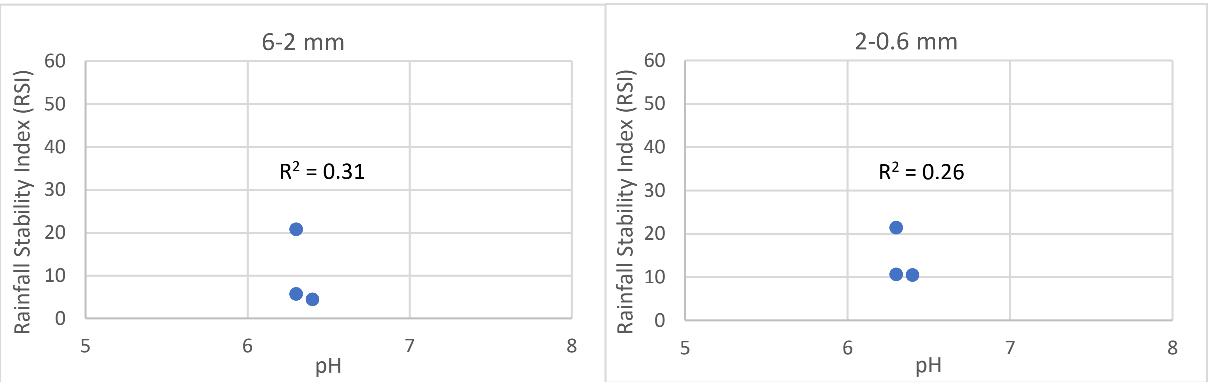

Figure 3.34 - Linear regression statistics showing the correlation between the Rainfall Stability Index (RSI) and pH in the soil. The chart displays fractions 6 – 2 mm and 2 – 0.6 mm.

Linear regression statistics are created to reveal if there is a correlation between the RSI and organic matter (g/100g) & pH (Fig. 3.33 & 3.34).

There is a strong but non-significant negative correlation between RSI and organic matter content in fraction 6 – 2 mm, with an R^2-value of 0.95 and a $p > 0.05$. In fraction 2 – 0.6 mm there is also a strong negative correlation, with an R^2-value of 0.92 and a $p > 0.05$ (not significant). Small sample size is the reason why the strong correlations seen in Figure 3.33 are not significant.

When it comes to the correlation between RSI and pH, there is a moderate negative correlation in fraction 6 – 2 mm ($R^2 = 0.31$), but the correlation is not significant ($p > 0.05$). There is a moderate negative correlation in fraction 2 – 0.6 mm as well ($R^2 = 0.26$), but again the correlation is not significant ($p > 0.05$).

3.3.4.2 – SLAKES

Box plots for both coefficient *a* and SI-600 are created to show the differences between treatments (Fig. 3.35 & 3.36). For both coefficient *a* and SI-600, Treatment 1 (spring ploughing) has the lowest aggregate stability (aggregates dispersing the most during slaking), while treatment 2 (direct sowing) and treatment 3 (spring harrowing) have the highest aggregate stability (aggregates dispersing the least during slaking). There is no way to confirm the significance of the results obtained in Figures 3.35 & 3.36 as there are no repetitions for either of the treatments.

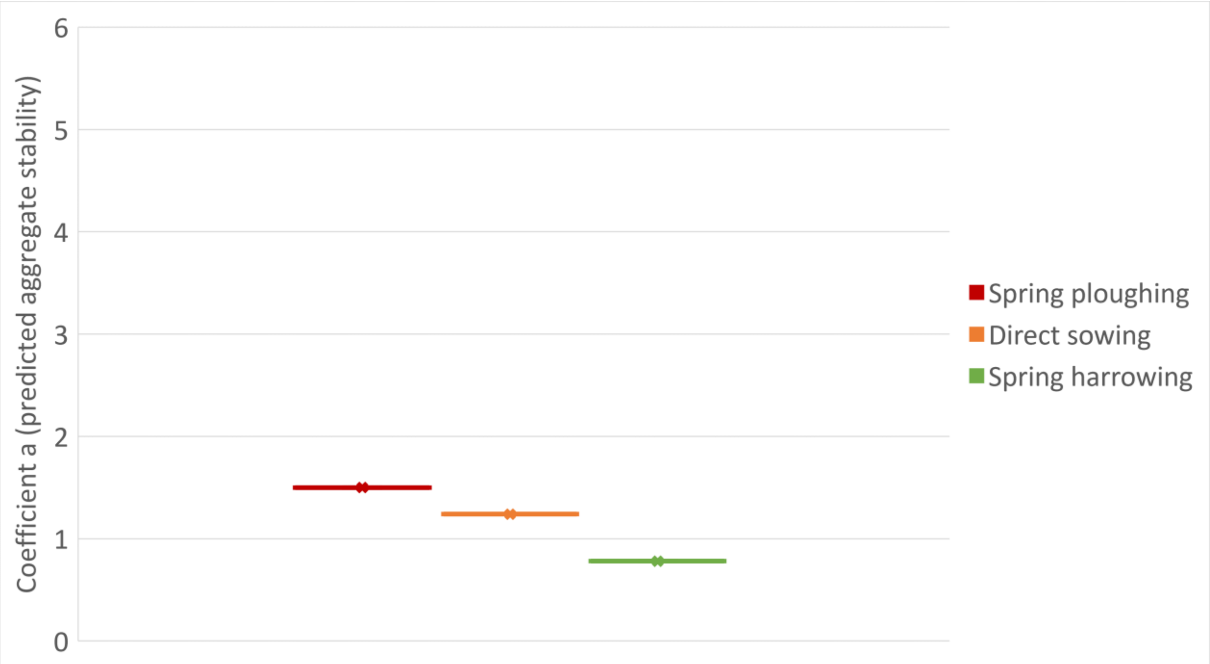

Figure 3.35 – Box plots showing average coefficient a-values for each treatment.

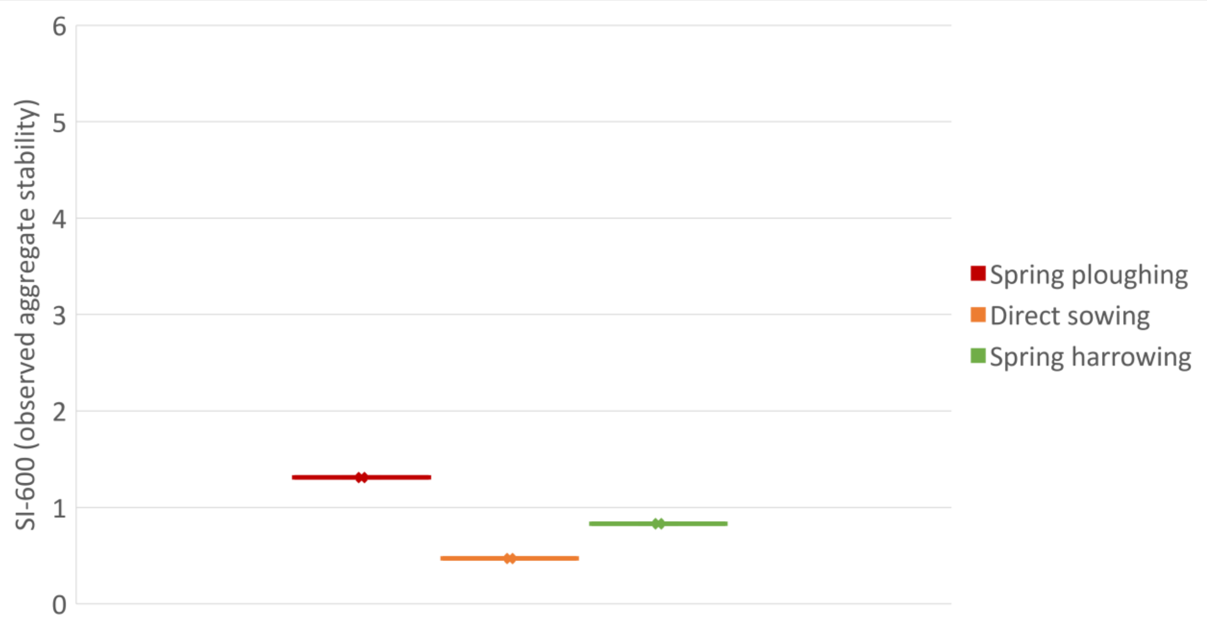

Figure 3.36 – Box plots showing average SI-600-values for each treatment.

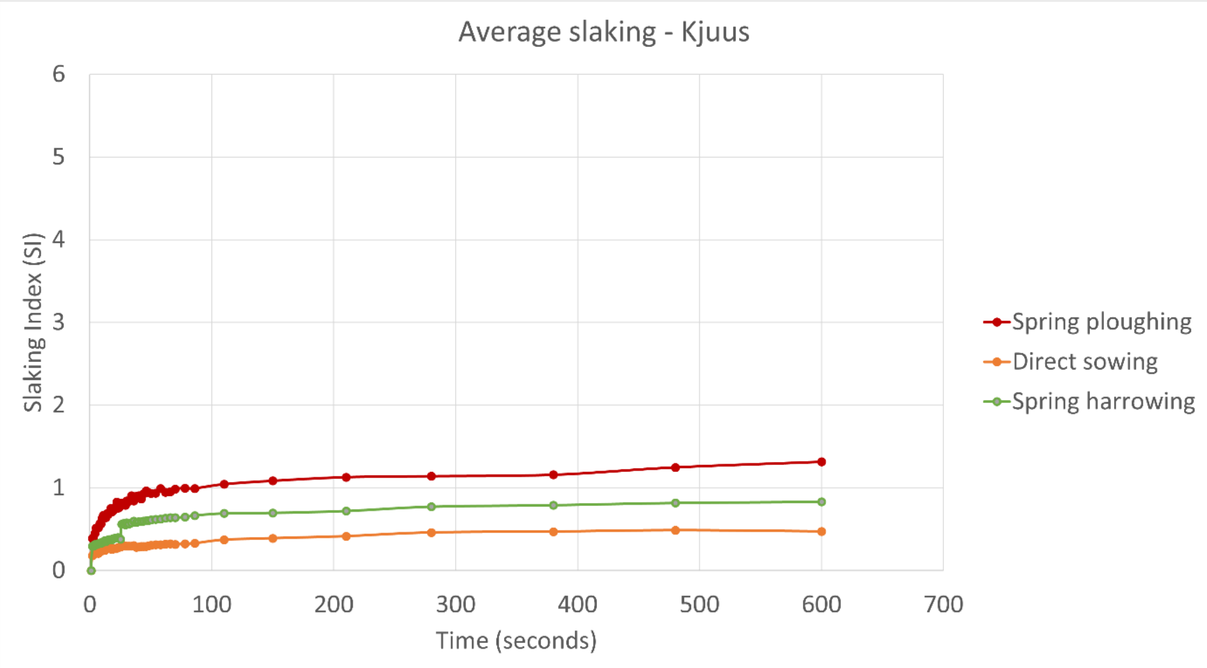

Figure 3.37 – Average slaking values for each treatment. Each data point is the mean slaking value of 3 soil aggregates at a particular time (t).

Figure 3.37 shows average SI-values over the 600 second slaking interval. The graph displays that treatment 1 (spring ploughing) has the highest mean SI-values from 54 image observations, whereas treatment 2 (direct sowing) has the lowest SI-values.

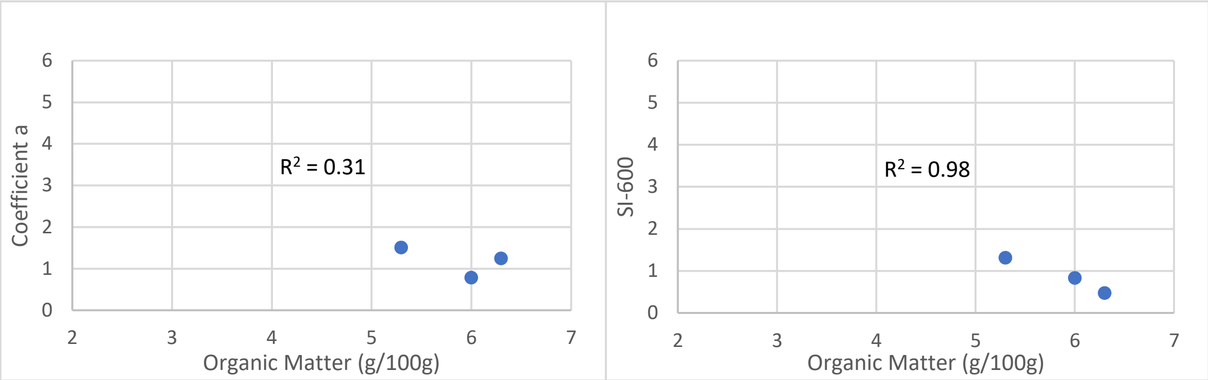

Figure 3.38 – Linear regression statistics showing the correlation between coefficient a & SI-600 and organic matter content in the soil.

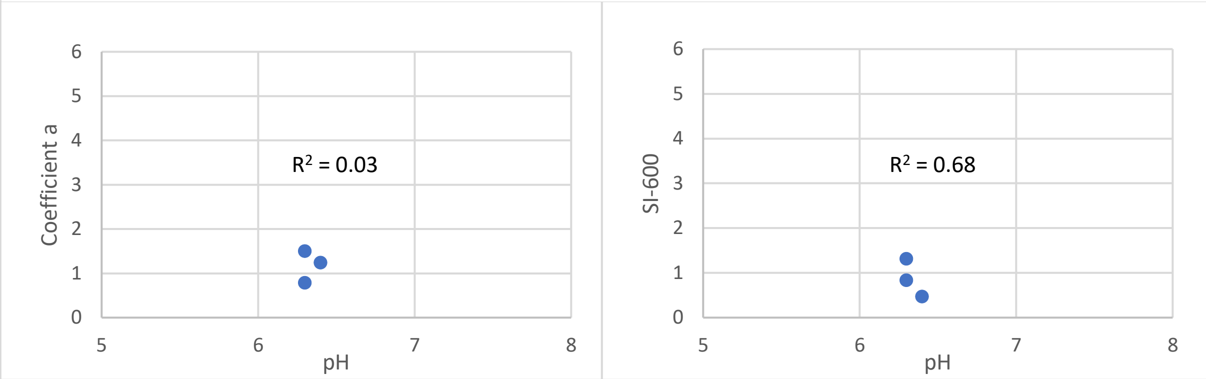

Figure 3.39 – Linear regression statistics showing the correlation between coefficient a & SI-600 and pH in the soil.

Linear regression statistics are created to reveal if there is a correlation between coefficient *a* & SI-600 and organic matter (g/100g) & pH (Fig. 3.38 & 3.39).

There is a moderate negative correlation between coefficient *a* and organic matter content ($R^2 = 0.31$), and a strong negative correlation for SI-600 ($R^2 = 0.98$). However, none of the correlations are significant, which is due to small sample size ($p > 0.05$).

There is no significant correlation between the Slaking Index and pH for coefficient *a* ($R^2 = 0.03$), with a $p > 0.05$. For SI-600 there is a strong correlation ($R^2 = 0.68$), but it is not significant ($p > 0.05$). Small sample size and hardly any variance in pH-values may be the reason for no significance.

3.3.4.3 – Comparison of rainfall simulator & SLAKES

To directly compare the rainfall simulator to SLAKES, values achieved from the rainfall simulator (6-2 mm) are plotted against the natural log of the values achieved from SLAKES (SI-600). This leads to a linear regression plot showing the relationship between the two methods for measuring aggregate stability (Fig. 3.40). There is a strong positive correlation ($R^2 = 0.76$) in Figure 3.40, but it is not significant due to small sample size ($p > 0.05$).

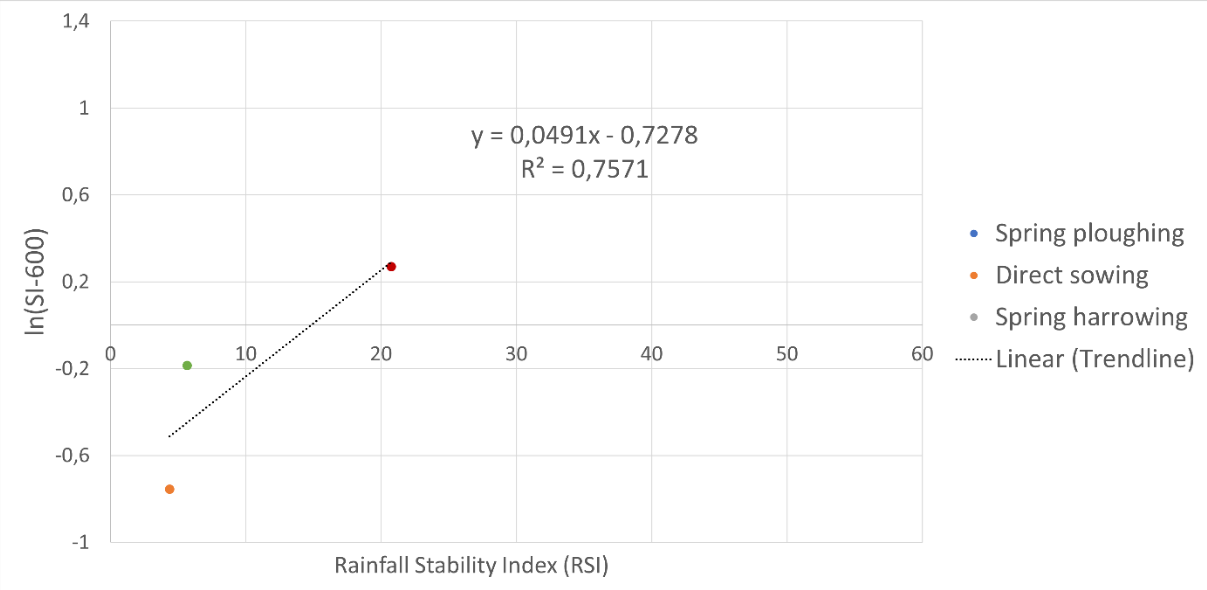

Figure 3.40 - Linear regression statistic showing the correlation between the natural log of SLAKES' Slaking Index at 600s and the % lost aggregate stability from fraction 6-2 mm.

3.3.5 – Combined linear regression comparisons (organic matter & aggregate stability)

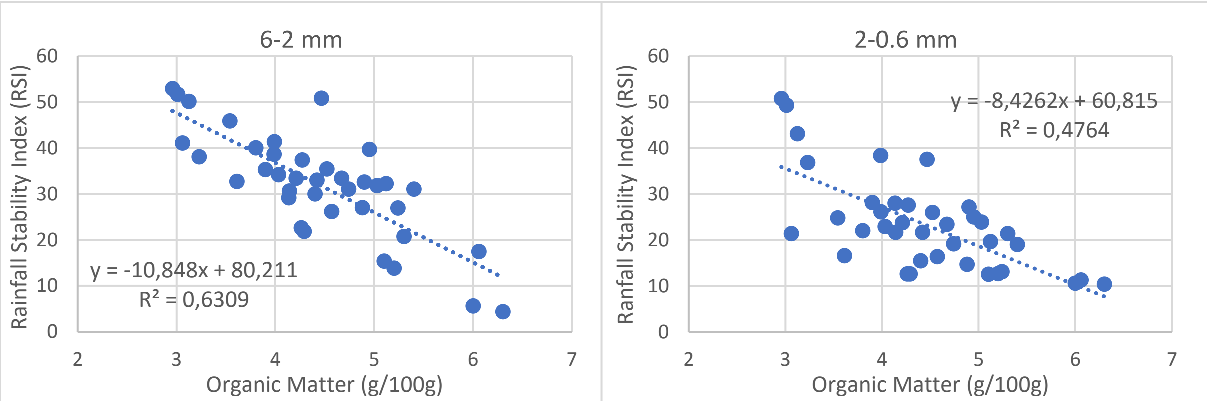

Figure 3.41 – Linear regression statistics showing the correlation between the Rainfall Stability Index (RSI) and organic matter content in the soil. The chart displays fractions 6 – 2 mm and 2 – 0.6 mm.

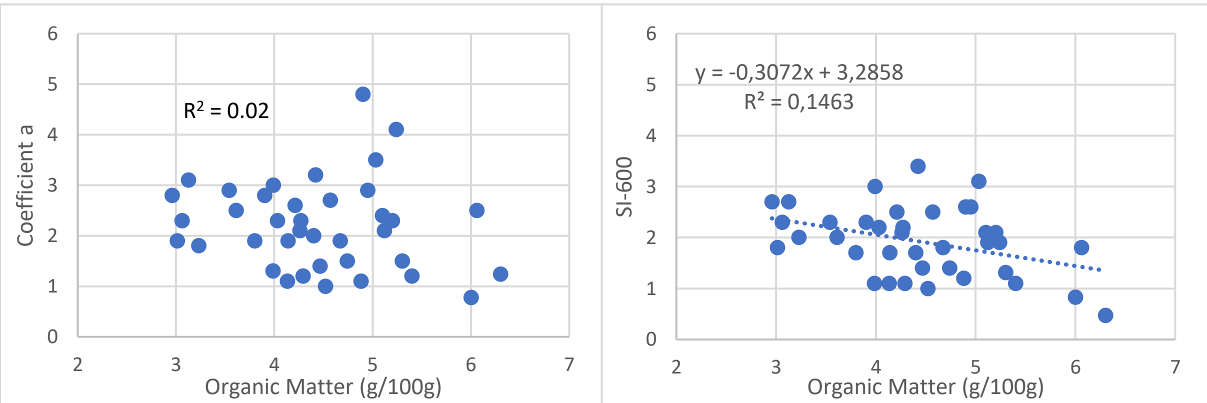

Figure 3.42 – Linear regression statistics showing the correlation between coefficient a & SI-600 and organic matter content in the soil.

Values from all fields (E166, A85, A45, Kjuus) are used to create a combined linear regression statistic to better see which aggregate stability measurement method is more sensitive to finding a correlation between aggregate stability and organic matter content (Fig. 3.41 & 3.42).

Both fractions 6-2 mm and 2-0.6 mm from the rainfall simulator have moderate/strong correlations ($R^2 = 0.63$ & $R^2 = 0.48$ respectively) between RSI and organic matter content, and both correlations are significant ($p < 0.05$). For SLAKES, there is a weak correlation between SI-600 and organic matter content ($R^2 = 0.15$), and the correlation is significant ($p < 0.05$). There is no correlation between coefficient *a* and organic matter content.

4 – Discussion

4.1 – Organic Matter and acidity

This section refers to Table 3.1.

As field E166 is a relatively short-term experiment, there is no surprise that the various treatments do not show any significant differences in organic matter content. However, the trend is clear: Both the control and mineral fertilizer treatments exhibit lower average organic matter content than all the organic fertilizer treatments. As explained in the introduction, organic matter is removed from the soil during harvest and must be replaced. This occurs with the organic fertilizer treatments, but not with the control or mineral fertilizer treatments. There are some significant differences in pH in field E166, and on average the mineral fertilizer treatment has the lowest pH. Studies suggest that the use of only mineral fertilizers may decrease the pH of soil over time (Wang et al., 2019; Bell & Mathesius, 2019). This is probably due to the excessive use of ammonium-based nitrogen fertilizers (NH_4^+). Manure-based fertilizers are suggested to increase the pH of soils due to often high content of calcium and magnesium (Bell & Mathesius, 2019), which is possibly why the animal manure treatment exhibits the highest pH. Also, the animal manure treatment has a significantly higher pH than the mineral fertilizer treatment. However, this thesis cannot conclusively state that the pH decreases using mineral fertilizers only – local soil variation must be considered and as mentioned this is a relatively short-term field experiment so far. Although the organic fertilizer treatments exhibit promising organic matter content and pH results, the continuation of this field experiment is important to assess the possibility of supplementing mineral fertilizers with organic fertilizers in the future.

Since field A85 is a long-term tillage experiment, it may be surprising that there are no significant differences in organic matter content between treatments. However, the reason for this could be due to the four soil samples taken at a depth of 10 – 20 cm rather than at a depth of 0 – 10 cm. Two of these samples are from the spring ploughing treatment and two are from the spring harrowing treatment. Organic matter content is almost always higher in upper layers of the soil (Debela & Gebrekidan, 2015), so these results are slightly biased. Nevertheless, average organic matter content is higher for the reduced tillage treatment (spring harrowing) compared to the conventional tillage treatments (autumn ploughing and spring ploughing). This is expected as conventional tillage often leaves soil vulnerable to erosion and thus also loss of organic matter (Bagnall & Morgan, 2021). pH does not differ significantly between tillage treatments, but the pH is on average highest for the autumn ploughing treatment. The pH results may unfortunately also be affected by soil sample depth.

In field A45, another long-term tillage experiment, there is quite a big difference in organic matter content between the two treatments. autumn & spring harrowing have a much higher organic matter content than Autumn ploughing. The difference is significant, and one can begin to comprehend the importance of tillage treatment on conserving organic matter in the soil. There is no significant difference in pH between tillage treatments, but also here the pH is on average slightly higher in the autumn ploughing treatment.

In field Kjuus, one can only make speculations based on the average results obtained. However, there is an indication that reduced tillage increases organic matter content. Direct sowing exhibits the highest organic matter content, closely followed by spring harrowing, whereas spring ploughing displays the lowest percentage of organic matter. Also here, there do not seem to be large differences in pH.

For all tillage experiments, the tendency is that organic matter content increases as a result of reduced tillage, whereas pH seems to be unaffected.

4.2 – Fraction 0.6 – 6 mm (from aggregate size distribution)

This section refers to Table 3.2.

Aggregation processes and therefore aggregate size distribution and soil structure are dynamic and highly dependent on moment in time and present conditions (Amézketa, 1999). The results are thus very dependent on the conditions that prevail during soil sampling.
In spring, aggregate size distribution is mostly governed by conditions during tillage, along with texture and organic matter, whereas in autumn, the weather throughout the growing season and water content at time of sampling are also contributing factors.

Soil samples were extracted in spring after tillage and fertilization in field E166. As mentioned, it is the mineral fertilizer treatment that on average has the highest percentage of aggregates in fraction 0.6 – 6 mm (47.5 g/100g). Interestingly the mineral fertilizer treatment also has one of the two lowest average organic matter contents. Both digestate treatments have a lower and significantly different aggregate size distribution (0.6 – 6 mm) than the mineral fertilizer treatment. At the same time the digestate treatments have higher average organic matter contents than the mineral fertilizer treatment. A possible explanation for this is the cementing nature of organic compounds, which is discussed in the introduction.

Increasing organic matter content possibly enables stronger bondage between soil particles and may slightly lower the ability of various tillage practises to separate aggregates. However, this is only speculation.

For the different tillage experiments, soil samples were extracted at different times of the year. Soil samples from fields A85 and Kjuus were extracted in autumn, whereas soil samples from field A45 were extracted in spring. Apart from the spring ploughing treatment in field A85 and direct sowing treatment in field Kjuus, more intensive tillage practises seem to increase the percentage of aggregates in fraction 0.6 – 6 mm compared to less intensive tillage practises. This is not that surprising as intensive tillage crushes, turns, and works the soil to a much greater extent than reduced tillage.

4.3 – Aggregate Stability

Two fractions (6-2 & 2-0.6 mm) are used to measure aggregate stability using the rainfall simulator. However, only fraction 6-2 mm can be used to directly compare the rainfall simulator and SLAKES, because SLAKES requires aggregates between 2-15 mm to measure aggregate stability, thus only fraction 6-2 mm is used for measuring aggregate stability with SLAKES.

4.3.1 – Organic waste fertilizer experiment (E166 – Digestate)

4.3.1.1 – Aggregate stability

This section discusses the aggregate stability indices obtained from the rainfall simulator and SLAKES (Fig. 3.1, 3.2, 3.5, 3.6) as well as interpreting the average slaking values from Figure 3.7.

Although there is only significant difference between the control treatment and animal manure treatment in fraction 6-2 mm, the differences between treatments in Rainfall Stability Index (RSI) resulting from the rainfall simulator show a clearer trend than the average values between treatments for both coefficient *a* and SI-600 (Fig. 3.1, 3.5 & 3.6). Fraction 2-0.6 displays clearer and even greater significant differences between treatments than 6-2 mm (Fig. 3.1 & 3.2). This suggests that the rainfall simulator is more sensitive to various fertilizer treatments than SLAKES is. Both fraction 6-2 mm and SI-600 do however exhibit the same tendency, which is that both the control and mineral fertilizer treatments on average have lower aggregate stability than the organic fertilizer treatments (Fig. 3.1 & 3.6). SI-600 appears to be a much more accurate measure of aggregate stability than coefficient *a*. SI-600 can on average distinguish between treatments, which coefficient *a* cannot. In addition, SI-600 standard deviations are much lower than those of coefficient *a*. Since E166 is a relatively short-term experiment, no big variations in aggregate stability are expected between treatments, which is probably why there are few significant differences. When it comes to the average RSI-values (rainfall simulator), none of the treatments' soil appear to have particularly good aggregate stability. Less soil is lost during rainfall simulation in fraction 6-2 mm than in fraction 2-0.6 mm. In fraction 6-2 mm, only the animal manure treatment can be considered as having moderate aggregate stability (less than 30 % soil loss), whereas the other treatments have poor stability (more than 30 % soil loss). Contrastingly, SLAKES suggests that all treatments have good aggregate stability, because all treatment averages for both coefficient *a* and SI-600 are below 3. These are contradictory results that may have a big impact on decision making in the field. If one is led to believe that one's soil is stable (SLAKES) when it might not be (rainfall simulator), important measures may not be taken to ensure the stability of the soil. However, rainfall intensity in the rainfall simulator is 1.5 bar, which is more intense than regular rainfall, and the amount of rain achieved per hour of rainfall simulation is 250 – 500 mm depending on how large the area of water distribution (Børresen, 2021[1]). In reality, one would never witness that amount of rain in one hour. Thus, there is a chance of increased loss of aggregate stability when the soil is exposed to the rainfall simulator rather than regular rainfall. This may lead the rainfall simulator to portray soils as more unstable than they actually are.

Figure 3.7 (average slaking) is not able to confirm that the trend seen between treatments in SI-600 (Fig. 3.6) is significant, but it strongly indicates that both the control and mineral fertilizer treatments have lower aggregate stability than the organic fertilizer treatments since all 54 SI-averages show the same tendency.

4.3.1.2 – Linear regression comparisons

This section compares linear regression statistics between the rainfall simulator and SLAKES (Fig. 3.3, 3.4, 3.8, 3.9).

Both fraction 6-2 mm from the rainfall simulator and SI-600 from SLAKES have significant correlations between organic matter and aggregate stability (Fig. 3.3 & 3.8), although the correlation is stronger for the rainfall simulator than for SLAKES. This suggests that the rainfall simulator is more sensitive in relation to finding correlations between organic matter and aggregate stability than SLAKES.

---

[1] Trond Børresen, personal communication.

Only fraction 2-0.6 mm shows a significant correlation between the pH and aggregate stability (Fig. 3.4). However, the difference in pH both within and between treatments varies by a maximum 0.5, which means that variation in aggregate stability is likely related to other factors, such as organic matter.

4.3.1.3 – Comparison of rainfall simulator and SLAKES

No significant correlation is found between the rainfall simulator and SLAKES (Fig. 3.10), and there are a few potential reasons as to why this is the case. Firstly, note that there is random difference within soil samples. This means that the 20 g of soil used to measure aggregate stability with the rainfall simulator is not exactly the same as the three aggregates used when measuring with SLAKES. Secondly, the forces causing disaggregation are different between the two methods. Thirdly, the rainfall simulator appears to be more sensitive to fertilizer treatment than SLAKES. All three factors mentioned affect the correlation, and although the correlation is not significant, it does indicate mean that one method is better at measuring aggregate stability than the other.

Judging from the main measurements of aggregate stability (Fig. 3.3, 3.4, 3.8, 3.9), the rainfall simulator seems like the most reliable option when measuring aggregate stability in fertilizer experiments, but this is just one experiment so further experimentation is required. However, SLAKES, and especially SI-600 shows promising results and should be considered as an alternative to the rainfall simulator. Still, one must be wary of SLAKES’ interpretation of good and bad aggregate stability. To be sure SLAKES is reliable, further experiments are needed. SLAKES long-term fertilizer experiments may help establish significant results over time.

4.3.2 – Ås – tillage spring and autumn (A85)

4.3.2.1 – Aggregate stability

This section discusses the aggregate stability indices obtained from the rainfall simulator and SLAKES (Fig. 3.11, 3.12, 3.15, 3.16) as well as interpreting the average slaking values from Figure 3.17.

SLAKES is able to determine that autumn ploughing has a significantly lower aggregate stability compared to the two other treatments, namely spring ploughing and spring harrowing. The rainfall simulator on the other hand cannot find a significant difference between autumn ploughing and spring ploughing. Both SLAKES and the rainfall simulator cannot find significant differences between spring ploughing and spring harrowing. However, both methods reveal that spring ploughing on average has lower aggregate stability than spring harrowing, which is as expected. Although both methods show the same tendency in all figures, the results suggest that SLAKES is more sensitive to tillage treatments than the rainfall simulator. This is because SLAKES can significantly distinguish between autumn ploughing and spring ploughing in both coefficient *a* and SI-600, whereas the rainfall simulator fails to do so in both fractions. As anticipated, box plots show clearer differences between treatments for both SLAKES and the rainfall simulator in this field (A85) than in E166. Most likely because this is a long-term experiment where contrasts between treatments have built up over time. As in field E166, the interpretation of aggregate stability is different between the rainfall simulator and SLAKES as the rainfall simulators interprets lower aggregate stability than SLAKES. Also here, the intensity of rainfall in the rainfall simulator must be taken into account.

Figure 3.17 (average slaking) displays the same tendency as coefficient *a* and SI-600. All 54 SI-averages suggest that autumn ploughing has lower aggregate stability than both spring ploughing and spring harrowing, supporting the results obtained from the box plots (Fig. 3.15 & 3.16).

4.3.2.2 – Linear regression comparisons

This section compares linear regression statistics between the rainfall simulator and SLAKES (Fig. 3.13, 3.14, 3.18, 3.19).

Both fractions from the rainfall simulator have significant correlations between organic matter and aggregate stability (Fig. 3.13), but there is no correlation between organic matter and aggregate stability in coefficient *a* and SI-600 (Fig. 3.18). This suggests that the rainfall simulator is more sensitive at detecting correlations between organic matter and aggregate stability than SLAKES.

Neither SLAKES nor the rainfall simulator display any significant correlation between the pH and aggregate stability (Fig. 3.14 & 3.19). As in field E166, the difference in pH both within and between treatments varies by a maximum of 0.5 pH units, which means that variation in aggregate stability is likely related to other factors, such as organic matter. Also, 4 pH samples are taken at a depth of 10 – 20 cm rather than 0 – 10 cm, which means these results need to be interpreted with some caution.

4.3.2.3 – Comparison of rainfall simulator and SLAKES

No significant correlation is found between the rainfall simulator and SLAKES (Fig. 3.20). The potential reasons as to why there is no correlation are the same as in field E166; samples are different between the two methods, and so is the mode of disaggregation. As opposed to E166, the third reason for no correlation is that SLAKES appears to be more sensitive to tillage treatment than the rainfall simulator. Also here, none of the reasons for non-significant correlation mean that one method is better at measuring aggregate stability than the other.

Based on the main aggregate stability results (Fig. Fig. 3.11, 3.12, 3.15, 3.16), it appears that SLAKES is the better option of the two aggregate stability methods because of better sensitivity to tillage treatment. Also here though, one must note the two methods' different interpretations of what is good and poor aggregate stability as to not be misled.

4.3.3 – Øsaker – tillage spring and autumn (A45)

4.3.3.1 – Aggregate stability

This section discusses the aggregate stability indices obtained from the rainfall simulator and SLAKES (Fig. 3.21, 3.22, 3.25, 3.26) as well as interpreting the average slaking values from Figure 3.27.

Both coefficient *a* and SI-600 are able to significantly differentiate between autumn ploughing and autumn & spring harrowing (Fig. 3.25 & 3.26), whereas only fraction 2-0.6 mm from rainfall simulation is able to do the same (Fig. 3.22). Both SLAKES and the rainfall simulator show the same tendency but SLAKES shows increased sensitivity to tillage treatment compared to the rainfall simulator. As seen from Figures 3.25 & 3.26, SI-600 has a lower standard deviation compared to coefficient *a*, further displaying the benefits of using SI-600 as a measure of aggregate stability rather than coefficient *a*. For the rainfall simulator, the average RSI-values display a soil loss of more than 30 % in autumn & spring harrowing and more than 40 % in autumn ploughing for both fractions, thus displaying poor and very poor aggregate stability respectively. Conversely, coefficient *a* and SI-600 have average values < 3 in both treatments, thus interpreting both treatments as having good aggregate stability. Although the autumn ploughing treatment is close to having moderate aggregate stability (coeff *a* & SI-600 > 3), SLAKES would still present this treatment as having good aggregate stability on the smartphone screen after the 10-min slaking interval.

As seen in Figure 3.27, the 54 average SI-values show that autumn ploughing has lower aggregate stability than autumn & spring harrowing. This strongly supports the results seen in the box plots (Fig. 3.25 & 3.26).

4.3.3.2 – Linear regression comparisons

This section compares linear regression statistics between the rainfall simulator and SLAKES (Fig. 3.23, 3.24, 3.28, 3.29).

Both SLAKES coefficient *a* and SI-600 have significant correlations between organic matter and aggregate stability (Fig. 3.28), whereas only rainfall simulator fraction 2-0.6 mm has a significant correlation between organic matter and aggregate stability (Fig. 3.23). This suggests that SLAKES may be better at detecting correlations between organic matter and aggregate stability than the rainfall simulator.

Neither SLAKES nor the rainfall simulator display any significant correlation between the pH and aggregate stability (Fig. 3.24 & 3.29). The difference in pH both within and between treatments varies by a maximum of 0.8 pH units, which indicates that variation in aggregate stability is likely related to other factors, such as organic matter.

4.3.3.3 – Comparison of rainfall simulator and SLAKES

In contrast to fields E166 and A85, there is found a significant correlation between the rainfall simulator and SLAKES (Fig. 3.30). Flynn et al. (2019) found an inverse relationship between SLAKES and the Cornell Wet Aggregate Stability method (CWAST), the expectation was that such a relationship exists between the rainfall simulator and SLAKES too. This result confirms such an inverse relationship between the rainfall simulator and SLAKES.

As in field A85, SLAKES appears to be a better aggregate stability measurement method than the rainfall simulator based on its superior ability to significantly distinguish between treatments in this field. As long as one is aware that SLAKES in general interprets higher aggregate stability than the rainfall simulator, important differences between treatments can be found by SLAKES that cannot be found by the rainfall simulator.

4.3.4 – Kjuus – tillage spring (Kjuus)

4.3.4.1 – Aggregate stability

This section discusses the aggregate stability indices obtained from the rainfall simulator and SLAKES (Fig. 3.31, 3.32, 3.35, 3.36) as well as interpreting the average slaking values from Figure 3.37.

For both the rainfall simulator and SLAKES, the tendency is the same in field Kjuus. On average, spring ploughing has the lowest aggregate stability, whereas both spring harrowing and direct sowing exhibit approximately the same stability. For the rainfall simulator there is an approximate RSI-value of 20 for the spring ploughing treatment in both fractions, corresponding to good aggregate stability (20 % soil loss). Direct sowing and spring harrowing treatments lose on average 10 % soil (RSI = 10) in fraction 6-2 mm, and 5 % in fraction 2-0.6 mm (RSI = 5), corresponding to excellent aggregate stability. SLAKES interprets all treatments as having good aggregate stability, since all average coefficient *a* and SI-600 values < 3. Yet again, the interpretation of SLAKES leads us to believe that there is no pronounced difference between conventional/intensive tillage treatments (spring ploughing) and reduced/no tillage treatments (spring harrowing & direct sowing), although there probably is.

Figure 3.37 presents the same tendency as the coefficient *a* and SI-600 box plots. All 54 average SI-values show that spring ploughing aggregates slake (disperse) to a higher degree than both spring harrowing and direct sowing treatments.

4.3.4.2 – Linear regression comparisons

This section compares linear regressions statistics between the rainfall simulator and SLAKES (Fig. 3.33, 3.34, 3.38, 3.39).

R^2-values are high for SI-600 (SLAKES) and fractions 6-2 mm and 2-0.6 mm (rainfall simulator), which could suggest correlations between organic matter and aggregate stability (Fig. 3.33 & 3.38). However, since there are no repetitions in field Kjuus there is too little data (*n*) to say that there are any correlations.

Nor can there be found correlations between pH and aggregate stability, also here due to a small sample size (*n*) (Fig. 3.34 & 3.39).

4.3.4.3 - Comparison of rainfall simulator and SLAKES

Although the correlation (R^2) is strong between SLAKES and the rainfall simulator in Figure 3.40, it is not significant due to small sample size. However, this result does suggest that both methods are inversely related as is significantly demonstrated in Figure 3.30.

The differences in aggregate stability interpretation are not very different between the rainfall simulator and SLAKES in this field. However, the common rainfall simulator interpretation does at least distinguish between conventional tillage and reduced/no tillage, which SLAKES interpretation does not. At the same time, both methods show similar tendencies between treatments, indicating that SLAKES is as good a measurement of aggregate stability as the rainfall simulator. Slaking difficulty did not increase despite higher amounts of sand and silt in this field, suggesting SLAKES can be useful in fields where sand and silt contents are higher.

4.3.5 – Combined linear regression comparisons (organic matter & aggregate stability)

This section compares combined linear regression statistics between the rainfall simulator and SLAKES (Fig. 3.41 & 3.42).

Both fractions (6-2 mm & 2-0.6 mm) from the rainfall simulator have moderate/strong significant correlations between organic matter and aggregate stability (Fig. 3.41), whereas only SLAKES SI-600 has a significant correlation between organic matter and aggregate stability (Fig. 3.42), and the correlation is weak. As these combined linear regression statistics sum up the correlation between organic matter and aggregate stability from all 4 experimental fields, this gives a strong indication to suggest that the rainfall simulator is better at detecting correlations between organic matter and aggregate stability than SLAKES.

4.3.6 – Overall comparison of rainfall simulator and SLAKES

As seen throughout this thesis, both the rainfall simulator and SLAKES have different issues related to them. Timewise, SLAKES is a much quicker way of measuring aggregate stability. Approximately it takes 20 mins per plot to measure aggregate stability using the rainfall simulator, however, the aggregates need to dry for approximately one week or be placed in a drying cabinet overnight. Then the aggregates need to be weighed before the data can be analysed. In comparison, slaking of one plot using SLAKES only takes 10 mins to perform, and the data is then ready for analysis immediately. At best, it takes the rainfall simulator a day longer than SLAKES to produce results. Furthermore, a laboratory setup is needed to make aggregate stability measurements using the rainfall simulator. A laboratory is usually not accessible to non-scientists and nor is the rainfall simulator method very intuitive. If a farmer wants to know how stable his/her soil is, soil samples must be extracted and sent to a laboratory for analysis, and this is expensive. SLAKES on the other hand can be downloaded for free by anyone owning a smartphone, the instructions are simple, and laboratory facilities are not required. Although there are negative aspects linked to the rainfall simulator, it has one important advantage, it is proven to yield valid results, whilst SLAKES is a relatively new method that should be developed further.

One point is that without proper lighting above the smartphone providing contrast between the background and the soil aggregates, SLAKES will likely mistake aggregates for the background, and give very inaccurate aggregate stability measurements. In addition, aggregates submerged in water need to be placed in the petri dish so that they have the same orientation as in the reference image, if not the magnitude of change in area is misinterpreted (Flynn et al., 2019). Another issue with SLAKES is coefficient *a*, which is the predicted aggregate stability displayed on the smartphone screen after the 10 min slaking interval. More precisely, coefficient *a* is a projection of further disaggregation made by the fitted Gompertz function (Equation 2). As Flynn et al. (2019) explains, there is a risk of misinterpreting the analysis by projecting further dispersion, and so the SI-600 value obtained from the text file is a much better parameter because it is an actual observation of the data. An example of further disaggregation as predicted by the Gompertz function can be seen in Figure 4.1. SI-600 stops at an SI-value of 0.57, whereas coefficient *a* continues until it has a value of 49. The amount of time needed to reach a value of 49 with the growth rate of this curve is 1,00E+230 seconds, which is an infinite amount of time and completely unrealistic. As Flynn et al. (2019) suggests, it is probably wise to display SI-600 alongside coefficient *a* on the smartphone screen post-slaking. This is so that one can easily identify when the Gompertz function has made an unlikely prediction through coefficient *a*.

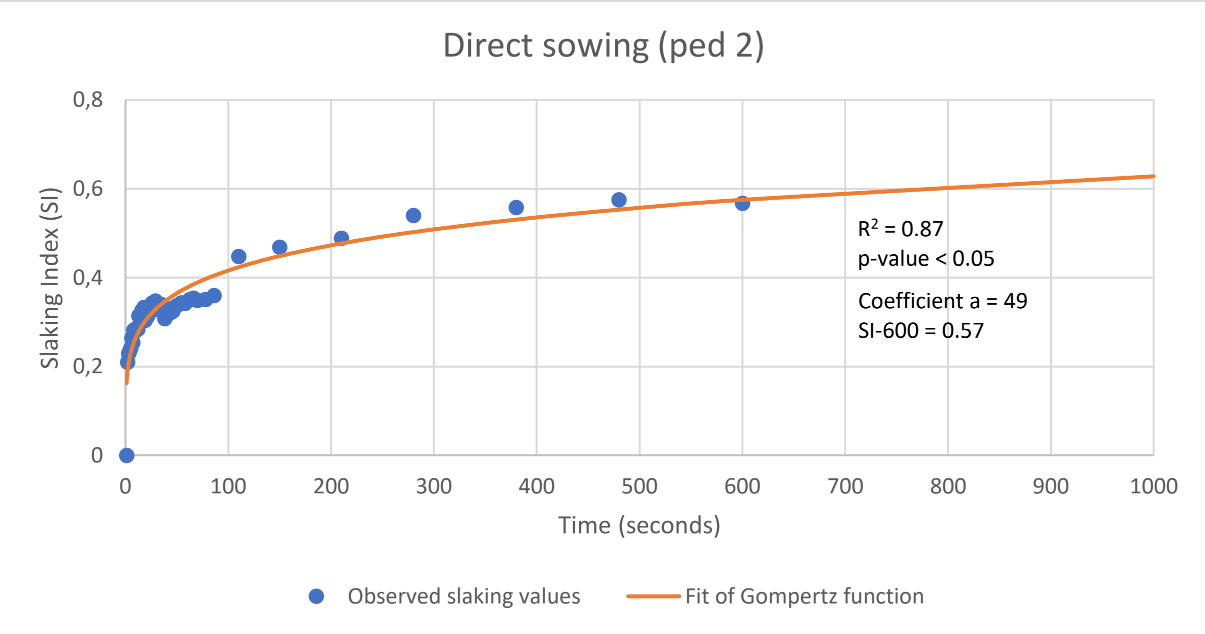

Figure 4.1 – Aggregate 2, Direct sowing, Kjuus. Fit of Gompertz function to the 54 observed slaking values, and the further projection of disaggregation by the Gompertz function. Significant and strong correlation between the observed slaking values and the Gompertz function.

Another matter that needs to be considered in future program software updates of SLAKES, is the SI-values that are considered as good; (0-3), moderate (3-7), and poor (> 7) aggregate stability. As discussed in sections 4.3.1, 4.3.2, 4.3.3 and 4.3.4, SI-values obtained from all fields exhibit too good aggregate stability compared to the RSI-values found by the rainfall simulator. Therefore, a suggestion is to lower the SI-values that are considered as good, moderate, and poor aggregate stability, as to calibrate SLAKES to more traditional methods like the rainfall simulator. E.g., SI-values: 0-1 = excellent aggregate stability; 1-2 = good aggregate stability; 2-3 = moderate aggregate stability; > 3 = poor aggregate stability. Although SLAKES (coefficient *a* and SI-600) and the rainfall simulator (6-2 mm and 2 – 0.6 mm) show the same tendency between treatments in all fields (box plots), the actual values that are considered as good, moderate, and poor are completely different between the two methods, which can lead to misinterpretation of the results. As long as one is aware of this issue and interpret the results accordingly, SLAKES can definitely yield valid results that can improve upon the rainfall simulator. In field E166, the rainfall simulator is more sensitive to fertilizer treatment than SLAKES, however, none of the methods yield particularly significant results in this field, which is as expected in a relatively short-term experiment. In fields A85 and A45, SLAKES displays superior sensitivity to tillage treatment when compared to the rainfall simulator, suggesting that SLAKES can be a valid alternative to the rainfall simulator. In addition, SI-600 shows increased sensitivity to tillage treatment in both A85 and A45 compared to coefficient *a*, backing up the proposition made by Flynn et al. (2019) of including SI-600 on the smartphone screen post-slaking. Field Kjuus cannot conclude whether SLAKES or the rainfall simulator is the superior method for measuring aggregate stability but suggests that SLAKES is as capable as the rainfall simulator in showing differences between treatments.

4 – Conclusion

In summary, this thesis confirms most assumptions of the hypothesis. SLAKES is simpler to use than the rainfall simulator because less equipment is needed to measure aggregate stability. In addition, clear instructions are provided by the SLAKES app so that anyone can perform measurements, not just persons with laboratory access. The application is also quicker than the rainfall simulator at providing data that can be analysed. Furthermore, SLAKES is cheaper than the rainfall simulator as the app is free and no laboratory or additional labour is needed. In 3 out of 4 fields (A85, A45, Kjuus vs E166) SLAKES indicates clearer and/or more significant variations between treatments compared to the rainfall simulator (SI-600 vs 6-2 mm). This suggests that SLAKES is at least as good at determining valid aggregate stability measurements as the rainfall simulator. However, long-term organic fertilizer experiments are needed to see if SLAKES can provide the same sensitivity to treatment differences as seen in the tillage experiments. Although this thesis finds evidence to suggest that SLAKES can substitute, or at least assist more traditional methods, some improvements are needed. For instance, SI-600 must be displayed on the smartphone screen along with coefficient *a* to avoid portraying false aggregate stability measurements. Also, SLAKES' interpretation of SI-values needs to be revised. This is so that treatments that clearly have different aggregate stability are not classified as having the same aggregate stability.

All things considered, SLAKES can provide a more than adequate alternative to traditional methods for measuring aggregate stability. However, more experiments and research are required because the application at present is still relatively new.

5 – References

In text

- Amézketa, E. (1999). Soil Aggregate Stability: A Review. *Journal of Sustainable Agriculture*, 14 (2-3): 83-151. https://doi.org/10.1300/J064v14n02_08
- Bagnall, D. K. & Morgan, C. L. S. (2021). SLAKES and 3D Scans characterize management effects on soil structure in farm fields. *Soil Tillage and Research*, 208 (Article 104893). https://doi.org/10.1016/j.still.2020.104893
- Bell, M. & Mathesius. (2019). Fertilizers and soil pH. *Agriculture and Natural Resources*, University of California. https://ucanr.edu/sites/soils/files/306283.pdf
- Birkhofer, K., Bezemer, T. M., Bloem, J., Bonkowski, M., Christensen, S., Dubois, D., Ekelund, F., Fließbach, A., Gunst, L., Hedlund, K., Mäder, P., Mikola, J., Robin, C., Setälä, H., Tatin-Froux, F., Van der Putten, W. H., Scheu, S. (2008). Long-term organic farming fosters below and aboveground biota: Implications for soil quality, biological control and productivity. *Soil biology and Biochemistry*, 40 (9): 2297-2308. https://doi.org/10.1016/j.soilbio.2008.05.007
- Børresen, T. & Lamandé, M. (2019). *Jordfysikk, øvelser JORD230*. JORD230-Jordfysikk_oevelsehefte.pdf, Canvas. Faculty of Environmental Sciences and Natural Resource Management (MINA), NMBU, Ås, Norway.
- Coleman, D. C. & Crossley, J. R. (1996). Fundamentals of soil ecology. *Academic Press*.
- De Leenheer, L. & De Boodt, M. (1958) Determination of Aggregate Stability by the Change in Mean Weight Diameter. *International Symposium on Soil Structure*, 24: 290-300.
- Debela, N. & Gebrekidan, H. (2015). Effect of land use changes and soil depth on soil organic matter, total nitrogen and available phosphorus contents of soils in Senbat watershed, western Ethiopia. *American Journal of Agricultural and Biological Science*, 8 (3): 206-212. https://www.researchgate.net/publication/264859040_Effect_of_land_use_changes_and_soil_depth_on_soil_organic_matter_total_nitrogen_and_available_phosphorus_contents_of_soils_in_Senbat_watershed_western_Ethiopia
- Fajardo, M. & McBratney, A. B. (2019). SLAKES: A soil aggregate stability smart-phone app [Mobile application software]. *The University of Sydney*, Australia. https://play.google.com/store/apps/details?id=slaker.sydneyuni.au.com.slaker&hl=en.

- Fajardo, M., McBratney, A.B., Field, D. J., Minasny, B. (2016). Soil slaking assessment using image recognition. *Elsevier, Soil Tillage & Research*, 163: 119-129. https://doi.org/10.1016/j.still.2016.05.018
- Flynn, K. D., Bagnall, D. K., Morgan, C. L. S. (2019). Evaluation of SLAKES, a smartphone application for quantifying aggregate stability, in high-clay soils. *Soil Science Society of Americal Journal*, 84 (2): 345-353. https://doi.org/10.1002/saj2.20012
- Getahun, G. T., Etana, A., Munkholm, L. J., Kirchmann, H. (2021). Liming with CaCO3 or CaO affects aggregate stability and dissolved reactive phosphorus in a heavy clay subsoil. *Soil and Tillage Research*, 214 (Article 105161). https://doi.org/10.1016/j.still.2021.105162.
- Gompertz, B. (1825). On the nature of the function expressive of the law of human mortality, and on a new mode of determining the value of life contingencies. *Philosophical Transactions of the Royal Society of London*, 2: 513-583. https://doi.org/10.1098/rspl.1815.0271.
- Hillel, D., Warrick, A. W., Baker, R.S. Rosenzweig, C. (1998). Environmental Soil Physics: Fundamentals, Applications, and Environmental Considerations. *Academic Press*, San Diego. https://search.ebscohost.com/login.aspx?direct=true&db=e000xww&AN=198941&site=ehost-live.
- Karlen, D. L., Mausbach, M. J., Doran, J. W., Cline, R. G., Harris, R. F., Schuman, G. E. (1997). Soil Quality: A Concept, Definition, and Framework for Evaluation. *Soil Science Society of America Journal*, 61 (1): 4-10. https://doi.org/10.2136/sssaj1997.03615995006100010001x.
- Krauss, M., Berner, A., Perrochet, F., Frei, R., Niggli, U., Mäder, P. (2020). Enhanced soil quality with reduced tillage and solid manures in organic farming – a synthesis of 15 years. *Sci Rep*, 10 (Article 4403). https://doi.org/10.1038/s41598-020-61320-8
- Krogstad, T. & Børresen, T. (2015). *JORD 200 Field and Laboratory Methods*. Canvas. Department of Environmental Sciences, NMBU, Ås, Norway.
- Lamandé, M. (2020). *Ø4_Aggregatstørrelsesfordeling.mp4*. JORD230, Canvas. Faculty of Environmental Sciences and Natural Resource Management (MINA), NMBU, Ås, Norway.

- Mamen, J. (2020). Köppens klimaklassifikasjon. *Store norske leksikon*. https://snl.no/K%C3%B6ppens_klimaklassifikasjon (Accessed 28.04.2021).
- Marinari, S., Mancinelli, R., Campiglia, E., Grego, S. (2006). Chemical and biological indicators of soil quality in organic and conventional farming systems in Central Italy. *Ecological Indicators*, 6 (4): 701-711. https://doi.org/10.1016/j.ecolind.2005.08.029.
- Marti, M. (1984). *Kontinuierlicher Getreidebau ohne Pflug im Südosten Norwegens – Wirkung auf Ertrag Phyisikalsche und Chemische Bodenparameter*. PhD thesis, page 155, Agricultural University of Norway, Ås.
- Masciandaro, G., Macci, C., Peruzzi, E., Doni, S. (2018). Chapter 1 – Soil Carbon in the World: Ecosystem Services Linked to Soil Carbon in Forest and Agricultural Soils. *The Future of Soil Carbon, Academic Press*, 1-38. https://doi.org/10.1016/B978-0-12-811687-6.00001-8.
- McCalla, T.M. (1944). Water-drop method of determining stability of soil structure. *Soil Science*, 58 (2): 117-122. https://journals.lww.com/soilsci/Citation/1944/08000/WATER_DROP_METHOD_OF_DETERMINING_STABILITY_OF_SOIL.2.aspx.
- Metting, F. B. (1993). Soil microbial ecology: applications in agriculture and environmental management. *Marcel Dekker*. New York, USA.
- NIBIO. (1992). *Jordsmonn – teksturgrupper i plogsjiktet*. Kilden. Available from: https://kilden.nibio.no/?topic=jordsmonn&lang=nb&X=6670597.37&Y=304986.74&zoom=10.924941376867775&bgLayer=graatone_cache&layers_opacity=0.75&layers=jm_tekstturgrupper_plogsjikt (accessed 19.05.2021).
- Norwegian Meteorological Institute. (2021). *It will become hotter*. Norwegian Meteorological Institute. Available from: https://www.met.no/en/weather-and-climate/It-will-become-hotter (accessed 28.04.2021).
- Oades, J.M. (1984). Soil organic matter and structural stability: mechanisms and implications for management. *Plant and Soil*, 76: 319-337. https://doi.org/10.1007/BF02205590.
- Ogden, C.B., van Es, H. M., Schindelbeck, R.R. (1997). Miniature rain simulator for measurement of infiltration and runoff. *Soil science Society of America Journal*, 61 (4): 1041-1043. http://dx.doi.org/10.2136/sssaj1997.03615995006100040008x.

- Ohnishi, A., Namekawa, Y., Fukui, T. (2020). Universality in COVID-19 spread in view of the Gompertz function. *Progress of Theoretical and Experimental Physics*, 202 (12). https://doi.org/10.1093/ptep/ptaa148.
- Rajani, A.V. (2019). Soil Quality and Soil Health. *Department of Agricultural Chemistry & Soil Science, Junagadh Agricultural University, Gujarat*. http://dx.doi.org/10.13140/RG.2.2.24060.08321.
- Reeve, R.C. (1965). Air-to-Water Permeability Ratio. *Methods of Soil Analysis*: 41: 520-531. https://doi.org/10.2134/agronmonogr9.1.c41.
- Scialabba, N. E-H., & Hattam, C. (2002). Organic agriculture, environment and food security. *Food and Agriculture Organization of the United Nations (FAO)*. Available from: https://www.fao.org/3/Y4137E/y4137e00.htm (accessed 25.01.2021).
- Six, J., Bossuyt, H., Degryze, S., Denef, K. (2004). A history of research on the link between (micro)aggregates, soil biota, and soil organic matter dynamics. *Soil and Tillage Research*, 79 (1): 7-31. https://doi.org/10.1016/j.still.2004.03.008.
- State of the Environment Norway. (2021). *Climate Change in Norway*. Environment Norway. Available from: https://www.environment.no/topics/climate/climate-change-in-norway/ (accessed 28.04.2021).
- Tisdall, J.M., & Oades, J. M. (1982). Organic matter and water stable aggregates in soils. *European Journal of Soil Science*, 33 (2): 141-163. https://doi.org/10.1111/j.1365-2389.1982.tb01755.x.
- Tiulin, A.F. (1928). Aggregate analysis as a method for determining soil structure. *Per. Agric. Exp. Sta. Div. Chem. Rep*, 3: 77-122.
- Tjørve, K. M. C., & Tjørve, E. (2017). The use of Gompertz models in growth analyses, and new Gompertz-model approach: An addition to the Unified-Richards family. *PLos One*. https://doi.org/10.1371/journal.pone.0178691.
- United Nations. (2015). *Paris Agreement*. United Nations Framework Convention on Climate Change. https://unfccc.int/sites/default/files/english_paris_agreement.pdf.
- Wang, H., Xu, J., Liu, X., Zhang, D., Li, L., Li, W., Sheng, L. (2019). Effects of long-term application of organic fertilizer on improving organic matter content and retarding acidity in red soil from China. *Soil and Tillage Research*, 195 (Article 104382). https://doi.org/10.1016/j.still.2019.104382.

- Yoder, R. E. (1936). A direct method of aggregate analysis of soils and a study of the physical nature of erosion losses. *Agronomy Journal*, 28 (5): 337-351. https://doi.org/10.2134/agronj1936.00021962002800050001x.

Tables

- Table 1.1: Figure 1: Karlen, D. L., Mausbach, M. J., Doran, J. W., Cline, R. G., Harris, R. F., Schuman, G. E. (1997). Soil Quality: A Concept, Definition, and Framework for Evaluation. *Soil Science Society of America Journal*, 61 (1): 4-10. https://doi.org/10.2136/sssaj1997.03615995006100010001x

Figures

- Figure 1.1: Jastrow, J.D. & Miller, R. M. (1998). Soil aggregate stabilization and carbon sequestration: feedbacks through organomineral associations. In: Lal, R., Kimble, J. M., Follett, R. F., Stewart, B. A. (1st ed.) *Soil Processes and the Carbon Cycle*. *CRC Press*, pp. 207-223. https://doi.org/10.1201/9780203739273.
- Figure 1.2: Keefer, R. F. (2000). Handbook of soils for Landscape Architects. *Oxford University Press*. New York, USA. https://search.ebscohost.com/login.aspx?direct=true&db=e000xww&AN=169126&site=ehost-live
- Figure 1.3: Hillel, D., Warrick, A. W., Baker, R.S. Rosenzweig, C. (1998). *Environmental Soil Physics: Fundamentals, Applications, and Environmental Considerations.* Academic Press. Available from: https://search.ebscohost.com/login.aspx?direct=true&db=e000xww&AN=198941&site=ehost-live
- Figure 2.1: Google. (n.d.). Map of the Oslofjord region. *Google maps*. Available from: https://www.google.com/maps/@59.5663537,10.6725013,9z?hl=en (Accessed 29.04.2021).

6 – Appendix

6.1 – Appendix 1: Aggregate size distribution

6.1.1 – E166

Table 6.1 – Aggregate size distribution. Mean weight (g/100g) of all fractions (mm).

Treatment	> 20 mm (g/100g)	6-20 mm (g/100g)	2-6 mm (g/100g)	2-0.6 mm (g/100g)	< 0.6 mm (g/100g)
Control (T1)	11.3	24.6	25.6	19.9	18.5
Mineral fertilizer (T3)	8.8	26.4	27.6	19.8	17.1
Animal mnaure (T5)	8.9	26.0	25.9	20.4	18.6
Digestate – food waste (T7)	9.8	26.1	24.7	18.6	20.6
Digestate (T9)	10.6	25.9	24.8	18.0	20.4

6.1.2 – A85

Table 6.2 – Aggregate size distribution. Mean weight (g/100g) of all fractions (mm).

Treatment	> 20 mm (g/100g)	6-20 mm (g/100g)	2-6 mm (g/100g)	2-0.6 mm (g/100g)	< 0.6 mm (g/100g)
Autumn ploughing (A)	3.5	18.8	33.5	29.1	15.8
Spring ploughing (B)	8.8	30.6	30.0	18.6	10.9
Spring harrowing (C)	5.9	19.4	30.6	27.6	15.5

6.1.3 – A45

Table 6.3 – Aggregate size distribution. Mean weight (g/100g) of all fractions (mm).

Treatment	> 20 mm (g/100g)	6-20 mm (g/100g)	2-6 mm (g/100g)	2-0.6 mm (g/100g)	< 0.6 mm (g/100g)
Autumn & spring harrowing (B)	15.0	32.1	27.3	16.5	8.5
Autumn ploughing (D)	11.9	24.8	23.9	22.9	16.2

6.1.4 – Kjuus

Table 6.4 – Aggregate size distribution. Mean weight (g/100g) of all fractions (mm).

Treatment	> 20 mm (g/100g)	6-20 mm (g/100g)	2-6 mm (g/100g)	2-0.6 mm (g/100g)	< 0.6 mm (g/100g)
Spring ploughing (T1)	39.1	25.3	16.8	9.7	9.0
Direct sowing (T2)	41.6	20.4	14.6	11.0	9.8
Spring harrowing (T3)	38.3	17.4	11.6	7.8	8.1

Norges miljø- og biovitenskapelige universitet
Noregs miljø- og biovitskapelege universitet
Norwegian University of Life Sciences

Postboks 5003
NO-1432 Ås
Norway